An Investigation into the Alkene Hydroformylation Reaction using Platinum Complexes

by

Deshen Kistamurthy

A thesis submitted in partial fulfillment of the requirements for the degree of

Master of Science

in the Department of Chemistry

University of Cape Town

South Africa

Supervisors: Prof. J. R. Moss and Dr. G. Smith

August 2009

DECLARATION

I declare that **An Investigation into the Alkene Hydroformylation Reaction using Platinum Complexes** is my own work and has not been presented for the award of any other degree at any university. All the sources I have used or quoted have been indicated and acknowledged by means of complete references.

Deshen Kistamurthy
17 August 2009

Signed by candidate

Table of Contents

ACKNOWLEDGEMENTS

I would like to extend my sincere gratitude and appreciation to the following people who have made invaluable contributions to the completion of this thesis:

Prof Moss, for the guidance, direction as well as motivational and enthusiastic discussions throughout this project.

Dr Smith, for the constant encouragement, inspiration and keen interest to provide advice in all aspects of this project.

Noel and Pete for the NMR spectra provided; Pierro for elemental analysis and mass spectra.

Dr S. Otto for the constant willingness to help and great assistance provided in the catalytic testing and GC analysis.

All members of the Organometallic research group for the pleasant working environment; Mokgolela Mogorosi for advice in synthesis of compounds; Banothile Makhubela for proof-reading this thesis.

To my parents Rani and Preggie and my sister Dashnee thank you for the inspiration and undying support; Rowena for making the past few years the best time of my life.

LIST OF ABBREVIATIONS AND SYMBOLS

Ph	phenyl
Me	methyl
COD	1,5-cyclooctadiene
dppm	1,1-bis(diphenylphosphino)methane
dppe	1,2-bis(diphenylphosphino)ethane
dppp	1,3-bis(diphenylphosphino)propane
dcpp	1,3-bis(dicyclohexylphosphino)propane
dbpp	1,3-bis(di-tertiary-butylphosphino)propane
dnpe	1,2-bis(8-bicyclo–2-6-dimethylphospha(3.3.1)- nonyl)ethane
syngas	synthesis gas
NMR	Nuclear Magnetic Resonance
s	singlet
d	doublet
t	triplet
m	multiplet
J	coupling constant
EI	Electron Impact
IR	Infrared
M^+	parent molecular ion
m/z	mass to charge ratio
°C	degrees Celsius
mg	milligrams
h	hour

ABSTRACT

Hydroformylation is the most widely applied homogeneous catalysis reaction used in industry. The aldehyde product is an important commodity in both the bulk and specialty chemical industry. Platinum catalysts have shown significant chemo- and regioselectivities in alkene hydroformylation. This thesis investigates the activity as well as selectivity of platinum complexes containing bidentate ligands in the hydroformylation reaction.

A series of metal complexes of the type $[MCl_2\{X\text{-}N(Ph_2P)_2\}]$ (where M = Pt, Pd; X = benzyl, 2-picolyl, ^{n}Pr) have been prepared. ^{1}H, ^{31}P and ^{13}C NMR, elemental analysis as well as mass spectrometry were used to characterize these complexes of which $[PtCl_2\{^n\text{Pr-}N(Ph_2P)_2\}]$ and $[PdCl_2\{^n\text{Pr-}N(Ph_2P)_2\}]$ were new. A new complex containing an iminophosphine ligand $[PtCl_2(o\text{-}Ph_2PC_6H_4CH{=}N^n\text{Pr})]$ was also synthesized. In addition, a series of platinum complexes of the type $[PtCl_2(P\text{-}P)]$ (where (P-P) = dppp, dppe, dcpp, dbpp, dnpe), of which $[PtCl_2(dnpe)]$ was new, were prepared and characterized.

The platinum complexes were employed in the hydroformylation of 1-octene at 100 °C using 80 bar syngas ($CO:H_2$ = 1:1) in the presence of $SnCl_2$. Complexes of the type $[PtCl_2\{X\text{-}N(Ph_2P)_2\}]$ (X = benzyl, 2-picolyl, ^{n}Pr) showed low activity even after extended reaction times. This was attributed to the small bite angle which has been reported to reduce catalytic activity in complexes containing similar bite angles. In addition, we have established that the group linking the phosphorus atoms is an important feature of the ligand backbone in $[PtCl_2(P\text{-}P)]$ complexes. The more flexible three-carbon chain such as that in $[PtCl_2(dppp)]$ showed higher activity than the rigid two-carbon bridge of $[PtCl_2(dppe)]$. The substituents on the phosphorus atoms also proved to be important since replacing the phenyl substituents of $[PtCl_2(dppp)]$ with cyclohexyl groups as in $[PtCl_2(dcpp)]$ significantly reduced catalytic activity.

Chapter 1

Review on hydroformylation studies using transition metal catalysts

1.1. Introduction

Hydroformylation is the oldest homogeneous catalysis reaction of olefins used in industry, producing aldehydes, acids and alcohols. This homogeneous reaction involves the catalyzed addition of carbon monoxide and hydrogen to an alkene to form an aldehyde with one more carbon atom than the initial alkene. The subsequent reaction with hydrogen produces the alcohol product. The combination of H_2 and CO is commonly known as synthesis gas (syngas). Three types of homogeneous transition metal catalysts are used industrially for the hydroformylation of olefins.[1] These include unmodified Co, modified Co and modified Rh catalysts. Hydroformylation products include linear (normal) and branched (iso) aldehydes (Scheme 1.1). The selectivity achieved is determined by the addition of the alkene to the metal catalyst as an anti-Markovnikov addition produces the linear aldehyde while a Markovnikov addition produces the branched aldehyde.[1]

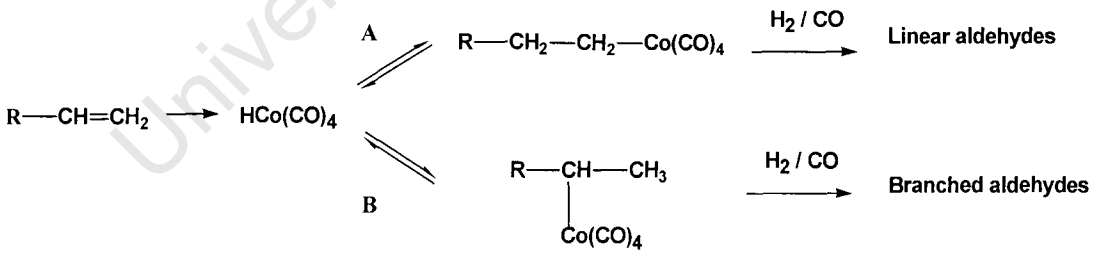

Scheme 1.1: Branched and linear aldehyde products of hydroformylation. (A) Anti-Markovnikov addition of alkene to metal catalyst resulting in linear aldehydes, (B) Markovnikov addition resulting in branched aldehydes.

1.1.1. Discovery and development of hydroformylation

The first product of hydroformylation was discovered by Otto Roelen on the 26th July 1938 at the Ruhrchemie AG laboratories at Oberhausen in Germany.[2] He had originally set out to investigate methods of increasing chain lengths of Fischer-Tropsch (FT) hydrocarbons by recycling generated olefins and found that he had isolated small amounts of propanal and diethyl ketone when ethylene and synthesis gas was passed over a cobalt catalyst at 150 °C and 100 bar.[2] Roelen demonstrated great experimental skill and a keen scientific awareness to characterize these compounds under conventional FT conditions.

The observation that ethylene could be used in this process to produce aldehydes and ketones led to the assumption that oxo compounds are generated, thus the process was aptly named 'the oxo synthesis'. The process later received a more accurate description, 'Hydroformylation' by Adkins and Krsek.[3]

Even 20 years after the discovery of hydroformylation, its full potential and industrial importance was not realised despite the chemical versatility of the products. Around the mid 1950's two significant developments were made that elevated the exploitation of hydroformylation tremendously. Initially, it was the rapid progression of the petrochemical industry and later the rise of PVC and detergent industries which proved to be the most significant traders of the alcohol products generated by hydroformylation.[1]

Prior to the development of the oxo synthesis, there had not been extensive discussion on the topic of homogeneous catalysis. Sabatier, the discoverer of nickel-catalyzed hydrogenation made an early classification of 'homogeneous systems' as those in which the catalysts are miscible with at least one of the compounds in the reaction while 'heterogeneous systems' involve a solid catalyst in contact with a reactive liquid or gas phase.[4] However, later work by Adkins and Kresk, Berty and Markoas as well as Storch and Natta confirmed oxo catalysts as homogeneous in nature.[3,5-7] Table 1.1 compares the features of homogeneous and heterogeneous catalysis.[8,9] Although heterogeneous catalysis has many important applications, a deeper mechanistic understanding of homogeneous systems has been established. Detailed

mechanistic studies into catalytic cycles allow steric and electronic properties of homogeneous catalysts to be adapted to solve a specific problem giving it a clear advantage over its heterogeneous counterpart.[10]

Table 1.1: Homogeneous vs heterogeneous catalysis.

	Homogeneous catalysis	**Heterogeneous catalysis**
Activity	High	Variable
Selectivity	High	Variable
Reaction conditions	Mild	Harsh
Catalyst recycling	Expensive	Not necessary
Mechanistic understanding	Plausible	Not plausible

The aldehyde product was found to be an invaluable commodity in both the bulk and specialty chemical industry.[11] This resulted in a number of applications from the hydroformylation process (Figure 1.1).

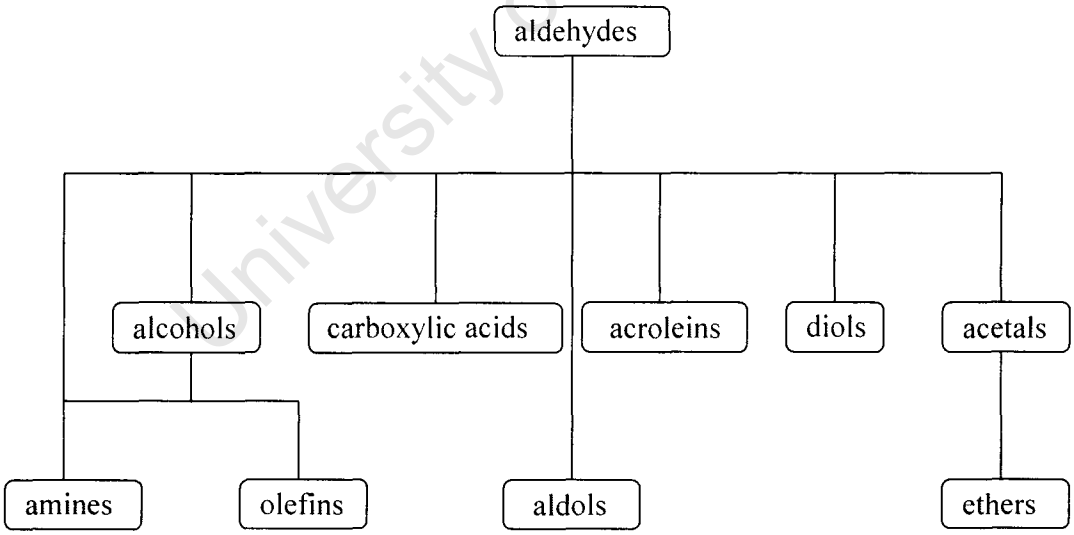

Figure 1.1: Compounds accessible *via* hydroformylation.

The first generation of hydroformylation processes such as BASF, ICI, Kuhlmann and Ruhrchemie utilized Co as the metal catalyst exclusively.[11] The processes using Co provided the desired products at a reasonable rate of reaction and the only major differences between these processes were the methods of separating product from

catalyst as well as catalyst recycling. However, reaction conditions were quite harsh and a need for further developments such as improved selectivity, lower by-product formation and milder reaction conditions became a priority. The Shell Process utilizing a ligand modified Co-phosphine catalyst served as the last of these first-generation hydroformylation processes.[9]

The second generation hydroformylation processes incorporated ligand modification with Rh as the metal catalyst. The Celanese Corporation conducted the first commercial process using a Rh-phosphine catalyst in a butyraldehyde plant in Texas in 1974.[12] Great advances then followed in efficient material and energy consumption using these second generation catalysts and it was expected that not many further developments would arise in this already effective hydroformylation system. However, it was later found that biphasic, yet still homogeneous, systems proved more efficient than single phase ones which resulted in intensive research into water-soluble phosphine ligands in hydroformylation.[11] These ligands demonstrated impressive features such as enhanced selectivity towards the linear aldehyde and minimal isomerisation of the substrate.[13]

1.1.2. Rh and Co catalyzed hydroformylation

Extensive spectroscopic studies have led to a greater understanding into the mechanism of hydroformylation using Co and Rh catalysts.[1] The use of various ligand systems and the subsequent effect on activity as well as regio- and chemoselectivity has also been well established. Heck and Breslow proposed a catalytic cycle as early as 1961 and since then tremendous strides have been made to identify the species involved in the hydroformylation cycle.[14] However, certain mechanistic details are still to be investigated since little is known about the kinetics of hydroformylation reactions. Table 1.2 shows the activity and selectivity of both unmodified and phosphine-modified Co and Rh catalysts used in industrial hydroformylation processes.[1]

Table 1.2: Co and Rh catalysts used in industrial hydroformylation processes.

Catalyst	$[HCo(CO)_4]$	$[HCo(CO)_3L]$[a]	$[HRh(CO)_4]$	$[HRh(CO)L_3]$
Temperature (°C)	150-180	160-200	100-140	110-130
Pressure (MPa)	20-30	5-15	20-30	4-6
Products	Aldehydes	Alcohols	Aldehydes	Aldehydes
n:iso	80:20	88:12	50:50	95:5
By-products	High	High	Low	Low

[a] L = monodentate phosphine ligand.

The modified catalysts react under significantly lower pressures and demonstrate far greater linearity of the products. The versatility of the homogeneous system is also clearly demonstrated as the catalysts can be used to isolate a particular target and are adaptable to meet a specific reaction requirement.[15-17]

Scheme 1.2 shows the hydroformylation of an olefin utilizing an unmodified Co catalyst. Only the formation of the linear product is shown for simplicity.[1] Heck and Breslow developed the steps in this catalytic cycle and the mechanism is generally accepted for unmodified Rh systems as well.[14]

The hydrido metal carbonyl **1-1** (Scheme 1.2) is formed from the reaction of $[Co_2(CO)_8]$ with H_2. Dissociation of CO leads to the unsaturated 16e species **1-2**. Coordination of the olefin produces **1-3** (18e) and *via* H migration the alkyl metal carbonyl **1-4** (16e) is formed. Coordination of CO leads to **1-5** (18e) and *via* an alkyl migration step, the acyl metal carbonyl **1-6** (16e) is formed. Oxidative addition of hydrogen then takes place to form **1-7** (18e) and subsequently the acyl metal carbonyl is cleaved to form the aldehyde **1-8** and regenerate the active catalyst **1-2**. The aldehyde can then be further reacted with hydrogen to produce the alcohol **1-9**.

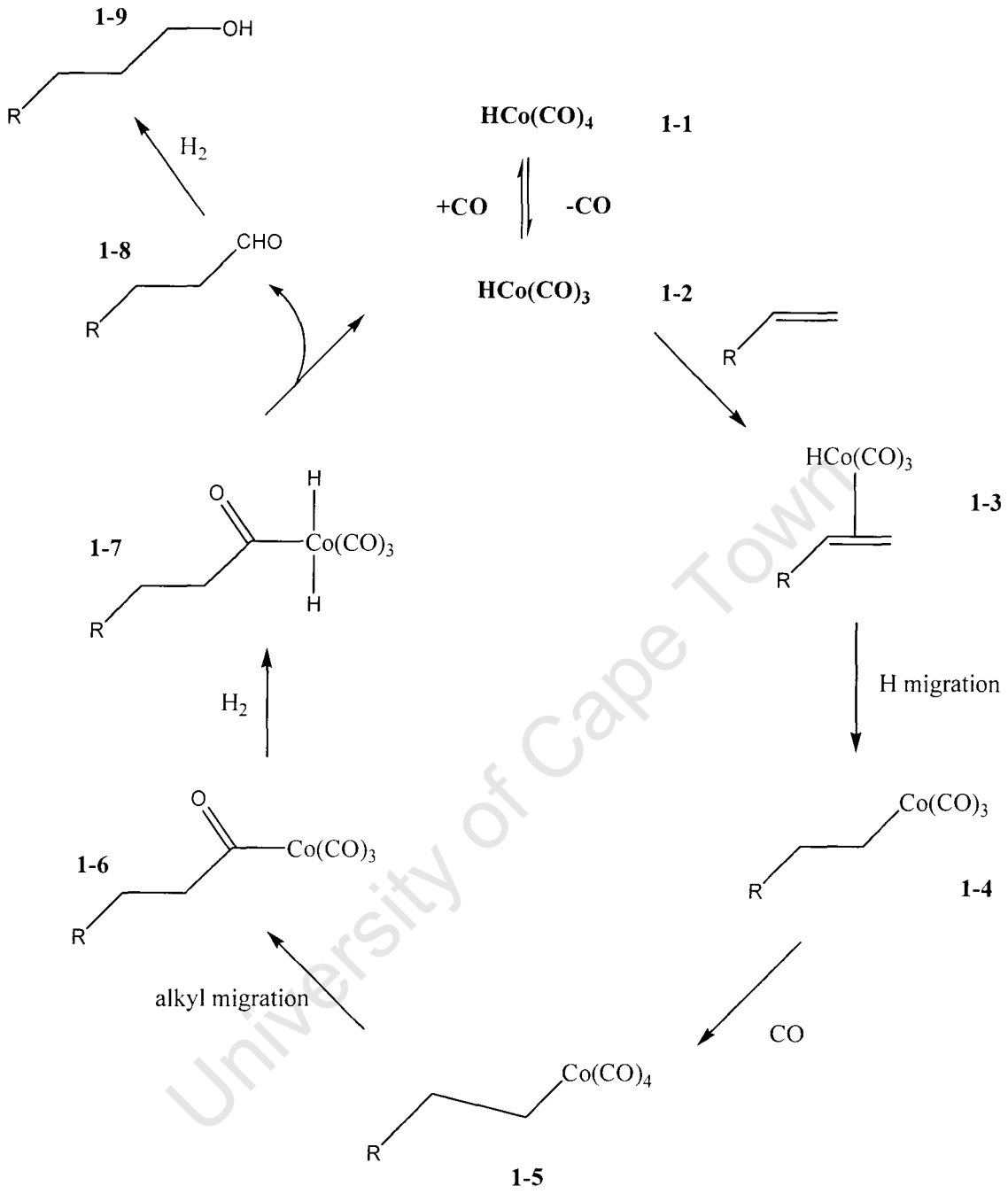

Scheme 1.2: The mechanism of unmodified Co catalyzed hydroformylation.

Scheme 1.3 depicts the mechanism for modified Rh-catalyzed hydroformylation *via* two mechanisms, the associative (A) and the dissociative (B) mechanisms. These were the two plausible pathways according to Wilkinson, who envisaged that the associative mechanism occurs *via* coordination of the alkene to form a six-coordinate Rh species and rapidly converts to a five-coordinate Rh-alkyl species, which is also generated in the dissociative mechanism.[18]

The dissociative mechanism begins in much the same way as the Co-catalyzed reaction does with dissociation of CO and then subsequent coordination of the alkene. Once the Rh-alkyl species has formed as the intermediate in both the dissociative and associative mechanisms, the subsequent catalytic steps are the same. Firstly, there is CO insertion, followed by oxidative addition of hydrogen and then reductive elimination to form the aldehyde product. The final step is coordination of CO to regenerate the active catalyst.

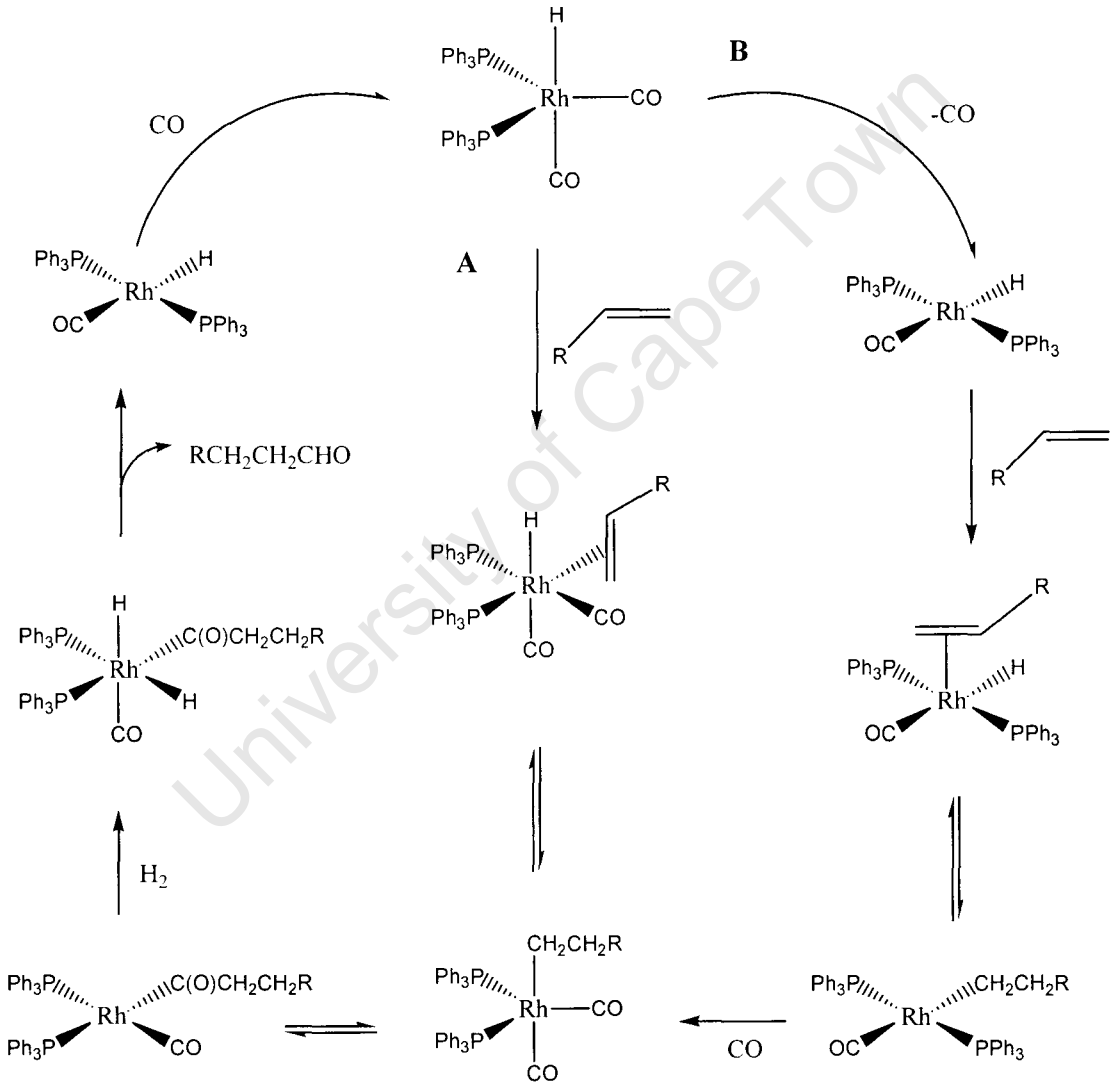

Scheme 1.3: Modified Rh-catalyzed hydroformylation.

The dissociative mechanism is favoured under common industrial operating conditions while the associative mechanism prevails at very high catalyst concentrations. Experimental evidence shows that at lower partial pressure of CO and

higher ligand concentration the environment around the metal centre is more sterically hindered. This results in favoured formation of the linear acyl species and subsequently the linear aldehyde.[19]

1.1.3. Important parameters in hydroformylation

When studying the parameters which define activity and selectivity of a modified Rh or Co catalyst a number of factors including temperature, pressure, catalyst concentration and ligand system play important roles. Thus, in keeping with the versatility of this homogeneous catalysis system, it is possible to fine tune certain parameters to achieve a desired activity or selectivity.

For modified Rh and Co systems, the n:i selectivity is reduced with higher temperatures as a lower concentration of coordinated species is present and the reduced steric congestion around the metal centre results in increased formation of the branched aldehyde.[20] However, higher temperatures are a drawback of modified catalysts as the introduction of phosphine ligands leads to lower activities even though selectivity and thermal stability are increased. Thus, temperatures are increased to counter-balance the reduction in activity.

Lower partial pressures of CO are known to increase n:i selectivity since ligand coordination is more pronounced resulting in increased steric congestion around the metal centre favouring formation of the linear aldehyde.[21] When using modified catalysts a hard and fast rule regarding the effect of changing catalyst concentration has not been established. Rupilius and Tucci both found that increasing catalyst concentration raises conversion of substrate overall but the trends in selectivity achieved were not the same.[22,23] The n:i ratio has been found to increase with an increasing ligand:metal ratio. Increased ligand coordination increases steric congestion around the metal centre leading to increased linear aldehyde formation. Also, coordination of phosphine ligands has shown elevated quantities of alcohol products. The metal-hydrogen bond is more hydridic with phosphine ligands leading to increased hydrogenation products.[11] Shell reported high n:i ratios when alkylphosphine–Co catalysts were used in the hydroformylation of terminal alkenes.[24]

There is no evidence of a specific correlation of ligand system and selectivity but it is accepted that more basic ligands result in higher n:i selectivities, suggesting that ligands may exhibit similar selectivities if their electronic structures are analogous. This is consistent with work of Tucci *et al.* that PPh_3 exhibits lower n:i selectivity than $P(n\text{-}C_4H_9)_3$ in the hydroformylation of 1-hexene with n:i ratios of 62.4 % and 89.6 % respectively.[25]

There has been a steady growth in the production capacities of aldehyde products from hydroformylation. Table 1.3 shows estimates of production capacities from the hydroformylation of ethylene, propene and higher olefins in different regions in 1998.[26]

From the estimates it is clear that C_4 or butanal products made up the largest production capacity and was in most demand with 73 % of total production. Ethylene hydroformylation to C_3 products appeared to be in lowest demand making up only 2 % of total production capacity, joined by the production of larger than C_{13} products at 6 % total capacity. The hydroformylation of olefins of medium chain length were of increasing availability accumulating up to 19 % of total production capacity. Approximately 70 % of C_4/n-butanal capacity was used to form 2-ethylhexanol used in plasticizer production and the increasing demand for this commodity only emphasizes the importance of hydroformylation in the polymer industry.[26]

Table 1.3: Production capacities of aldehydes worldwide.

Region	Capacity (1000 t)[a]			
	C_3[b]	C_4	C_5-C_{13}	>C_{13}
West Europe	25	1600	535	85
East Europe		785		
North America	75	970	450	270
South America		120	55	
East Asia		1040	140	30
% Total	2	73	19	6

[a]Estimates for 1998

[b]Propanal products.

1.2. A review of other metals as hydroformylation catalysts

A number of metal complexes other than those of Co and Rh have been used in the hydroformylation reaction. In principle, any metal atom capable of forming a reactive metal carbonyl hydride species under suitable reaction conditions is a potential hydroformylation catalyst.[11] Modern research is based mainly on four transition metals as catalysts in hydroformylation, namely, Rh, Co, Pt and Ru. The generally accepted order of activity for unmodified monometallic catalysts is: Rh > Co > Ru/Ir > Os > Pt > Pd > Fe > Ni.[27] Pt and Ru catalysts have been studied mainly for academic interest while Co and Rh have been used industrially for many years.[28] The development of metal complexes as the next generation of hydroformylation catalysts is the topic of ongoing research worldwide. The next section reviews some of the metals other than Co and Rh that have been tested as catalysts in the hydroformylation reaction.

1.2.1. Fe catalysts

The complex [Fe(η^6-CHT)(η^4-cod)] (CHT: 1,3,5-cycloheptatriene) was studied in the hydroformylation of 1-hexene under 100 atm syngas (CO/H_2 = 1:1) pressure and 100 °C over 24 h. The selectivity observed was 58 % of the linear aldehyde (heptanal), 38 % of the branched aldehyde (2-methylhexanal) and 4 % of isomerised product 2-hexene.[29]

1.2.2. Ru catalysts

(i) Ruthenium-catalyzed hydroformylation was carried out using 1-hexene and carbon dioxide. The reaction medium was an ionic liquid containing [bmim][Cl + NTf_2] (bmim :1-butyl-3-methylimidazolium cation) and the reaction was carried out without the use of CO or volatile organic solvents. [$Ru_3(CO)_{12}$] (0.1 mmol) was tested in the hydroformylation of 1-hexene (20 mmol) at 160 °C and 40 bar $CO:H_2$ (1:1) for 10 h. The conversion achieved was 94 % and the yield of heptanol an impressive 82 %. The products showed that no linear aldehydes were present and a minimal hydrogenation yield of 8.5 % was achieved. The major product was readily separated by distillation and the reaction medium containing the Ru catalyst recycled for further use.[30]

(ii) Moreno *et al.* showed that ruthenium-carbonyl complexes with 2-substituted pyrazine ligands (pz–R; R = Cl, OMe, SMe, CN, NH_2) exhibit activity in the hydroformylation of 1-hexene at 120 °C and 20 bar syngas pressure. Reactions of $[Ru(CO)_3Cl_2]_2$ with the pyrazines produced the mononuclear compound $[Ru(CO)_3Cl_2(R–pz)]$ (Figure 1.2).[31]

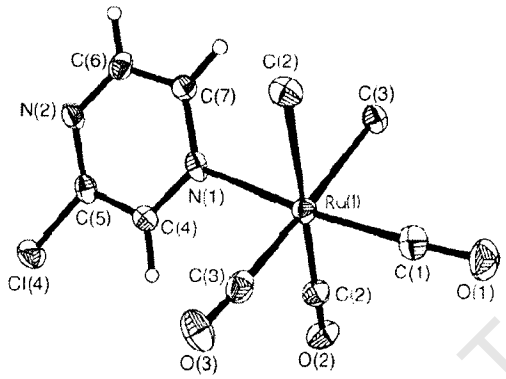

Figure 1.2: Crystal structure of $[Ru(CO)_3Cl_2(2\text{-}Cl–pz)]$[31].

The catalytic activities of all but the amino-pyrazine complexes were found to be higher than the activity of the simple pyrazine $[Ru(CO)_3Cl_2(pz)]$. The trend in activity followed the order of [Ru–(2-Cl–pz)] > [Ru–(2-OMe–pz)] > [Ru–(2-SMe–pz)] > [Ru–(2-CN–pz)] > [Ru–(pz)] > [Ru–(2-NH_2–pz)]. The superior $[Ru(CO)_3Cl_2(2\text{-}Cl\text{-}pz)]$ showed a 72 % yield of hydroformylation products with a total alcohol production of 40 %, of which 26 % was the linear product. The n:i ratio was found to be 1.8.[31]

(iii) The complex $[HRu(CO)(CH_3CN)(TPPTS)_3]BF_4$ (TPPTS = tris[(*m*-sulfonated)phenyl]phosphine P(*m*-$C_6H_4SO_3Na)_3$) was synthesized with the aim of producing a catalyst which is cheaper than Rh, utilizes longer chain olefins and is sulfur tolerant (Figure 1.3).[32]

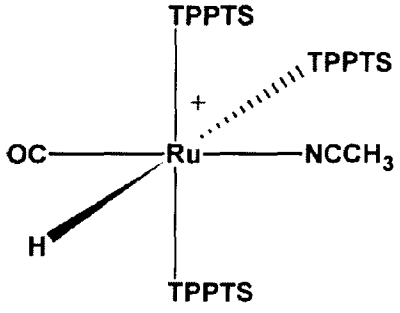

Figure 1.3: Structure proposed for the complex $[HRu(CO)(CH_3CN)(TPPTS)_3]BF_4$.

The aqueous biphasic hydroformylation of 1-hexene catalyzed by $[HRu(CO)(CH_3CN)(TPPTS)_3]BF_4$ was studied and the catalytic performance is summarized in Table 1.4. In a typical experiment, the ruthenium catalyst was added to an aqueous mixture containing the olefin in a water/heptane solution.

Table 1.4: Aqueous biphasic hydroformylation using $[HRu(CO)(CH_3CN)(TPPTS)_3]BF_4$.

Substrate	Product	Product Yield (%)
1-hexene	heptanal	54
	2-methylhexanal	27
	hex-2-ene	20

*P(H_2:CO) = 6288.8 kPa, 353 K, [Subst]/[Cat] = 100, 24 h.

The formation of 2-ethylpentanal was not observed and this was attributed to the fact that the formation of the linear aldehyde must occur faster than the isomerisation to 2-hexene (Scheme 1.4).

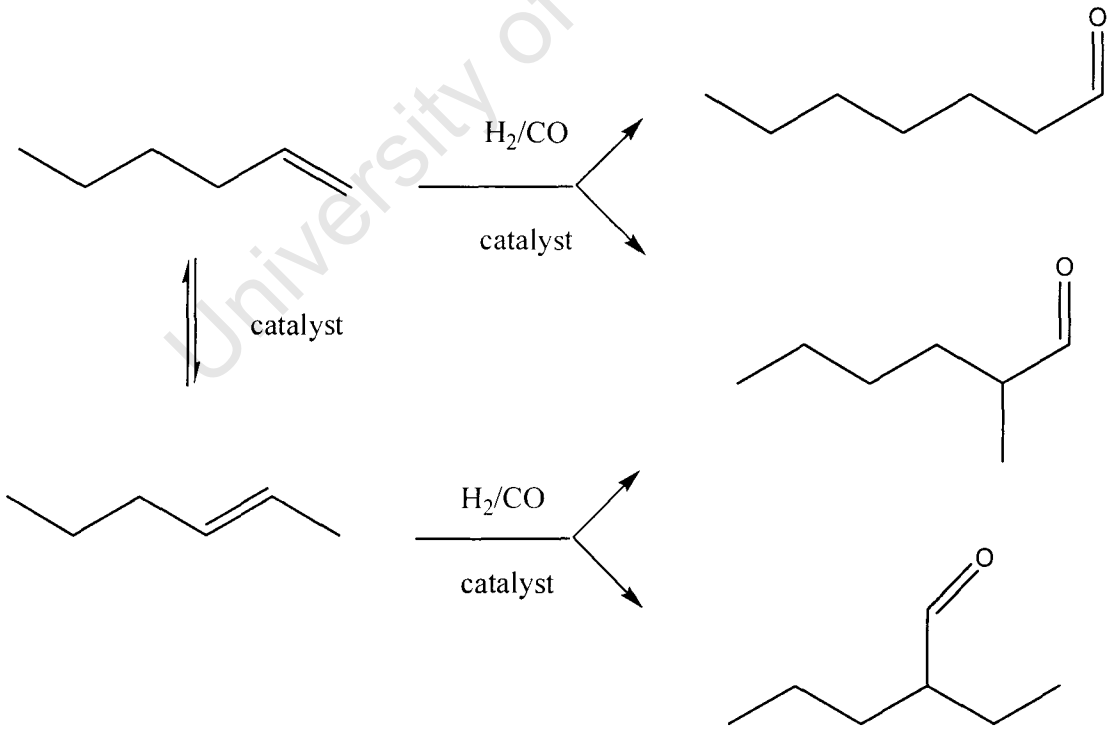

Scheme 1.4: Products from the hydroformylation of 1-hexene.

The trend in catalytic activity with regards to the olefin used was: 1-hexene > allylbenzene > 2,3-dimethyl-1-butene > styrene > cyclohexene. Hydroformylation of

an alkene mixture was performed to simulate the hydroformylation of a C_6 - C_8 cut of naptha. The yield of aldehydes was found to be 82 % and the total conversion of each olefin is shown in Table 1.5.[32]

Table 1.5: Aqueous biphasic hydroformylation using $HRu(CO)(CH_3CN)(TPPTS)_3]BF_4$

Alkene Mixture[a]	Conversion (%)
1-hexene	54
allylbenzene	22
2.3-dimethyl-1-butene	6
styrene	0
cyclohexene	0

[a]Real quantities present in naphtha cuts.

$P(H_2 + CO)$ = 6288.8 kPa, 353 K, Substrate/Catalyst = 100, 24 h.

(iv) The hydroformylation of 1-hexene was studied using rhodium, cobalt and ruthenium complexes consisting of triphenylphosphine, triphenylarsine and triphenylantimony ligands at 80 °C and 60 bar syngas (1:1). There are many factors affecting hydroformylation activity and the σ- and π-character of the particular ligand is an important one. The electronic properties that the ligand possesses will have a significant effect on the intermediates through which the catalytic cycle takes place. Equation 1 describes the ligand association-dissociation equilibrium in this system and shows the hydrido complex produced with an equilibrium shift to the right. This intermediate is inactive in the catalytic cycle.[33]

$$HRu(CO)_n(EPh_3)_m \rightleftharpoons RuH(CO)_n(EPh_3)_{m-1} + EPh_3 \qquad \text{(Eqn 1)}$$

where n = 2, m = 3 and E = P, As or Sb.

The σ-donor and π-acceptor character of the ligand determines the strength of the Ru-EPh_3 bond. Tucci *et al.* reported that the rate of hydroformylation was strongly dependent on the basicity of the ligand and that one of low basic character results in a faster rate of hydroformylation.[25] The order of basicity for the ligands used in this study was $SbPh_3 > PPh_3 > AsPh_3$, thus it was expected that $AsPh_3$ would afford higher reaction rates.[34] The activities resulting from the various ligands were studied in the hydroformylation of 1-hexene. The results are summarized in Table 1.6.

Table 1.6: Hydroformylation of 1-hexene.

Catalyst	Conversion (%)	Selectivity (%)		
		Hydrogenation	Heptanal	n/iso
$[RuCl_2(PPh_3)_3]$	12	60	40	-
$[RuCl_3(AsPh_3)_2CH_3OH]$	23	46	54	-
$[RuCl_2(SbPh_3)_3]$	20	44	56	-
$[RhCl(PPh_3)_3]$	100	0	86	1.0
$[RhCl(AsPh_3)_3]$	100	0	85	0.8
$[RhCl(SbPh_3)_3]$	99	20	68	2.0
$[Co/PPh_3]$	30	0	100	3.1
$[Co/AsPh_3]$	30	0	86	2.6
$[Co/SbPh_3]$	18	4	84	2.9

As expected the conversions and even selectivities using the $AsPh_3$ system were comparable and in some cases higher than its counterparts. One common trend was that complexes containing the $AsPh_3$ ligand consistently produced lower n:i ratios of the aldehyde products under the same reaction conditions. This can be attributed to electronic or steric factors or a synergetic effect of both. The linear aldehyde is formed when anti-Markovnikov addition of the olefin to the hydrido complex $HM(CO)_n(EPh_3)_{m-1}$ takes place. The mode of addition was found to be dependant on the M-H bond as enhanced polarity favoured a Markovnikov addition of the olefin.[35] The ligand $AsPh_3$ with high π-acidity will enhance the polarity of the M-H bond, thus promoting Markovnikov addition and lowering the n:i ratio as is observed in the catalysis.[33]

Interestingly, no branched aldehyde product was observed using the Ru complexes. The results indicated that the trend of activity followed the order of $Ru/AsPh_3 \approx Ru/SbPh_3 > Ru/PPh_3$. Also, it was found that the Ru/PPh_3 complex showed significant hydrogenation and reduced conversion in comparison to its counterparts. This was attributed to the possible formation of $[HRuCl(CO)_2(PPh_3)_2]$ and $[RuCl_2(CO)_2(PPh_3)_2]$ under syngas pressure.[36]

(v) The metal clusters $[Ru_3(CO)_{10}(dcpm)]$ (**1-10**), $[Ru_3(CO)_{10}(F\text{-}dppe)]$ (**1-11**), $[Ru_3(CO)_8(dcpm)_2]$ (**1-12**) and $[Ru_3(CO)_8(F\text{-}dppe)_2]$ (**1-13**) were synthesised from $[Ru_3(CO)_{12}]$ and the bulky diphosphine ligands 1,2-bis[bis(pentafluorophenyl)-phosphino]ethane (F-dppe) and bis(dicyclohexylphosphino)methane (dcpm). Single-crystal X-ray structure analyses of **1-10**, **1-11** and **1-12** showed μ_2-η^2 coordination of the diphosphine ligands, while that of **1-13** consisted of μ_2-η^2 –diphosphine and μ_1-η^2 –diphosphine ligand coordination (Figure 1.4).[37]

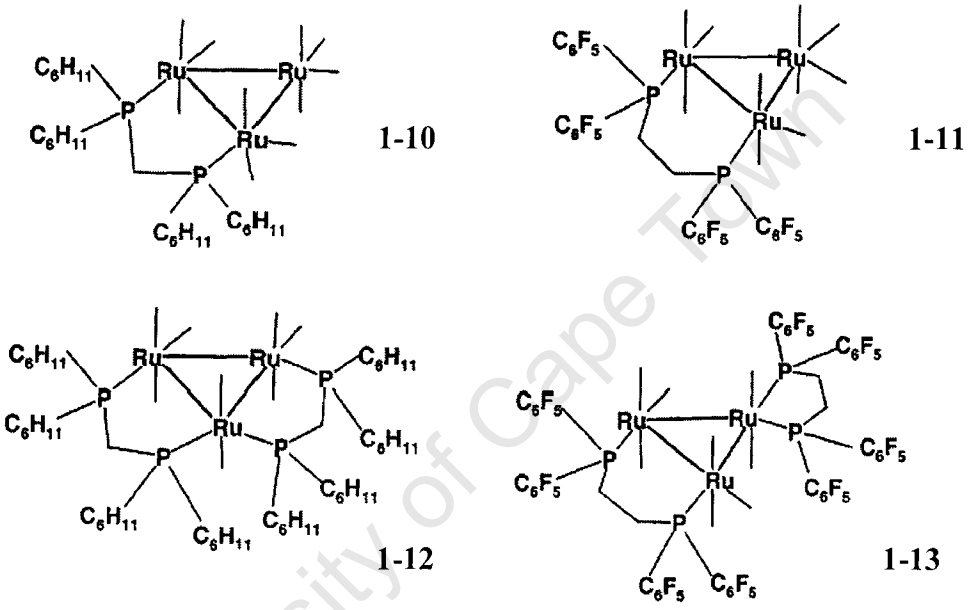

Figure 1.4: Ru complexes tested for their hydroformylation activity.

The clusters **1-10** to **1-13** were tested in the hydroformylation of ethylene and propylene (Table 1.7). The activity of $[Ru_3(CO)_{12}]$ and $[Ru_3(CO)_{10}(dppe)]$ were also studied to infer certain structural details of substituted complexes **1-10** to **1-13** (Table 1.7). Complex **1-10** resulted in better conversion when compared to $[Ru_3(CO)_{12}]$, however it also showed a lower n:i ratio in the hydroformylation of propylene. Complex **1-11** proved more active than **1-10** but achieved this at the expense of its selectivity. Complexes **1-12** and **1-13** showed lower activity but increased selectivity than their mono-substituted counterparts **1-10** and **1-11**. The highest turnover was observed with complex **1-11** with 429 cycles in 24 h in the hydroformylation of ethylene.

Complex **1-11** demonstrated significant activity under the initial conditions and as a result the temperature dependence was studied over the range 50 – 80 °C for 6 h. The

results indicated an exponential increase in catalytic activity with temperature over this range.[37]

Table 1.7: Hydroformylation activity of Ru complexes using ethylene and propylene.

Catalyst*	Ethylene P(bar)	Propylene P(bar)	Turnover	Selectivity (%)
1-10	10	-	274	-
	-	9	130	71/29
1-11	10	-	429	-
	-	9	145	57/41
1-12	10	-	127	-
	-	9	72	83/17
1-13	10	-	143	-
	-	9	130	67/33
$[Ru_3(CO)_{12}]$	10	-	157	-
	-	9	63	85/5
$[Ru_3(CO)_{10}(dppe)]$	10	-	289	-
	-	9	128	63/37

*Conditions: 10 ml dmf, 10 bar CO, 10 bar H_2, 80 °C, 24 h.

Turnover: mol product/mol catalyst, Selectivity: n-propionaldehyde/i-propionaldehyde.

1.2.3. Ir catalysts

(i) Fox *et al.* carried out the hydroformylation of 1-hexene using the Ir complexes $[IrH(CO)_2(XanthPhos)]$, $[IrH_3(CO)(XanthPhos)]$ and the propionyl complex $[Ir(COEt)(CO)_2(XanthPhos)]$ (XanthPhos = 4,5-bis(diphenylphosphino)-9.9-dimethyl-xanthene) (Figure 1.5).[38]

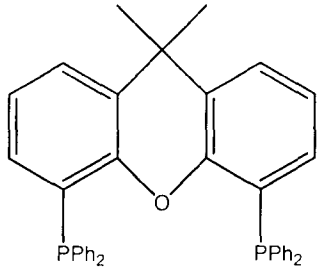

Figure 1.5: XanthPhos

The catalysis was performed at 75 °C under 3 atm of a 2:1 mixture of H_2:CO for 24 h. Low aldehyde yields and modest conversions were achieved. One interesting finding was that complete catalyst inhibition was observed when excess xanthphos was added suggesting that ligand dissociation may have been necessary for catalysis to take place.[38]

(ii) The iridium complexes $[Ir_4(CO)_{12}]$, $[IrCl_3]$, and $[IrCl(CO)_3]$ were used as catalysts in the hydroformylation of 1-hexene at 150 °C under 40 bar $CO:H_2$ (1:1) for 17 h. Inorganic salts such as LiCl, Li_2CO_3, KCl, $CaCl_2$, and LiBr were used as promoters to enhance activity and selectivity by suppressing hydrogenation. The results showed that the activity of the complexes followed the trend $[IrCl_3] < [IrCl(CO)_3] < [Ir_4(CO)_{12}]$. The $[Ir_4(CO)_{12}]$ catalyst was tested in the presence of a LiCl promoter and this resulted in a 25 % yield of 2-methylhexanal and 48 % 1-heptanal.[39]

(iii) The catalyst $[(cod)Ir(OSiMe_3)]_2$ was used as a catalyst in the hydroformylation of the vinylsilane, $Me_3SiCH{=}CH_2$ at 80 °C, 10 atm of H_2/CO (1/1) for 1 h. The major products were aldehydes with yields reaching 100 %. Hydrogenation products were also obtained as a significant quantity of ethylsilane (40 %) was detected.[40]

(iv) Cationic complexes of the type $[M(cod)(PPh_3)_2]PF_6$ (M = Rh or Ir) were used in the hydroformylation of 1-hexene at 60 °C and 100 °C for Rh and Ir respectively. The pressure of syngas used was in the range of 2 to 5 bar. The n:i ratio of the aldehyde products observed varied between 3.0 and 3.7 for Rh and approximately 2.0 for Ir.[41]

1.2.4. Pd catalysts

(i) Halide anion-promoted palladium-catalyzed hydroformylation has shown impressive selectivity towards linear alcohols using internal alkenes. The complex $[(bcope)Pd(OTf)_2]$, where bcope = bis(cyclooctyl)phosphinoethane, proved an effective catalyst in the hydroformylation of an equilibrated mixture of internal C_8-C_{10} alkenes (12 % C_8, 44% C_9, and 44 % C_{10}) at 105 °C under 60 bar $CO:H_2$ = 1:1. Hydrogenation products found were less than 1 % while 99 % of the products formed were alcohols of which 72 % was the linear alcohol.[42]

(ii) Drent *et al.* have reported catalyst systems consisting of a palladium(II)-diphosphine system using weakly or non-coordinating counterions. These catalysts were found to be highly active in the hydrocarbonylation of both aliphatic and functionalized olefins. Numerous experiments were carried out using various ligand, anion and solvent combinations to establish a reaction system that would promote substantial aldehyde and alcohol yields. The complexes were formed *via* a ligand complexation/anion displacement reaction using a bidentate ligand (L_2) and an acid containing the anion (X^-) (Equation 2).[43]

$$L_2 + Pd(OAc)_2 + 2HX \rightarrow L_2PdX_2 + 2HOAc \qquad \text{(Eqn 2)}$$

The hydroformylation of propene using $Pd(OAc)_2$ and the ligand DsBPP {(*sec*-Bu)$_2$ P(CH$_2$)$_3$P(*sec*-Bu)$_2$} in the presence of trifluoroacetic acid (CF_3COOH) at 125 °C and 30 bar syngas produced a turnover frequency of 500 (mol product /mol reactant / h) with 84 % linear aldehyde selectivity.[43]

(iii) In a later study, Drent *et al.* carried out the hydroformylation of terminal alkenes using Pd(II) acetate, an anion source and a diphosphine ligand. Results of catalytic performance are summarised in Table 1.8.[44]

Table 1.8: Pd(II)acetate catalyzed hydroformylation of 1-octene.

Ligand	Acid (mmol)	T (°C)	Turnover	Alcohol (linear) (%)
BPBE*	MSA(1) /HCl(0.2)	120	1380	>99 (68)
BPBE	MSA(0.5) / HCl(0.1)	120	920	>99 (65)
BPBE	FSA(0.5) / HCl(0.2)	110	680	>99 (72)
BPBE	MSA(0.5)	120	156	75 (63)
BPBU	MSA(0.5) / HCl(0.1)	105	119	75 (58)

*BPBE: 1, 2-PP'bis(9-phosphabicyclo[3.3.1]nonyl)benzene,

BPBU: 2, 3-PP'bis(9-phosphabicyclo[3.3.1]nonyl)butane,

MSA: Methane sulfonic acid,

FSA: Trifluoromethane sulfonic acid.

Turnover: mol product/(mol Pd/h)

Conditions: 20 ml substrate, 0.4 mmol 1-octene, 20 bar CO, 40 bar H_2, reaction time 5 h.

The highest turnover was obtained when BPBE was used and resulted in moderate formation of the linear alcohol product (68 %) using 1-octene. Less than 1 % hydrogenation products were obtained. The effect of the acid on hydroformylation activity was also studied and the trend observed indicated that the turnover was reduced considerably when the reaction quantity of MSA and HCl was reduced.[44]

1.2.5. Pt catalysts

(i) [$PtCl_2$(diphosphine)] complexes were used in the hydroformylation of styrene where *in situ* catalysts were formed using tin(II) chloride and silver/tin(II) triflate. The linear and branched regioisomers achiral 3-phenyl-propanal and chiral 2-phenyl-propanal were produced. When the optically active Pt-bdpp (bdpp = (2S,4S)-2,4-bis(diphenylphosphino)pentane) was used, high enantiomeric excess (ee-s) was achieved. However, ee-s were lowered significantly in the presence of triflate anion.

The addition of silver triflate resulted in a reduction in catalytic activity and a further excess resulted in completely inactive systems. However, this diminished activity also brought about a greater regioselectivity with both achiral and chiral catalysts. The hydroformylation of styrene using platinum-phosphine-tin(II)chloride in the presence of tin(II)triflate resulted in subsequent hydrogenation of the aldehyde products.[45]

(ii) The hydroformylation of methyl 3-pentenoate (M3P) (Fig 1.6) using Pt/Sn catalyst systems modified with diphosphine ligands were studied by Meessen and co-workers. Specifically, the regioselective formation of 5-formyl methyl pentanoate (5-FMP) was targeted (Fig 1.6). Heteroaromatic xanthene-type hydrocarbons were employed as the ligands as they possess a large bite angle combined with a rigid backbone.

Figure 1.6: Structures of M3P and 5-FMP.

The modified catalysts showed high regioselectivity towards the linear aldehyde and hydrogenation of the substrate and products were largely suppressed (Table 1.9). The findings reiterated the fact that catalytic activity and selectivity are controlled by both the bite angle and backbone rigidity of the ligands.[46]

Table 1.9: Hydroformylation of M3P catalyzed by $[L_2PtCl_2]/SnCl_2$.

Complex	Time (h)	Conversion (%)	TOF (h^{-1})	n/iso ratio
$[PtCl_2(PPh_3)_2]$	2	18	45	0.7
$[PtCl_2(dppe)]$	16	32	11	1.8
$[PtCl_2(dppp)]$	16	95	31	0.5
$[PtCl_2(thixanthphos)]$	16	66	22	3.2

*PPh_3: Triphenylphosphine,

dppe: 1,2-bis(diphenylphosphino)ethane,

dppp: 1,3-bis(diphenylphosphino)propane,

thixanthphos: 2,8-dimethyl-4,6-bis(diphenylphosphino)phenoxathiin.

Conditions: 25 bar CO/H_2, 120 °C.

(iii) Platinum(II) catalyzed hydroformylation in the presence of a $SnCl_2$ co-catalyst has been extensively studied due to the high regioselectivity toward the linear aldehyde observed in such systems. The platinum/tin system is particularly useful in asymmetric reactions where high stereoselectivity is prevalent.[47]

The $[PtCl_2(diphosphine)]/SnCl_2$ catalyzed hydroformylation of (-)-β-pinene, *R*-(+)-limonene and (-)-camphene was studied using dppp, dppe and dppb (1,4-bis(diphenylphosphino)butane) diphosphine sytems. The catalysts showed high regioselectivity towards the linear aldehyde product. The hydroformylation of β-pinene produced *trans*-10-formylpinane with a 98 % diastereoisomeric excess (d.e.), while limonene and camphene produced diastereoisomers in approximately equivalent quantities of 10 and 15 % d.e. respectively.[47]

Previous studies in hydroformylation have emphasised the strong synergetic effect of $SnCl_2$ and Pt(II). Studies using the $[PtCl(SnCl_3)(PPh_3)_2]$ precursor suggested that the Pt–$SnCl_3$ fragment is involved in the formation of intermediates such as hydride,

alkyl and acyl platinum complexes formed in the catalytic reaction.[48-50] The $SnCl_3^-$ ligand removes electron density away from the platinum centre due to its high π-acceptor ability and in turn enhances coordination of the olefin while inhibiting the reduction of Pt.[51] Subsequently, the strong *trans*-activation effect of the $SnCl_3^-$ ligand contributes favourably to the ligand-exchange reactions necessary for catalytic activity.[52] Studies suggest that the catalytic cycle proceeds *via* a penta-coordinated Pt(II) species which facilitates olefin insertion into a Pt–H bond via a trigonal bipyramidal species. The $SnCl_3^-$ ligand stabilizes this intermediate and decreases the activation energies of both the olefin insertion and hydrogenolysis reactions.[53]

(iv) Platinum-catalyzed hydroformylation of functionalized and non-functionalized olefins was carried out using room temperature chlorostannate ionic liquids (salts that melt at ambient temperature). The Pt catalyst was activated due to the Lewis-acidity of the ionic liquids and versatility in the functional groups of the substrate.

The catalyst precursor $[PtCl_2(PPh_3)_2]$ dissolved in either 1-butyl-3-methylimidazolium chloride (BMIM Cl) or 1-butyl-4-methylpyridinium chloride (4-MBP Cl) was tested in the in the hydroformylation of methyl-3-pentenoate (M3P) at 120 °C and 50 bar (CO/H_2) for 2 h. The catalyst demonstrated enhanced stability and selectivity when compared to the identical reaction in conventional organic solvents such as CH_2Cl_2 (Table 1.10). This finding was attributed to the fact that the catalyst experiences increased lifetimes in the chlorostannate liquid but is deactivated in CH_2Cl_2.[54]

Table 1.10: Hydroformylation of M3P catalyzed by $[PtCl_2(PPh_3)_2]$

Solvent	Conversion (%)	TOF (h^{-1})	5-FMP (%)
(4-MBP Cl)/$SnCl_2$	5.4	31	56.5
(BMIM Cl)/$SnCl_2$	6.3	37	56.5
CH_2Cl_2	1.5	9	44.4

*Conditions: 50 bar (CO/H_2), T = 120 °C, 2 h., 5-FMP = amt 5-FMP / amt of all products.

The hydroformylation of 1-octene using the biphasic reaction system resulted in low reaction rates in all systems and this was attributed to poor olefin solubility in water. However, high selectivity toward the linear aldehyde was maintained. The reaction in

CH_2Cl_2 produced elevated reaction rates as well as selectivity when compared to the reactions in the chlorostannate ionic liquids (Table 1.11).[54]

Table 1.11: Hydroformylation of 1-octene catalyzed by $[PtCl_2(PPh_3)_2]$.

Solvent	Conversion (%)	TOF (h^{-1})	n-nonanal (%)
(4-MBP Cl)/$SnCl_2$	19.7	103	96.0
(BMIM Cl)/$SnCl_2$	22.3	126	95.0
CH_2Cl_2	25.7	140	98.3

*Conditions: 50 bar (CO/H_2), T = 120 °C, 2 h.

n-nonanal = amt n-nonanal / amt of all products.

(v) The hydroformylation of styrene was studied using using platinum(II) complexes modified with the diphosphine ligand xanthphos. The ligand consisted of a large bite angle and was isolated as a parent complex [*cis*-$PtCl_2$(xanthphos)] as well as a square planar *trans*-chelating complex *trans*-$PtCl_2$(xanthphos). The system was studied using $SnCl_2$ as a co-catalyst and a significant finding was the high chemo- and regioselectivities obtained of up to 99.8 % and 88 % respectively.[55]

(vi) Marteel *et al.* used platinum–phosphine complexes anchored on silica and mesoporous MCM-41 supports in the hydroformylation of 1-hexene at 100 °C in supercritical carbon dioxide (pressure = 2700 psi).[56] The co-catalyst used was $SnCl_2 \cdot 2H_2O$ (Sn:Pt = 3.5:1). Hydrogenation was completely inhibited and high regioselectivity toward heptanal was observed.[56]

(vii) Illner *et al.* studied the kinetics of the formation of [*cis*-$Pt(PPh_3)_2Cl(SnCl_3)$] and [*cis*-$Pt(PPh_3)_2(SnCl_3)_2$] from the hydroformylation catalyst precursor [*cis*-$Pt(PPh_3)_2Cl_2$] in the presence of co-catalyst $SnCl_2$ (Scheme 1.5). The study was conducted in two imidazolium-based ionic liquids. Various chlorostannate melts consisting of 1-butyl-3-methyl-imidazolium cations and Sn anions with varying molar fraction of $SnCl_2$ were prepared and characterized by ^1H and ^{119}Sn NMR. The study suggested that formation of $[Pt(PPh_3)_2Cl(SnCl_3)]$ in chlorostannate melts with a greater then equimolar composition of $SnCl_2$ proceeds *via* insertion of $SnCl_2$ in a Pt–Cl bond.[57]

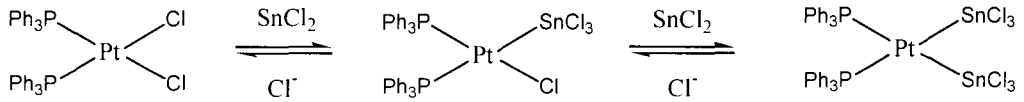

Scheme 1.5: Formation of the catalytically active species on addition of $SnCl_2$ to [*cis*-$PtCl_2(PPh_3)_2$].

(viii) The molecular structure and spectroscopic data for [$PtCl_2$(Sixantphos)] was described in studies conducted by van Duren and co-workers.[58] The hydroformylation of 1-octene and internal octenes was carried out at various temperatures and 40 bar syngas. UV/Vis-spectroscopy was used to identify the rapid formation of the Pt–stannate species upon addition of $SnCl_2$ (Scheme 1.6). High-pressure *in situ* IR-spectroscopy was used to identify formation of the Pt–CO species and a short-lived Pt–H species under syngas. Complex **1-14** was used in the hydroformylation of 1-octene and the catalytic performance with increasing temperature is shown in Table 1.12.[58]

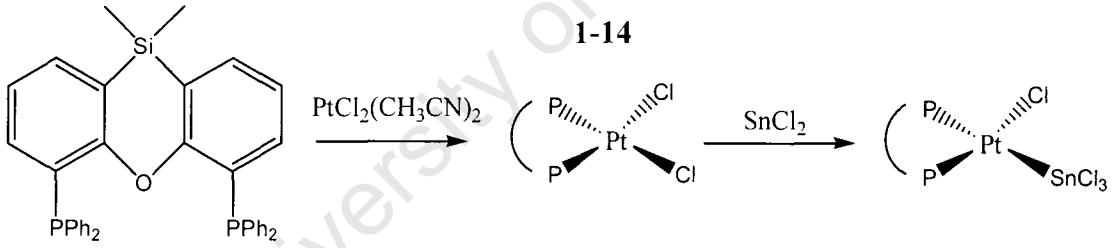

Scheme 1.6: Complexation of Sixantphos to Pt(II) species **1-14** and subsequent generation of the Pt/Sn-precatalyst by reaction with $SnCl_2$.

Table 1.12: Hydroformylation of 1-octene catalyzed by Pt species **1-14**.

Temp (°C)	Time (h)	Conversion (%)	TOF (h^{-1})	n/iso ratio
90	0.3	1060	72	39
100	0.2	1228	50	22
110	0.1	2533	36	23
120	0.1	4356	25	21

Conditions: CO/H_2 (1:1) = 40 bar, CH_2Cl_2.

The highest turnover frequency as well as n:i ratio was obtained at 90 °C, while superior conversion was obtained at 120 °C. The data obtained was used to create an Eyring plot (ln TOF vs T^{-1}) at the various reaction temperatures. Two different linear regions were apparent on this plot suggesting that the rate determining step is not the same at low and high temperatures. Hydrogenolysis of the acyl complex is the rate limiting step at high temperatures while alkene coordination is believed be the rate limiting step at lower temperatures. This agrees with previous work that showed a temperature dependence on the rate of alkene insertion.[46,59]

(ix) XanthPhos has been widely used as a diphosphine ligand in Pt catalyzed hydroformylation mainly due to its large bite angle. Xantarsine and xantphoarsine ligands (**1-16** and **1-17**) were used in a wide bite angle study to observe catalytic efficiency of terminal olefins under hydroformylation conditions (Figure 1.7). Table 1.13 summarizes the catalytic performances observed.[60]

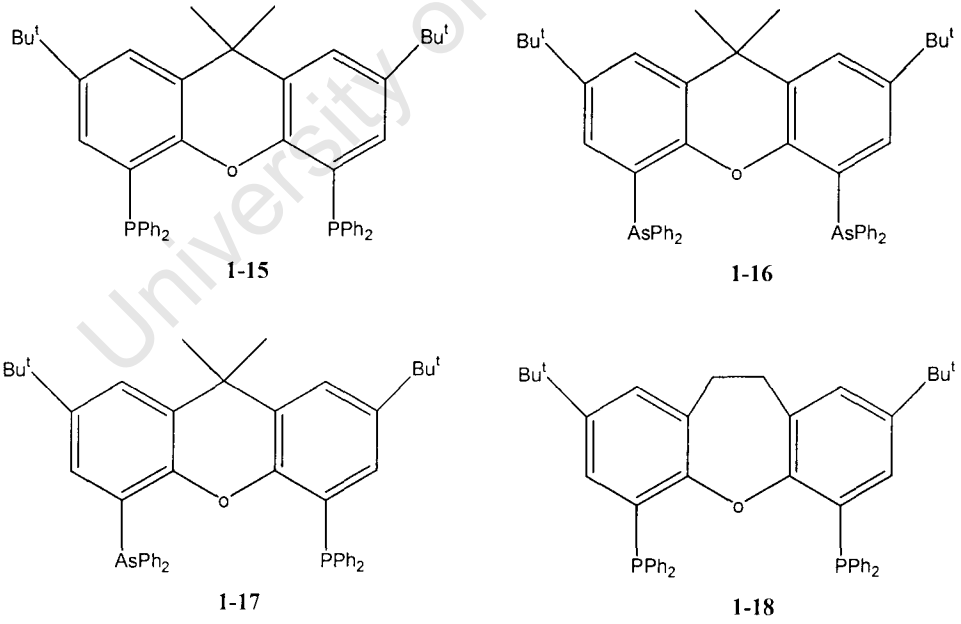

Figure 1.7: XanthPhos modified ligands used in Pt/Sn catalyzed hydroformylation.

Table 1.13: Pt/Sn catalyzed hydroformylation of 1-octene.

Ligand	n:i ratio	TOF*	n-Nonanal (%)	Isomerisation (%)
1-15	230	18	95	4.5
1-16	>250	210	92	8.0
1-17	200	350	96	3.1
1-18	>250	720	88	12

*Conditions: 60 °C under 40 bar of $CO:H_2$ (1:1), Turnover frequencies (TOF) (mol of aldehyde/mol Pt/h) at 20–30 % conversion.

The bite angle of ligands **1-15**, **1-16**, **1-17** and **1-18** are 110, 113, 111 and 102° respectively.[61] Results revealed that decreasing the bite angle increased the rate of reaction significantly. This was apparent when ligand **1-18** showed superior activity when compared to its counterparts. However, this is accompanied by a considerable increase in isomerisation and a decline in selectivity toward the linear aldehyde.

Ligands **1-16** and **1-17** were highly efficient in the hydroformylation of 1-octene. The xantarsine ligand **1-16** was less selective for the linear aldehyde than its xanthphos counterpart **1-15** but more than 10 times as active. The xantphoarsine ligand **1-17** was more then 20 times as active as xanthphos but showed the same excellent selectivity.

The rationale behind the effect of the bite angle remains that the wide angle increases steric crowding around the platinum centre resulting in formation of the sterically less hindered linear aldehyde product. The significant finding of this study was that arsine based platinum/tin catalyst systems are capable of competing with rhodium catalysts when considering catalytic performance in hydroformylation.[57]

(x) Platinum complexes containing the monodentate ligands *o*-1, *m*-1, *p*-1 (Figure 1.8) were tested in the hydroformylation of 1-butene.

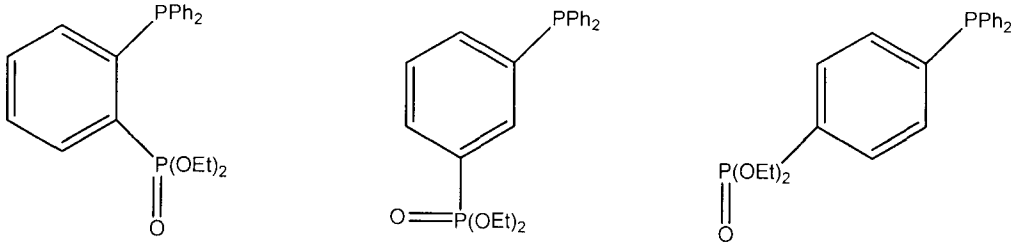

o-1 *m*-1 *p*-1

Figure 1.8: Platinum complexes containing monodentate ligands.

The complex featuring ligand *o*-1 was isolated in a *trans* configuration while those featuring ligands *m*-1 and *p*-1 were *cis* (Figure 1.8). This was attributed to the greater bulk associated with *o*-1. The conversion and activity achieved followed the order ***p*-1** > PPh_3 ≈ ***m*-1** > ***o*-1** (Table 1.14). The low activity of ***o*-1** was attributed to the steric hinderance brought about by the bulkiness of the ligand. Also, the effect of P=O coordination on overall activity could not be ruled out. The superior efficiency of ***p*-1** was suspected to be a function of the electron-withdrawing effect resulting from the phosphonate group in the *para* position.[62]

Table 1.14: Pt(II) catalyzed hydroformylation of 1-butene.

Ligand	Conversion (%)	n:i	TOF
PPh_3	60	6.3	213
o-1	13	2.5	48
m-1	47	3.0	94
p-1	91	6.8	272

*Conditions: 80 bar CO/H_2, 120 °C.

(xi) Knifton *et al.* studied the synthesis of alkyl primary amines from α-olefins, syngas and ammonia. The initial hydroformylation step prior to reductive amination to form the desired amine included the hydroformylation of 1-heptene using a $[PtX_2(PPh_3)_2]$/ SnX_2 (X = Cl, Br, I) co-catalyst system. The results obtained which are summarised in Table 1.15, indicated that the $[PtCl_2(PPh_3)_2]/SnCl_2$ system proved to be the most efficient at achieving excellent conversion as well as selectivity toward the linear aldehyde.[63]

Table 1.15: Pt(II) catalyzed hydroformylation of 1-heptene.[63]

Catalyst	Conversion (%)	Octanal (%)	n-Octanal (%)
$[PtCl_2(PPh_3)_2]/SnCl_2$	100	85	90
$[PtBr_2(PPh_3)_2]/SnBr_2$	100	64	85
$[PtI_2(PPh_3)_2]/SnI_2$	< 2	0.6	-

*Conditions: 103 bar CO/H_2, 66 °C, 3h.

(xii) Lofu *et al.* performed the hydroformylation of 1-octene using platinum complexes of the general formula $[\kappa^2P,S\text{-}(dppmS)Pt(CH_3)(Cl)]$ (**1-19**), $[\kappa^2P,S\text{-}(dppeS)Pt(CH_3)(Cl)]$ (**1-20**) and $[\kappa^2P,S\text{-}(dpppS)\text{-}Pt(CH_3)(Cl)]$ (**1-21**) (dppmS = $Ph_2PCH_2P(S)Ph_2$, dppeS = $Ph_2P(CH_2)_2P(S)Ph_2$ dpppS = $Ph_2P(CH_2)_3P(S)Ph_2$) (Figure 1.9). The order of reactivity was found to be **1-21** > **1-20** > **1-19** (Table 1.16).[64]

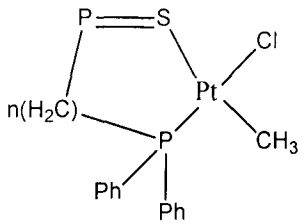

Figure 1.9: Platinum complexes **1-19** (n = 1), **1-20** (n = 2), **1-21** (n = 3).

Table 1.16: Pt(II) catalyzed hydroformylation of 1-octene.

Complex	Conversion (%)	Aldehydes (%)	TOF (h^{-1})
1-19	63	25	6
1-20	100	56	16
1-21	100	60	48

*Conditions: 25 bar CO/H_2, 80 °C, 1-5 h.

Results indicated that increasing the size of the ring in the chelating ligand increased both activity and selectivity and agreed with previous observations.[65] The effect of a larger metallacycle has previously been reported to assist in lowering the activation energy of the hydrogenolysis step in the catalytic cycle.[66,67]

1.2.6. Fe/Rh catalysts

The cluster $[PPh_4][Fe_5RhC(CO)_{16}]$ was used in the hydroformylation of 1-pentene at 100 °C and 60 atm syngas. The reaction produced both $[Fe_4Rh_2C(CO)_{16}]$ and $[PPh_4][Fe_3Rh_3C(CO)_{15}]$.

The structure of $[PPh_4][Fe_3Rh_3C(CO)_{15}]$ was found to consist of an octahedral cluster anion with the three rhodium and the three iron atoms in *fac* positions. The encapsulated carbido-carbon atom is octahedrally coordinated to the six metal atoms. The cluster was used in the hydroformylation of 1-pentene and resulted in a 1:1 mixture of hexanal and 2-methylpentanal after 5 h. Also, trace amounts of the hydrogenated substrate were detected. The n:i ratio was found to be 2.5:1 and this ratio decreased as the conversion of pentene increased.[68]

1.2.7. Mn/Rh

(i) The hydroformylation of 3,3-dimethylbut-1-ene was performed using unmodified rhodium and manganese carbonyls at T = 298 K and 1.0-4.0 MPa CO/ 0.5-2.0 MPa H_2. The reaction underwent a dramatic increase in rate when both metals were used simultaneously. $[RCORh(CO)_4]$, $[Rh_4(CO)_{12}]$, $[Rh_6(CO)_{16}]$, $[HMn(CO)_5]$ and $[Mn_2(CO)_{10}]$ species were detected during the reaction and characterized using *in-situ* FT-IR spectroscopy. The kinetics of product formation show a distinct linear-bilinear form in observables: $k_1[RCORh(CO)_4][CO]^{-1}[H_2] + k_2[RCORh(CO)_4]-[HMn(CO)_5][CO]^{-1.5}$, where the first term represents the classic unicyclic rhodium catalysis and the second a hydride attack on an acyl species. The results obtained from the characterization and kinetic studies suggested that the synergetic effect is a result of bimetallic catalytic binuclear elimination and not cluster catalysis.[69]

(ii) The hydroformylation of styrene at 60 °C and 2.0 MPa of CO/H_2 (1:1) was carried out using the cluster $[\mu^3\text{-}CC_6H_5)(\mu\text{-}CC_6H_5)Rh_2Mn_2Cp_2(\mu\text{-}CO)_3(CO)_3]$ (**1-22**) (Figure 1.10). This compound was produced by reacting a cationic carbyne complex $[Cp(CO)_2Mn{\equiv}CC_6H_5]BBr_4$ with $PPN[Rh(CO)_4]$. Complete conversion (100 %) was achieved within 4 h and a mixture of 3-phenylpropanal and 2-phenylpropanal products were detected with an n:i ratio of approximately 1:0.07. [70]

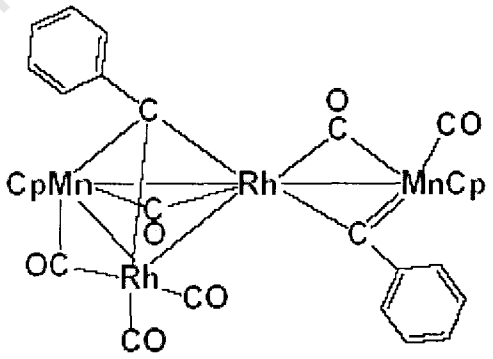

Figure 1.10: $[\mu^3\text{-}CC_6H_5)(\mu\text{-}CC_6H_5)\ Rh_2Mn_2Cp_2(\mu\text{-}CO)_3(CO)_3\ ]$ (**1-22**).

1.3. Conclusion

Rh and Co catalysts have been extensively studied and much of their mechanistic detail has already been uncovered.[14,18] Other metal catalysts have not been able to compete with the efficiency of Co and Rh as industrially viable hydroformylation catalysts.[28]

Platinum catalysts have been the subject of growing interest in recent years, especially in asymmetric hydroformylation.[71] Platinum catalysts modified with phosphine ligands in the presence of Lewis acids were found to achieve high activities and elevated selectivities toward the linear aldehyde. The role of the Lewis acid such as $SnCl_2$ is to be the co-catalyst, promoting olefin coordination, CO insertion and hydrogenolysis.[72] One of the primary objectives in this field of research would now be identifying a Pt catalyst that exhibits the desired activity and selectivity at mild reactions conditions with the least prevalence of unwanted by-products.

1.4. Scope of thesis

From the literature review in **Chapter 1**, it is clear that there are a number of metal catalysts capable of achieving good activity and selectivity in the hydroformylation reaction. Specifically, Pd and Pt catalysts containing bidentate ligands have demonstrated good activity and selectivity. Therefore, we have synthesized a series of Pd and Pt complexes containing bidentate ligands and further employed the Pt complexes in the hydroformylation of 1-octene.

The synthesis and characterization of the compounds prepared are discussed in **Chapter 2**. The complexes containing aminodiphosphine ligands have not been previously tested as hydroformylation catalysts and those containing alkyldiphosphine ligands were used to compare relative catalytic activity. The results obtained from the catalytic testing are discussed in **Chapter 3. Chapter 4** describes all experimental details.

1.5. References

1. B. Cornils, W. A. Herrman, *Applied Homogeneous Catalysis with Organometallic Compounds*, Vol. 1, VCH Publishers, New York, 1996, pp 29-33.
2. O. Roelen, *Chemische Verwertungsgesellschaft Oberhausen m.b.H*, DE 849.548, 1938/1952, US 2.327.066, 1943.
3. H. Adkins, G. Krsek, *J. Am. Chem. Soc.*, 1948, **70**, 383.
4. P. Sabatier, *Die Katalyse in der Organischen Chemie*, Akademische Verlagsgesellschaft, Liepzig, 1927, **8**.
5. H. H. Storch, N. Golumbic, R. B. Anderson, *The Fischer-Tropsch and Related Syntheses*, Wiley, Chapman and Hall, New York, London, 1951, 441.
6. J. Berty, L. Marko, *Acta Chim. Aca. Sci. Hung.*, 1953, **3**, 177.
7. G. Natta, *Brennst. Chem.*, 1955, **36**, 176.
8. B. Cornils, J. Falbe, *4th Int. Symp. Homogeneous Catalysis*, Leningrad, 1984, 487.
9. W. Keim, *Chem. Ing. Tech.*, 1984, **56**, 850.
10. B. Cornils, W. A. Herrman, *Applied Homogeneous Catalysis with Organometallic Compounds 2nd ed.*, Wiley-VCH, Weinheim, 2002, pp 29-33.
11. B. Cornils, J. Falbe, *New Syntheses with Carbon Monoxide*, Springer, Berlin, 1980, Chapter 1.
12. *Celanese Corp. Annual Business Report*, 1974, 9.
13. M. Schreuder-Goedheijt, P. C. J. Kamer, P. W. N. M van Leeuwen, *J. Mol.Catal.*, 1998, **134**, 243.
14. D. S. Breslow, R. F. Heck, *Chem. Ind. (London)*, 1960, 467.
15. J. A. Godfrey, R. A. Searles, *Chemie-Technik*, 1981, **10**, 1271.
16. B. Cornils, L. Marko, *Methoden Org. Chem. (Houben-Weyl) 4th Ed*, 1986, Vol **E18**, 759.
17. J. Gauthier-Lafaye, R. Perron, *LActualite Chimique*, *Mars/Avril*, 1989, 49.
18. D. Evans, J. A. Osborn, G. Wilkinson, *J. Chem. Soc. (A)*, 1968, 3133.
19. R. L. Pruett, *Adv. Organomet. Chem.*, 1979, **17**, 1.
20. B. Cornils, J. Falbe, H. Tummes, *Chem. Zig.*, 1973, **97**, 368.
21. F. Piacenti, M. Bianchi, E. Benedetti, P. Frediani, *J. Organomet. Chem.*, 1970, **23**, 257.
22. W. Rupilius, J. J. Mcoy, M. Orchin, *Ind. Eng. Chem., Prod. Res. Dev.*, 1971, **10**, 142.

23. E. R. Tucci, *Ind. Eng. Chem., Prod. Res. Dev.*, 1968, **7**, 32.
24. L. H. Slaugh, R. D. Mullineaux , Shell Oil, 1996, US 3.239.569.
25. E. R. Tucci, *Ind. Eng. Chem., Prod. Res. Dev.*, 1971, **9**, 516.
26. B. Cornils, H. W. Bohnen, *Adv. Catalysis*, 2002, **2**, 121.
27. F. P. Pruchnik, *Organometallic Chemistry of Transition Metals*, Plenum Press, New York, 1990, 691.
28. H. Bahrmann, H. Bach, *Ullman's Encycl. Ind. Chem., 5th Ed.*, 1991, **A18**, 321.
29. C. Breschi, L. Piparo, P. Pertici , A. M. Caporusso and G. Vitulli, *J. Organomet. Chem.*, 2000, **607**, 57.
30. K. Tominaga, *Catal. Today*, 2006, **115**, 70.
31. M. A. Moreno, M. Haukka, A. Turunen, T. A. Pakkanen, *J. Mol. Catal. A: Chem.*, 2005, **240**, 7.
32. P. J. Baricelli, K. Segovia, E. Lujano, M. Modrono-Alonso, F. López-Linares, R. A. Sánchez-Delgado, *J. Mol. Catal. A: Chem.*, 2006, **252**, 70.
33. V. K. Srivastava, R. S. Shukla, H. C. Bajaj, R. V. Jasra, *Applied Catalysis A: General*, 2005, **282**, 31.
34. N. Kuznik, O. F. Wendt, *J. Chem. Soc., Dalton Trans.*, 2002, 3074.
35. D. Evans, J. A. Osborn, G. Wilkinson, *J. Chem. Soc. (A),* 1968, 3133.
36. V. K. Srivastava, R. S. Shukla, H. C. Bajaj, R. V. Jasra, *J. Mol. Catal. A: Chem.*, 2003, **202**, 65.
37. E. L. Diz, A. Neels, H. Stoeckli-Evans, G. Süss-Fink, *Polyhedron*, 2001, **20**, 2771.
38. D. J. Fox, S. B. Duckett, C. Flaschenriem, W. W. Brennessel, J. Schneider, A. Gunay, R. Eisenberg, *Inorg. Chem.*, 2006, **45**, 7197.
39. M. A. Moreno, M. Haukka, A. Pakkanen, *J. Catal.*, 2003, **215**, 326.
40. E. Mieczynska, A. M. Trzeciak, J. J. Ziolkowski, I. Kownacki, B. Marciniec, *J. Mol. Catal. A: Chem.*, 2005, **237**, 246.
41. M. Rosales, J. A. Durán, A. González , I. Pacheco, R. A. Sánchez-Delgado, *J. Mol. Cat. A: Chem.*, 2007, **270**, 250.
42. D. Konya, K. Q. A. Lenero, E. Drent, *Organometallics*, 2006, **25**, 3166.
43. E. Drent, P. H. M. Budzelaar , *J. Org. Chem.*, 2000, 593.
44. E. Drent, R. van Ginkel, W. Jager, U.S. Patent WO 028689 A2, 2004.
45. T. Kegl, L. Kollar, *J. Mol. Catal. A: Chem.*, 1997, **122**, 95.

46. P. Meessen, D. Vogt, W. Keim, *J. Org. Chem.*,1998, **551**, 165.
47. E. V. Gusevskaya, E. N. dos Santo, R. Augusti, A. Dias, C. M. Foca., *J. Mol. Cat. A. Chem.*, 2000, **152**, 15.
48. C. Y. Hsu, M. Orchin, *J. Am. Chem. Soc.*, 1975, **97,** 3553.
49. I. Schwager, J. F. Knifton, *J. Catal.*, 1976, **45**, 256.
50. M. Gómez, G. Muller, D. Sainz, J. Sales, *Organometallics*, 1991, **10**, 4036.
51. M. S. Holt, W. L.Wilson, J. H. Nelson, *Chem. Rev.*, 1989, **89**, 11.
52. R.V. Lindsey Jr., G. W. Parshall, U.G. Stolberg, *J. Am. Chem. Soc.*, 1965, **87**, 658.
53. R. D. Cramer, R.V. Lindsey Jr., C.T. Prewitt, U.G. Stolberg, *J. Am. Chem. Soc.*, 1965, **87**, 658.
54. P. Wasserscheid, H. Waffenschmidt, *J. Mol. Cat. A: Chem.*, 2000 **164**, 61.
55. G. Petocz, Z. Berente, T. Kegl, L. Kollar, *J. Org. Chem.*, 2004, **689**, 1188.
56. A. Marteel, J. A. Davies, M. R. Mason, T. Tack, S. Bektesevic , M. A. Abraham., *Cat. Commun.*, 2003, **4**, 309.
57. P. Illner, A. Zahl, R. Puchta, N. van Eikema, Hommes , P. Wasserscheid, R van Eldik, *J. Org. Chem.*, 2005, **690**, 3567.
58. R. van Duren, J. van der Vlugt, H. Kooijman, A. L. Spek and D. Vogt, *Dalton Trans.*, 2007, 1053.
59. H. C. Clark and H. Kurosawa, *Inorg. Chem.*, 1972, **11**, 1275.
60. L. A. van der Veen, P. K. Keeven, P. C. J. Kamer and P. W. N. M. van Leeuwen, *Chem. Commun.*, 2000, 333.
61. C. P. Casey and G. T. Whiteker, *Isr. J. Chem.*, 1990, **30**, 299.
62. D. D. Ellis, G. Harrison, A. G. Orpen, H. Phetmung, P. G. Pringle, J. G. de Vries, H. Oevering, *J. Chem. Soc., Dalton Trans.*, 2000, 671.
63. J. F. Knifton, *Catalysis Today,* 1997, **36**, 305.
64. A. Lofù, P. Mastrorilli, C. F. Nobile, G. P. Suranna, P. Frediani, J. Iggo, *Eur. J. Inorg. Chem.*, 2006, 2268.
65. T. Hayashi, Y. Kawabata, T. Isoyama, I.Ogata, *Bull. Chem. Soc. Jpn.,* 1981, **54**, 3438.
66. Y. Kawabata, T. Hayashi, I. Ogata, *J. Chem. Soc., Chem. Commun.,* 1979, 462.
67. A. Scrivanti, C. Botteghi, L. Toniolo, A. Berton, *J. Organomet. Chem.*, 1988, **344**, 261.
68. M. K. Alami, F. Dahan and R. Mathieu, *J. Chem. Soc. Dalton Trans.*, 1987, 1983.
69. C. Li, E. Widjaja and M. Garland, *J. Am. Chem. Soc.*, 2003, **125**, 5540.

70. B. Zhu, L. Zhang , N. Xiao, J. Chen, Y. Yin, J. Sun., *Inorg. Chim. Acta*, 2004, **357**, 864.

71. C. Botteghi, S. Paganelli, A. Schionato, M. Marchetti, *Chiralty*, 1991, **3**, 335.

72. G. K. Anderson, H. C. Clark, J. A. Davies, *Organometallics*, 1982, **1**, 64.

Chapter 2

Synthesis and characterization of Pt and Pd complexes containing bidentate ligands

2.1. Introduction

A review of previous hydroformylation studies has revealed that a combination of electronic as well as steric factors imposed by a particular ligand system determines the regio- and chemoselectivity achieved.[1] In addition, the activity achieved also depends on the metal centre used.[1] This creates an incentive for investigations into many new complexes as potential catalysts in hydroformylation.

The discovery of phosphine-modified catalysts initiated tremendous growth in hydroformylation.[1] Phosphines were able to replace carbon monoxide as an electron donating ligand. This was an important step in the development of the reaction since the imposed steric and electronic contribution of these ligands allowed for catalysts to be designed to meet selectivity requirements.[1] Also, reaction conditions such as the carbon monoxide pressure required was considerably lower when phosphine-modified catalysts were used.[2-4]

2.2. Aminophosphine ligands

Metal catalysts containing P,N bidentate (aminophosphine) ligands have acquired a growing interest in recent years. Shell International used phosphinoamines, $Ph_2P(CH_2)_xNMe_2$ (x = 1, 2), in the Rh catalyzed hydroformylation of allyl alcohol under mild conditions and found high reaction rates and an overall linearity of 69 %.[5] Amer and Abu-Gnim showed that the ligand $Ph_2P(O)CH_2NMe_2$ resulted in 100 % conversion and a 9:91 n:i ratio in the Rh catalyzed hydroformylation of styrene.[6] These ligands have not been as extensively researched as their diphosphine counterparts and further studies are required to fully realise the potential of these systems.[7-9]

The P,N bidentate ligands *o*-$Ph_2PC_6H_4CH{=}NR$ (where R is an alkyl group such as Et, ^{n}Pr, ^{i}Pr and ^{t}Bu) have been well researched.[10] This type of ligand provides an opportunity to manipulate steric crowding around the metal centre by varying the alkylimine functionality.

2.3. Synthesis and characterization of *o*-$Ph_2PC_6H_4CH{=}N^nPr$ (2-1) and $PtCl_2$[*o*-$Ph_2PC_6H_4CH{=}N^nPr$] (2-2)

The P,N bidentate ligand *o*-$Ph_2PC_6H_4CH{=}N^nPr$ was prepared *via* a Schiff-base reaction (Scheme 2.1).[8] Reacting *o*-(diphenylphosphino)benzaldehyde with propylamine in dichloromethane produced **2-1** after 4 hours. Since the reaction involved the loss of water, anhydrous $MgSO_4$ was added to drive the reaction forward. The ligand was isolated as an air stable yellow oil which was soluble in most polar organic solvents.

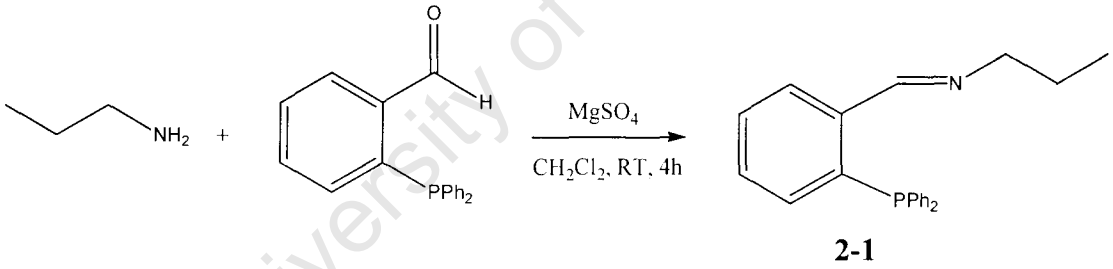

2-1

Scheme 2.1: Synthesis of *o*-$Ph_2PC_6H_4CH{=}N^nPr$ using a Schiff-base condensation reaction.

The subsequent complexation was carried out by reacting **2-1** with $[PtCl_2(cod)]$ in dichloromethane to produce complex **2-2** (Scheme 2.2).

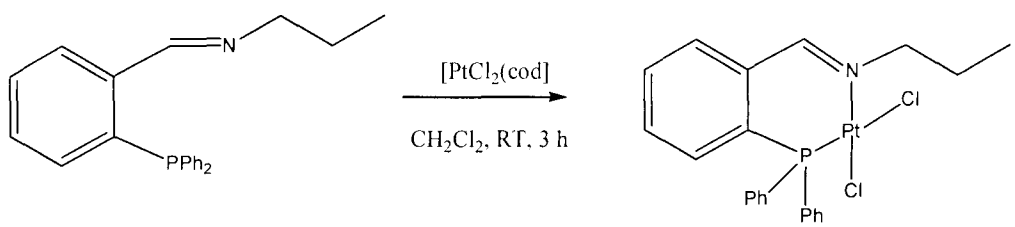

2-2

Scheme 2.2: Synthesis of $[PtCl_2$(*o*-$Ph_2PC_6H_4CH{=}N^nPr)]$.

The product was recrystallized from a dichloromethane/hexane (50/50 %) solution and a bright yellow solid was recovered. NMR and IR spectroscopy, elemental analysis as well as mass spectrometry were used to identify the product as [$PtCl_2$(*o*-$Ph_2PC_6H_4CH=N^nPr$)] (**2-2**). To our knowledge, this complex has not previously been reported.

2.3.1. NMR spectroscopy

2.3.1.1. *^1H NMR*

The ^1H, ^{31}P and ^{13}C NMR spectra reported in this chapter were recorded in deuterated-chloroform ($CDCl_3$) unless otherwise stated. The ^1H NMR spectrum of the free ligand, **2-1**, displayed signals at δ 3.42, 1.46 and 0.68 ppm for the protons on the propyl chain. The methyl protons displayed a triplet (^2J(H-H) = 7 Hz) peak due to coupling to the neighbouring methylene group. A peak at δ 8.85 ppm was indicative of the imine proton which appeared as a doublet (^4J(P-H) = 5 Hz). Previous studies have suggested that this coupling is the result of through space interactions, which implies that the free ligand adopts a conformation whereby the imine proton points towards the lone pair of the phosphorus atom.[11]

Figure 2.1 shows the ^1H NMR spectrum of **2-2**. Upon complexation to Pt, the peak for the imine proton, H_a, appeared as a singlet at δ 8.79 ppm, which was a slight upfield shift from the free ligand. This change in multiplicity has been reported previously in complexation reactions using iminophosphine ligands.[11,12] There were also significant changes in chemical shifts for the protons on the alkyl chain. Protons H_b and H_c shifted downfield to δ 4.45 and 1.72 ppm respectively, while protons H_d displayed an upfield shift to δ 0.49 ppm upon complexation.

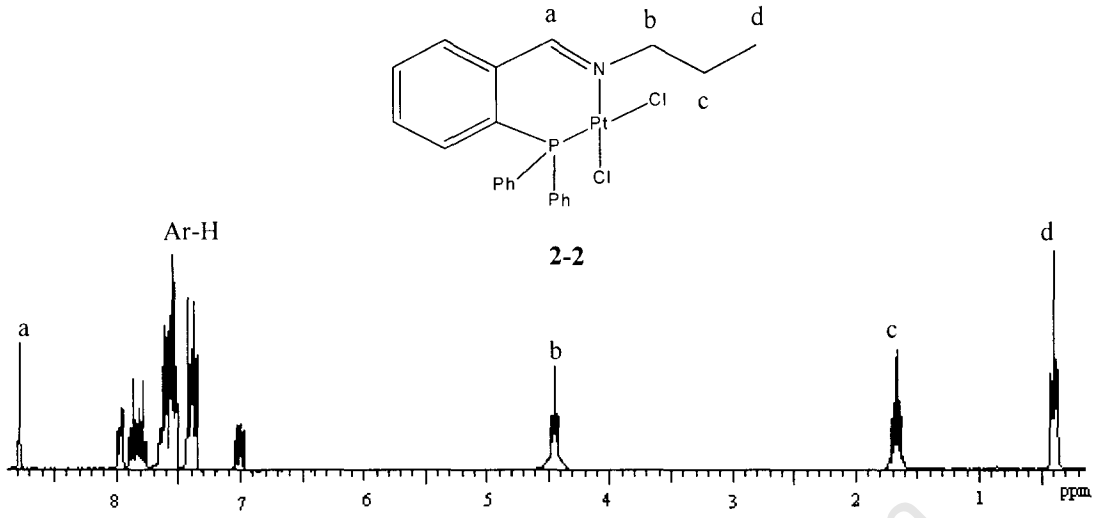

Figure 2.1: ^{1}H NMR spectrum of **2-2**. ($CDCl_3$, room temp (RT), internal standard: tetramethylsilane (TMS).

2.3.1.2. *^{31}P NMR*

The ^{31}P NMR spectra of platinum complexes provides a sensitive probe for the structures of complexes. The one-bond coupling ^{1}J(Pt-P) is characteristic of these complexes and those which contain Cl atoms *trans* to phosphorus atoms have been found to possess coupling constants greater than 3500 Hz.[13]

The ^{31}P NMR spectrum of **2-1** displayed a singlet peak at δ -13.4 ppm. Upon complexation, a singlet at δ 5.81 ppm flanked by two platinum satellites was observed (Figure 2.2). The calculated coupling constant was 3741 Hz (^{1}J(Pt -P)).

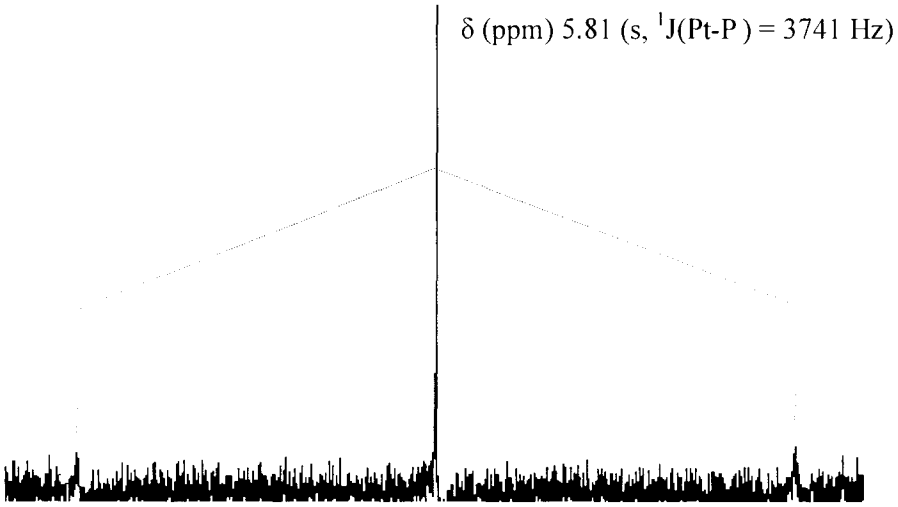

Figure 2.2: ^{31}P NMR spectrum of **2-2** ($CDCl_3$, RT, internal standard: H_3PO_4).

2.3.1.3. *^{13}C NMR*

Figure 2.3 shows the ^{13}C NMR spectrum of **2-2**. The imine carbon, C_a, displayed a singlet at δ 159.8 ppm, a downfield shift from the corresponding carbon in **2-1** which appeared at δ 152.5 ppm. Carbons C_b and C_c displayed singlets at δ 60.4 and 22.9 ppm in **2-1** and displayed downfield shifts to δ 62.3 and 23.3 ppm in **2-2** respectively. Carbon C_d was the only upfield shift, as was the case in the ^{1}H NMR, from 11.9 ppm in **2-1** to 11.3 ppm in **2-2**.

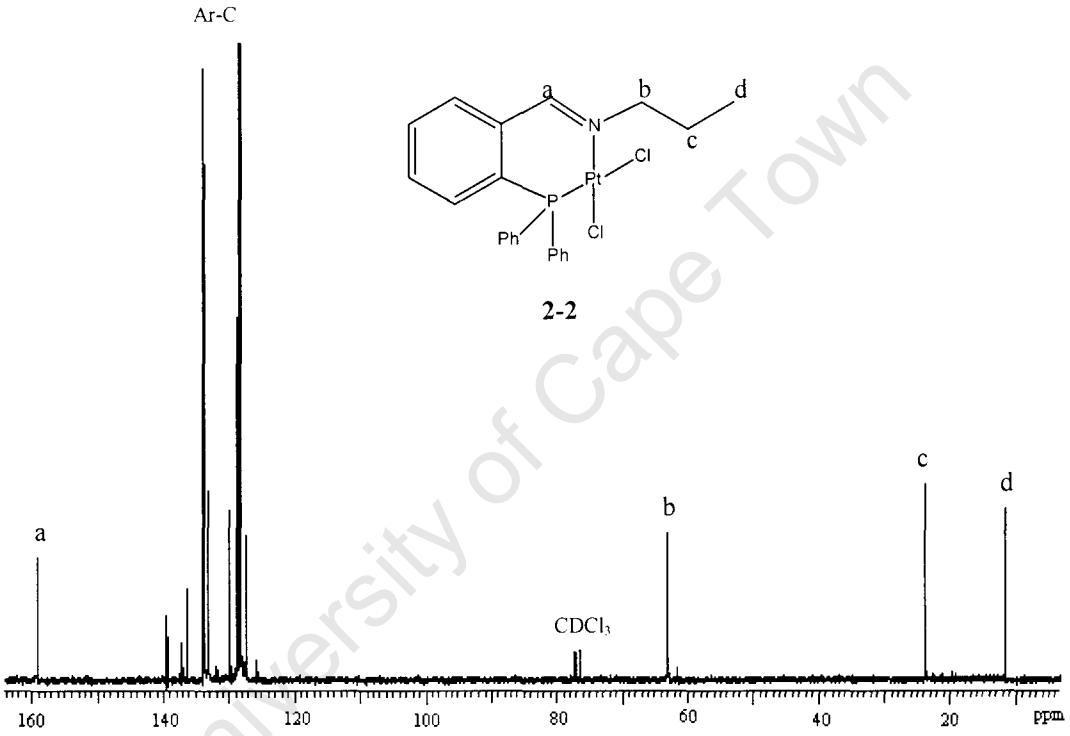

2-2

Figure 2.3: ^{13}C NMR spectrum of **2-2** ($CDCl_3$, RT, internal standard: TMS).

2.3.2. Mass spectrometry

Figure 2.4 shows the mass spectrum (EI) of **2-2**. The complex displays a peak corresponding to the parent ion with loss of a chloride ion $[M\text{-}Cl]^+$ (Table 2.1). The complex fragments by initial loss of the remaining chloride ion and subsequent loss of the phenyl group and imine moiety (m/z = 429.9, $[M\text{-}(Cl)_2\text{-}C_6H_4\text{-}CH]^+$). This is followed by sequential loss of the alkylamino group and eventually both phenyl groups (m/z = 225.3, $[M\text{-}(Cl)_2\text{-}C_6H_4\text{-}CH\text{-}(CH_2)_2\text{-}CH_3\text{-}N\text{-}(Ph)_2]^+$).

Table 2.1: Assignment of fragment ions in the mass spectrum of **2-2**.

Fragment ion	m/z
$[M\text{-}Cl]^+$	559.5
$[M\text{-}(Cl)_2\text{-}C_6H_4\text{-}CH]^+$	429.9
$[M\text{-}(Cl)_2\text{-}C_6H_4\text{-}CH\text{-}(CH_2)_2\text{-}CH_3]^+$	393.8
$[M\text{-}(Cl)_2\text{-}C_6H_4\text{-}CH\text{-}(CH_2)_2\text{-}CH_3\text{-}N\text{-}Ph]^+$	303.1
$[M\text{-}(Cl)_2\text{-}C_6H_4\text{-}CH\text{-}(CH_2)_2\text{-}CH_3\text{-}N\text{-}(Ph)_2]^+$	225.3

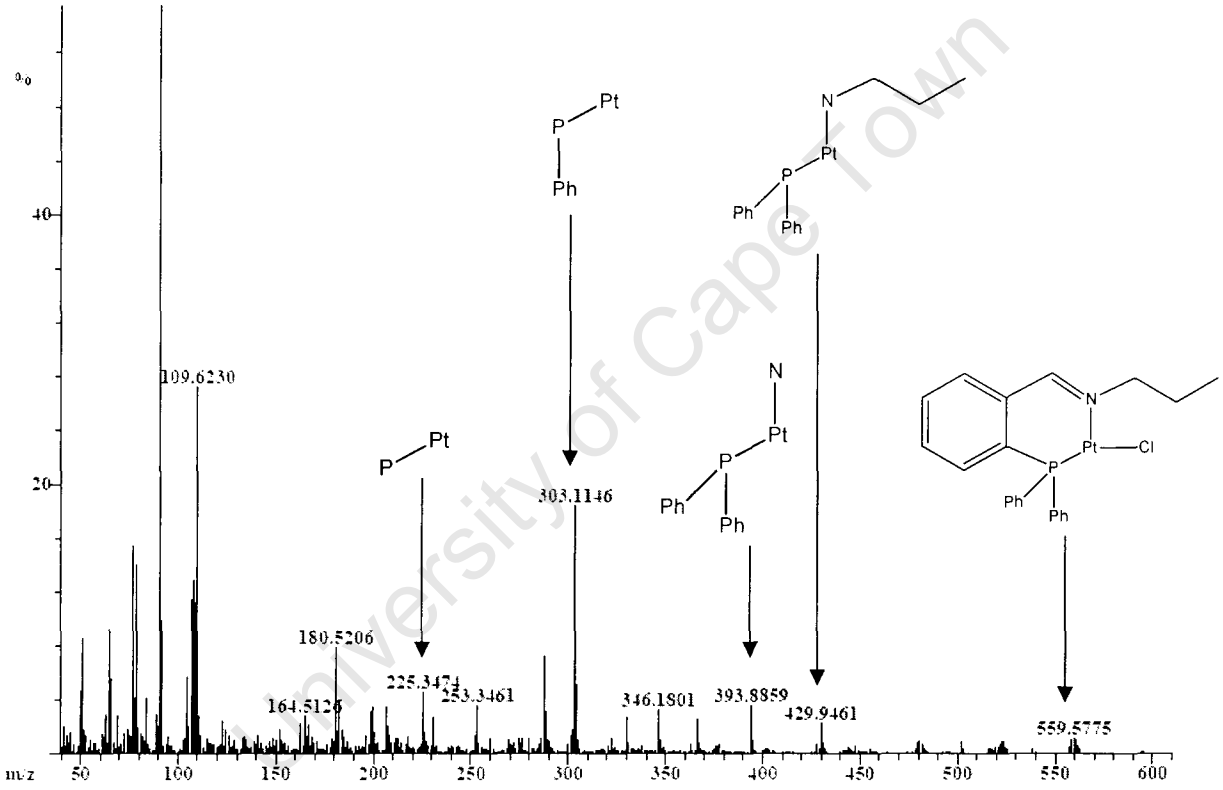

Figure 2.4: Mass spectrum (EI) of **2-2**.

2.3.3. Infrared spectroscopy

Ligand **2-1** shows a distinctive stretching frequency, ν(C=N) at 1637 cm^{-1} (CH_2Cl_2, NaCl plates) which agrees with previously reported values for iminophosphine ligands.[10] Upon complexation, this peak shifts to 1606 cm^{-1}. This is due to increased electron density on the metal upon coordination of the imine moiety to the metal centre.

2.4. Aminodiphosphine ligands

Aminodiphosphine ligands have seen many applications in the field of phosphorus-nitrogen chemistry.[14] They have proven particularly useful due to their facile synthesis that produces high yields. A wide range of ligands can be prepared by simple variations of the alkylamine functionality. This functionality allows for the introduction of additional donor atoms such as O- and N-donors as well as π–donors such as allyl groups.[14,15] They have been found to be particularly stable to hydrolysis when bulky groups are attached to the phosphorus atoms.[16] One major advantage is that these ligands behave as diphosphine ligands with coordination occurring *via* the two phosphorus atoms. This produces highly stable compounds that react readily to form complexes with Pt, Pd and Cu.[17]

The ligands NR(P-P) (R= Me, Et, ^{n}Pr) can be converted to the corresponding dioxides *via* oxidation reactions with ozone or activated manganese.[18,19] The aminodiphosphine ligands, benzyl-N(Ph_2P)$_2$ and 2-picolyl-N(Ph_2P)$_2$ were first synthesized by Biricik *et al.* in 2008.[20] The ligands were complexed to Pd and investigated as potential catalysts in C-C cross-coupling reactions. They demonstrated high catalytic activity in the coupling of unactivated, activated and deactivated aryl bromides.

Complexes containing other aminodiphosphine ligands have also been used in a number of studies as potential anticancer drugs, herbicides as well as antimicrobial and neuroactive agents.[21-24] Several examples of aminodiphosphine ligands with halogeno, alkyl and aryl substituents on the phosphorus atoms have been synthesized and the NMR data has been well documented.[25-27]

Cross and co-workers have investigated the possible conformations adopted by these ligands.[28] They reported that the conformation would depend on the lone pair on one phosphorus atom and the position of the second on the remaining phosphorus atom. The method used to investigate this was a study of the dihedral angle, θ, between the plane bisecting the phosphorus substituents and the plane containing the P-N-P unit about the P-N bond as in Figure 2.5.

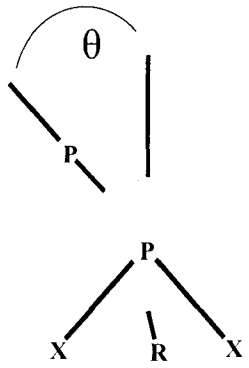

Figure 2.5: The dihedral angle, (θ), in R-N(PPX_2)systems.

Previous work has shown that lone pairs of electrons on phosphorus atoms tend to lie orthogonal to each other.[29,30] Taking this into account and excluding conformations where groups on adjacent phosphorus atoms are eclipsed, conformations (**I-III**) are possible (Figure 2.6). Construction of molecular models suggested that (**I**) was the most likely conformation when R groups impose few steric constraints. Conformations (**II**) and (**III**) became more important in molecules containing larger R groups. Electron diffraction studies of R-N(PPX_2) compounds, when R = Me and X = F, revealed that (**I**) is the preferred conformation ($\theta = 0^{\circ}$).[12]

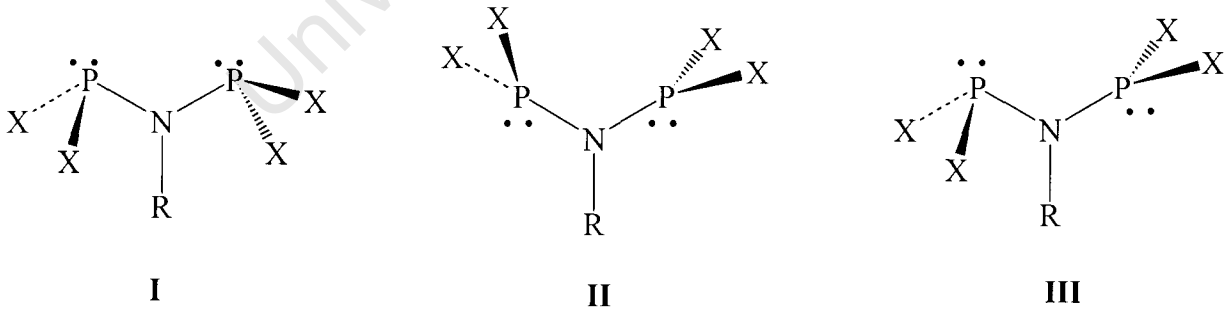

I **II** **III**

Figure 2.6: Possible conformations adopted in R-N(PPX_2)systems.

2.5. Synthesis and characterization of aminodiphosphine ligands (2-3 to 2-8)

Ligands **2-3** to **2-8** (Table 2.2) were prepared *via* an aminolysis reaction by slowly adding chlorodiphenylphosphine (PPh_2Cl) to a solution of the corresponding amine and triethylamine (Et_3N) in dichloromethane (CH_2Cl_2) at 0 °C (Scheme 2.3). Ligands **2-3** to **2-8** were characterised by IR spectroscopy as well as ^{1}H, ^{31}P and ^{13}C NMR. The spectroscopic data obtained agrees with literature values.[20,28,31-32]

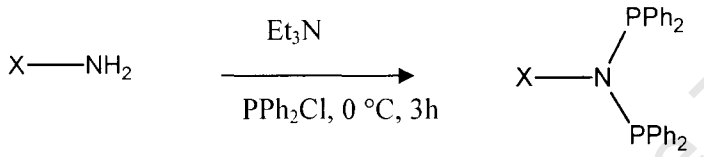

X = $(CH_2)C_6H_5$	**(2-3)**
X = $(CH_2)C_5H_4N$	**(2-4)**
X = $(CH_2)_2CH_3$	**(2-5)**
X = $C_6H_4(OMe)$	**(2-6)**
X = $C_6H_4(NO_2)$	**(2-7)**
X = $CH(CH_3)_2$	**(2-8)**

Scheme 2.3: Synthetic route to aminodiphosphine ligands *via* an aminolysis reaction.

Table 2.2: List of N-(PPh_2) ligands prepared.

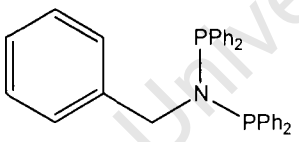 **(2-3)**	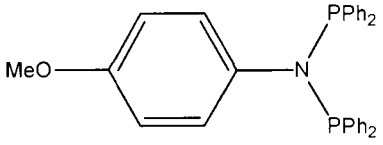 **(2-6)**
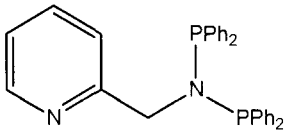 **(2-4)**	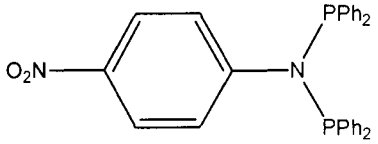 **(2-7)**
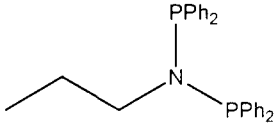 **(2-5)**	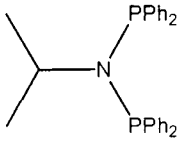 **(2-8)**

2.5.1. NMR spectroscopy

2.5.1.1. *^{1}H NMR*

The ^{1}H NMR spectra of the ligands **2-3** to **2-8** displayed peaks for the aromatic protons in the region of 6.49 - 8.44 ppm. The CH_2 groups of the benzylamine moiety of **2-3** and picolylamine moiety of **2-4** display singlets at 4.55 ppm and 4.67 ppm respectively. The spectrum of **2-5** (Figure 2.7) displayed the terminal methyl protons, H_e, as a triplet at δ 0.59 ppm (^{2}J(H-H) = 7 Hz).

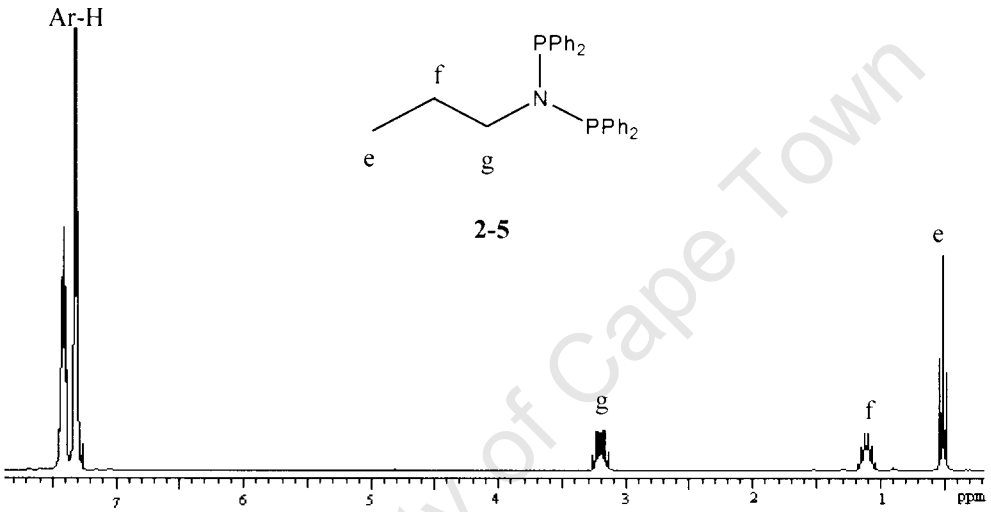

Figure 2.7: ^{1}H NMR spectrum of **2-5** ($CDCl_3$, RT, internal standard: TMS).

The coupling-interactions of **2-5** were identified using Correlation Spectroscopy (COSY) which showed that protons, H_e, coupled to neighbouring methylene protons (H_f) resulting in the triplet signal observed (Figure 2.8).

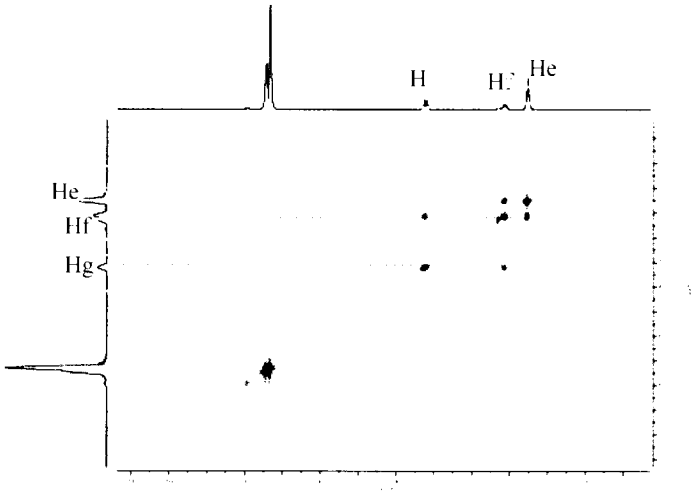

Figure 2.8: COSY spectrum of **2-5** ($CDCl_3$, RT, internal standard:TMS).

The peak for protons H_f appeared as a multiplet at δ 1.11 ppm. The COSY spectrum revealed that this was a result of geminal coupling to neighbouring methylene (H_g) and methyl protons (H_e). The peaks for protons H_g, directly coordinated to the nitrogen atom, also displayed a multiplet further downfield at δ 3.20 ppm. The high multiplicity of this peak suggested that not only geminal coupling to H_f was taking place, but also long-range coupling to the methyl group or through-space coupling to the phosphorus atom or both. Heteronuclear Multiple Bond Correlation (HMBC) revealed that indeed, there was long range coupling of H_g to H_e (Figure 2.9).

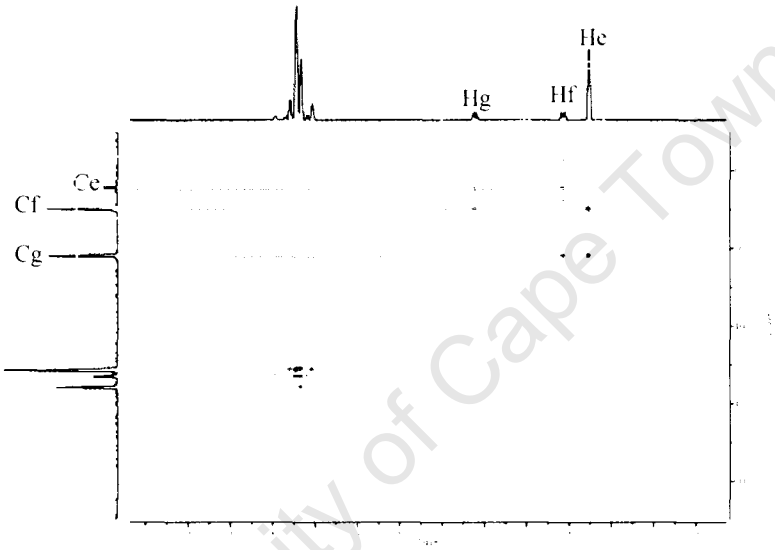

Figure 2.9: HMBC spectrum of **2-5** ($CDCl_3$, RT, internal standard: TMS).

The *p*-anisidine analogue of the aminodiphosphine ligand, **2-6**, displayed a singlet at δ 3.69 ppm for the CH_3 of the methoxy group and overlapping peaks due to the aromatic protons between δ 6.49 – 7.41 ppm in the ^1H NMR spectra. The 4-nitro-aniline analogue, **2-7**, displayed overlapping signals in the aromatic region between δ 6.91 – 8.21 ppm. The isopropyl group of **2-8** was identified by a multiplet for the CH group at δ 3.68 ppm and a doublet for the $(CH_3)_2$ protons at δ 1.17 ppm (^2J(H-H) = 6 Hz) in the ^1H NMR spectrum.

2.5.1.2. *^{31}P NMR*

The ^{31}P NMR spectra of the aminodiphosphine ligands displayed singlet resonances (Table 2.3). Figure 2.10 shows the sharp singlet in the ^{31}P NMR spectrum of **2-5**. The presence of an electron-withdrawing group on these ligands resulted in a chemical shift further downfield. This was demonstrated when **2-8** containing the isopropyl moiety displayed the lowest chemical shift at δ 48.8 ppm, while ligands **2-6** and **2-7** containing 4-methoxy-and 4-nitroaniline groups displayed peaks at δ 70.5 and 68.7 ppm respectively.

Table 2.3: ^{31}P NMR of **2-3** to **2-8**.

Ligand	δ (ppm) ($CDCl_3$)
2-3	60.2
2-4	62.6
2-5	62.9
2-6	70.5
2-7	68.7
2-8	48.8

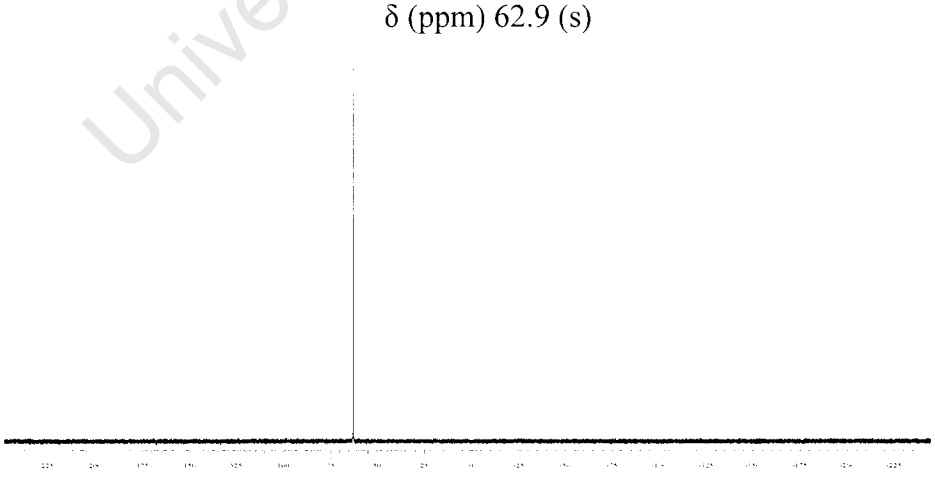

Figure 2.10: ^{31}P NMR spectrum of **2-5** ($CDCl_3$, RT, internal standard: H_3PO_4).

2.5.1.3. *^{13}C NMR*

In the ^{13}C NMR spectra, the ligands displayed signals for the aromatic carbons in the region of δ 113.2 - 139.8 ppm. Ligand **2-3** displayed a singlet for the bridging methylene carbon at δ 56.1 ppm while **2-4** displayed the corresponding peak at δ 57.8 ppm. This was a slight downfield shift, attributed to the only structural difference between the two ligands i.e the pyridyl group of **2-4**. Ligand **2-5** displayed three singlets for the carbons on the alkyl chain (Figure 2.11). Carbon C_e displayed a singlet at δ 10.9 ppm while its methylene counterparts C_g and C_f displayed peaks further downfield at δ 54.8 and 24.7 ppm respectively.

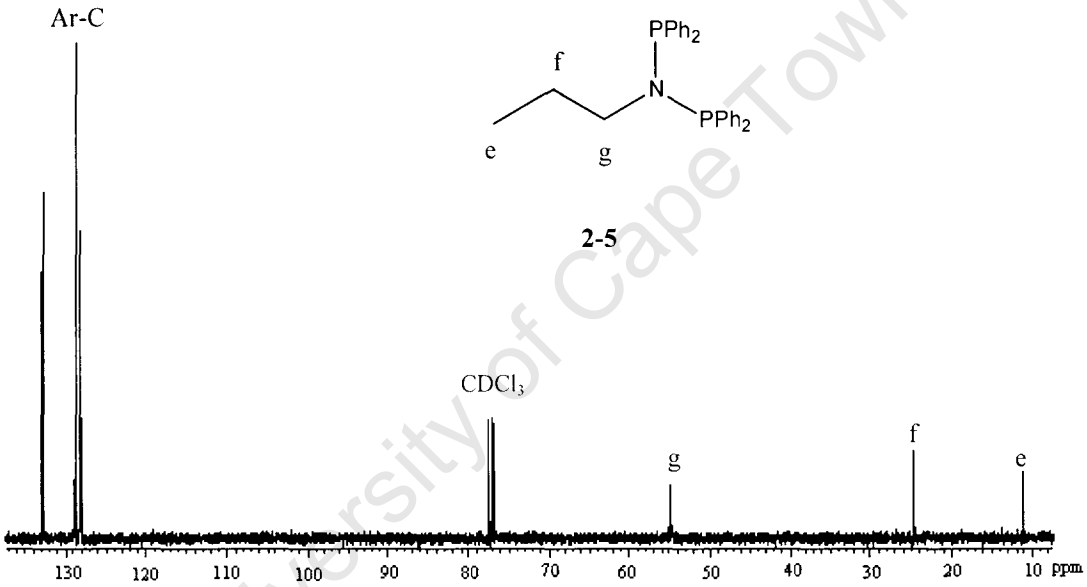

Figure 2.11: ^{13}C NMR spectrum of **2-5** ($CDCl_3$, RT, internal standard: TMS).

2.5.2. Physical properties

Ligands **2-3** to **2-8** were all air stable solids and were obtained in yields ranging between 63 – 89 % (Table 2.4). One possible explanation for the differences in yields obtained is the basicity of the protons from the primary amines used. The less basic the protons on the amine, the more difficult it would be for subsequent deprotonation using the base, Et_3N. Higher yields were obtained with those ligands containing more electron releasing amine groups such as **2-3**, **2-4** and **2-5**, while ligands with more electron withdrawing groups such as **2-6** and **2-7** resulted in lower yields.

The ligands were isolated as white solids with the exception of **2-6** and **2-7** which were pale yellow and pale purple solids respectively. Ligand **2-5** had the lowest melting range between 85–87 °C and **2-4** the highest between 162-164 °C. Interestingly, the presence of the pyridyl group on **2-4**, the only structural difference between **2-3** and **2-4**, resulted in a compound with a higher melting point. The data obtained agrees with previously reported values for these compounds.[20]

Table 2.4: Yields and physical properties of ligands **2-3** to **2-8**.

Ligand	Yield (%)	Colour of Solid	Melting point (°C)
2-3	87	White	146-148
2-4	89	White	162-164
2-5	71	White	85-87
2-6	75	Pale purple	118-120
2-7	66	Pale yellow	141-143
2-8	63	White	133-134

2.6. Synthesis and characterization of Pd complexes (2-9 to 2-12)

Palladium complexes **2-9** to **2-12** (Table 2.5) were prepared by reacting the appropriate aminodiphosphine ligand with $[PdCl_2(cod)]$ in dichloromethane (Scheme 2.4).

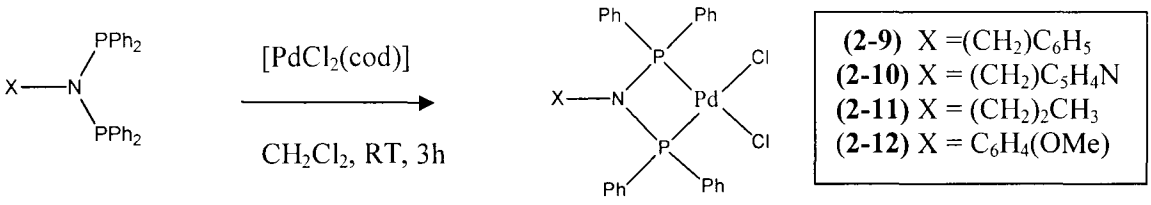

Scheme 2.4: Complexation reactions using aminodiphosphine ligands and $[PdCl_2(cod)]$.

Table 2.5: Palladium complexes prepared.

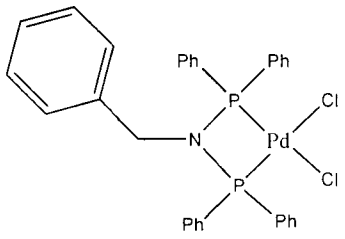 **(2-9)**	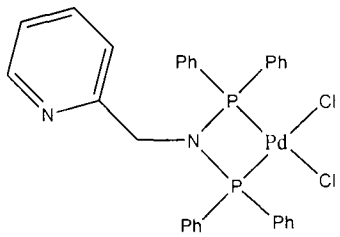 **(2-10)**
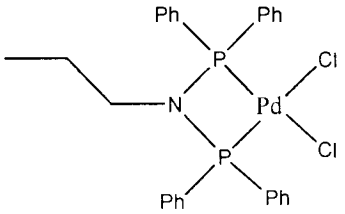 **(2-11)**	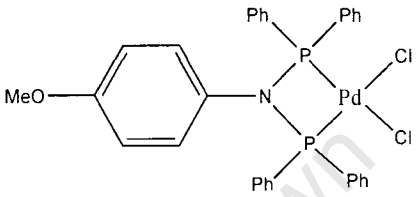 **(2-12)**

Ligands **2-7** and **2-8** did not form complexes with Pd under identical reaction conditions to their aminodiphosphine counterparts. Even with a change of solvent to toluene and heating to 70 °C, the reactions did not proceed and resulted only in unreacted metal complex and ligand. This inhibition of complexation is possibly due to the presence of electron withdrawing groups on these ligands resulting in weaker metal-ligand interactions. The spectroscopic data obtained for complexes **2-9** and **2-10** agree with literature values.[20] To the best of our knowledge, palladium complexes **2-11** and **2-12** have not been previously reported.

2.6.1. NMR spectroscopy

2.6.1.1. *^1H NMR*

Table 2.6 shows the chemical shifts observed for the ligands **2-3** to **2-6** and the corresponding palladium complexes **2-9** to **2-12**.

Table 2.6: ^{1}H NMR data for ligands **2-3** to **2-6** and complexes **2-9** to **2-12.**

Compound	Protons					
	Ar-H	C<u>H</u>$_2$	H$_g$	H$_f$	H$_e$ (t, ^{2}J(H-H))	O-C<u>H</u>$_3$
2-3	6.82 – 7.33	4.55	-	-	-	-
2-9	6.44 – 7.81	4.21	-	-	-	-
2-4	6.98 – 8.44	4.67	-	-	-	-
2-10	6.35 – 7.92	4.26	-	-	-	-
2-5	7.31 – 7.40	-	3.20	1.11	0.59 (7 Hz)	-
2-11	7.54 – 7.89	-	2.95	1.2	0.52 (7 Hz)	-
2-6[a]	6.49 – 7.41	-	-	-	-	3.69
2-12[a]	6.51 – 7.96	-	-	-	-	4.26

($CDCl_3$, RT, internal standard: TMS).

[a]NMR obtained in d_6-dmso.

Complexes **2-9** and **2-10** were most easily identified by the peak for the methylene protons on the benzyl and picolyl moieties respectively. The complexes also displayed upfield shifts in the ^{1}H NMR when compared to the ligand for both the aromatic and methylene protons. The nitrogen atom in the pyridyl group of complex **2-10** was not involved in the coordination to the metal centre since there was no significant shift in the resonance of the aromatic protons observed in the ^{1}H NMR spectrum upon complexation (δ 6.98 – 8.44 ppm to 6.35 – 7.92 ppm). Thus, the phosphorus atoms of the aminodiphosphine groups proved to be much stronger donor atoms and preferentially coordinated to the metal centre.

Complex **2-11** displayed a slight upfield shift in peak position for the methylene group directly attached to the nitrogen (H$_g$) from δ 3.20 ppm in the ligand to δ 2.95 ppm in the corresponding complex (Figure 2.12).

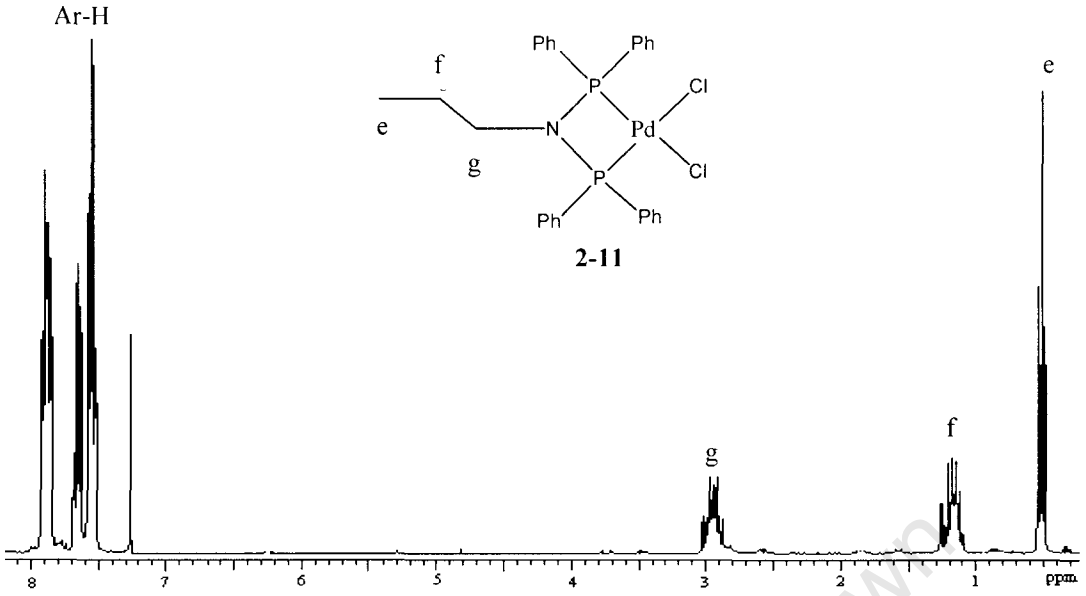

Figure 2.12: ^{1}H NMR spectrum of complex **2-11** ($CDCl_3$, RT, internal standard: TMS).

Complex **2-12** demonstrated poor solubility in most common organic solvents, thus NMR data were obtained in deuterated-dimethyl sulfoxide (d_6-dmso). Ligand **2-6** showed a distinctive signal for the protons of the methoxy group at δ 3.69 ppm and a significant downfield shift to δ 4.26 ppm was observed upon complexation.

2.6.1.2. *^{31}P NMR*

Palladium complexes **2-9** to **2-12** displayed sharp singlets in their ^{31}P NMR spectra (Table 2.7).

Table 2.7: ^{31}P NMR spectra for **2-3** to **2-6** and **2-9** to **2-12**.

Ligand	δ (ppm)	Pd Complex	δ (ppm)
2-3	60.2	**2-9**	34.6
2-4	62.6	**2-10**	34.5
2-5	62.9	**2-11**	31.3
2-6[a]	79.9	**2-12**	70.1

($CDCl_3$, RT, internal standard: H_3PO_4).

[a]NMR obtained in d_6-dmso.

Significant upfield shifts of approximately 30 ppm were observed in all cases. Complexes **2-9** and **2-10** displayed similar signals at δ 34.6 and 34.5 ppm respectively. Complex **2-11** displayed the furthest upfield shift upon complexation from δ 62.9 ppm to δ 31.3 ppm.

2.6.1.3. *^{13}C NMR*

The aromatic carbons displayed signals in the range of δ 121.4 - 139.8 for complexes **2-9** to **2-11** (Table 2.8).

Table 2.8: ^{13}C NMR of **2-3** to **2-6** and **2-9** to **2-12**.

Compound	Carbon					
	Ar-C	$\underline{C}H_2$	C_g	C_f	C_e	O-$\underline{C}H_3$
2-3	127.9 - 139.8	56.1	-	-	-	-
2-9	128.6 - 133.8	52.9	-	-	-	-
2-4	121.4 - 139.6	57.8	-	-	-	-
2-10	123.2 - 139.3	54.1	-	-	-	-
2-5	128.4 - 132.9	-	54.8	24.7	10.9	-
2-11	129.4 - 133.6	-	51.1	23.1	11.2	-
2-6[a]	113.2 - 139.5	-	-	-	-	55.2
2-12[a]	129.5 - 135.1	-	-	-	-	56.1

($CDCl_3$, room temp, internal standard: TMS).

*NMR obtained in d_6-dmso.

Complexes **2-9** and **2-10** displayed upfield shifts of the methylene carbons when compared to the free ligand at δ 52.9 and 54.1 ppm respectively. Complex **2-11** displayed slight upfield shifts for carbons C_g and C_f to δ 51.1 and 23.1 ppm respectively (Figure 2.13). The aromatic signals for complex **2-12** included those of the phenyl group of the *p*-anisidine moiety.

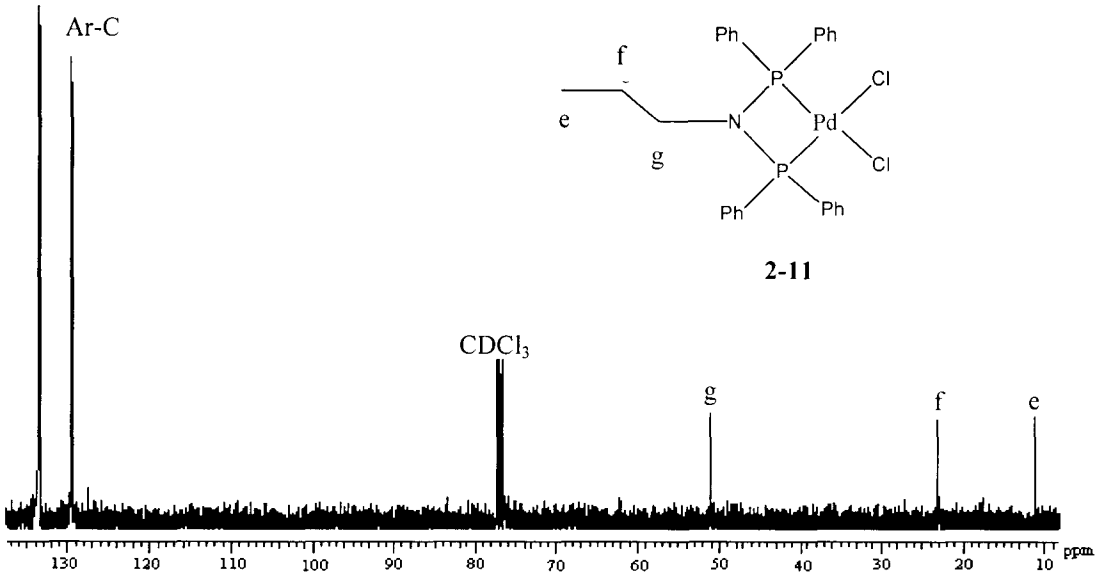

Figure 2.13: ^{13}C NMR spectrum of **2-11** ($CDCl_3$, room temp, internal standard: TMS).

2.7. Synthesis and characterization of Pt complexes (2-13 to 2-16)

Platinum complexes **2-13** to **2-15** (Table 2.9) were prepared by reacting the appropriate aminodiphosphine ligand with [$PtCl_2$(cod)] in dichloromethane (Scheme 2.5). The spectroscopic data obtained agrees with literature reported values for complexes **2-13** and **2-14.**[20] Complex **2-16** was prepared *via* a halide exchange reaction of **2-15** with NaI in acetone (Scheme 2.6). To our knowledge, complexes **2-15** and **2-16** have not previously been reported.

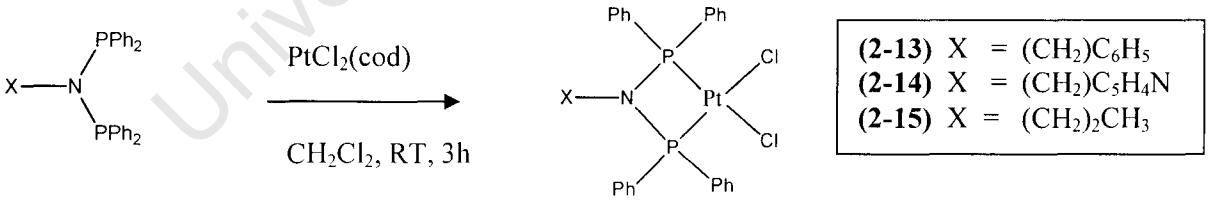

Scheme 2.5: Complexation reactions using aminodiphosphine ligands and [$PtCl_2$(cod)].

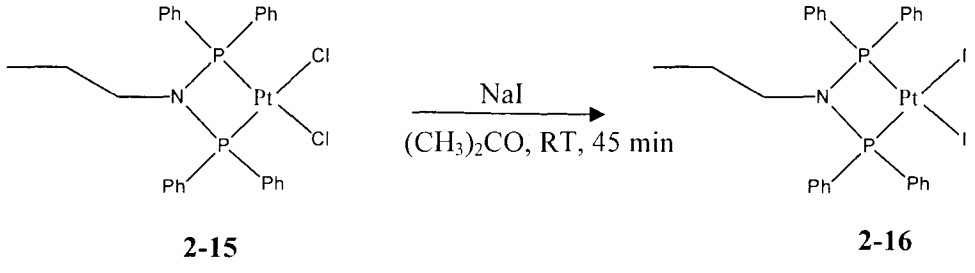

2-15 **2-16**

Scheme 2.6: Complex **2-16** via a halide exchange reaction using NaI and **2-15** in acetone.

Table 2.9: Platinum complexes **2-13** to **2 -16**.

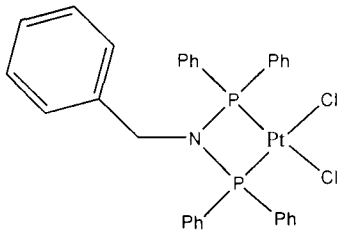 **(2-13)**	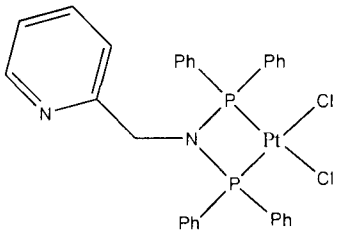 **(2-14)**
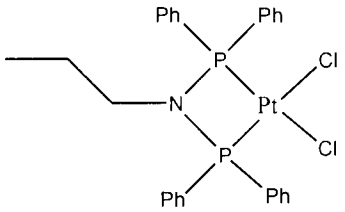 **(2-15)**	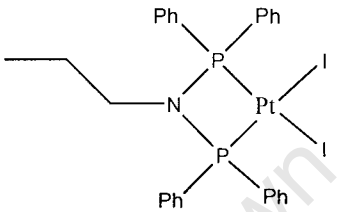 **(2-16)**

2.7.1. NMR spectroscopy

2.7.1.1. *^{1}H NMR*

Table 2.10: ^{1}H NMR data for ligands **2-3** to **2-5** and complexes **2-13** to **2–16**.

Compound	Protons				
	Ar-H	**C<u>H</u>$_2$**	**H$_g$**	**H$_f$**	**H$_e$** (t, ^{2}J(H-H))
2-3	6.82 – 7.33	4.55	-	-	-
2-13	6.25 – 8.05	4.14	-	-	-
2-4	6.98 – 8.44	4.67	-	-	-
2-14	6.49 – 8.11	4.18	-	-	-
2-5	7.31 – 7.40	-	3.20	1.11	0.59 (7 Hz)
2-15	7.26 – 7.87	-	2.94	1.15	0.51 (7 Hz)
2-16	7.18 – 7.49	-	2.75	1.05	0.44 (7 Hz)

($CDCl_3$, RT, internal standard: TMS).

The peaks for the aromatic protons ranged between δ 6.25 to 8.11 ppm for complexes **2-13** to **2-15** and were upfield compared to those observed for the ligands (Table 2.10).

Complex **2-13** was identified by the peak for the methylene protons on the benzyl moiety at δ 4.14 ppm, a significant shift from that of the free ligand (δ 4.55 to 4.14 ppm). Complex **2-14** was also identified by the methylene group slightly downfield compared to **2-13** at δ 4.18 ppm.

Complexes **2-15** and **2-16** differ only in the coordinating halide groups and displayed similar signals in their ^{1}H NMR spectra. The protons on the alkylamino groups displayed signals within 0.2 ppm of each other with the only significant variant being the peak for the methyl group of **2-15** which appeared at δ 0.51 ppm compared to δ 0.44 ppm in **2-16**.

2.7.1.2. *^{31}P NMR*

The platinum complexes **2-13** to **2-16** displayed sharp singlets flanked by platinum satellites in their ^{31}P NMR spectra (Table 2.11).

Table 2.11: ^{31}P NMR of **2-13** to **2-16**.

Ligand	δ (ppm)	Pt Complex	δ (ppm)	^{1}J(Pt-P) (Hz)
2-3	60.2	**2-13**	20.5	3305
2-4	62.6	**2-14**	20.3	3308
2-5	62.9	**2-15**	17.3	3300
		2-16	13.3	3019

($CDCl_3$, RT, internal standard: H_3PO_4).

The coupling constants of the dichloride complexes were in the range of 3300-3308 Hz (^{1}J(Pt-P)). The largest coupling observed was that of the dichloro complex **2-14** (3308 Hz) while the smallest was that of the diiodo complex **2-16** (3019 Hz). Similar reductions in coupling constants upon exchange of Cl with I atoms in platinum complexes have been reported.[33] There were upfield shifts of approximately 40 ppm from ligand to complex, with the most significant shift arising from formation of complex **2-15** (Figure 2.14).

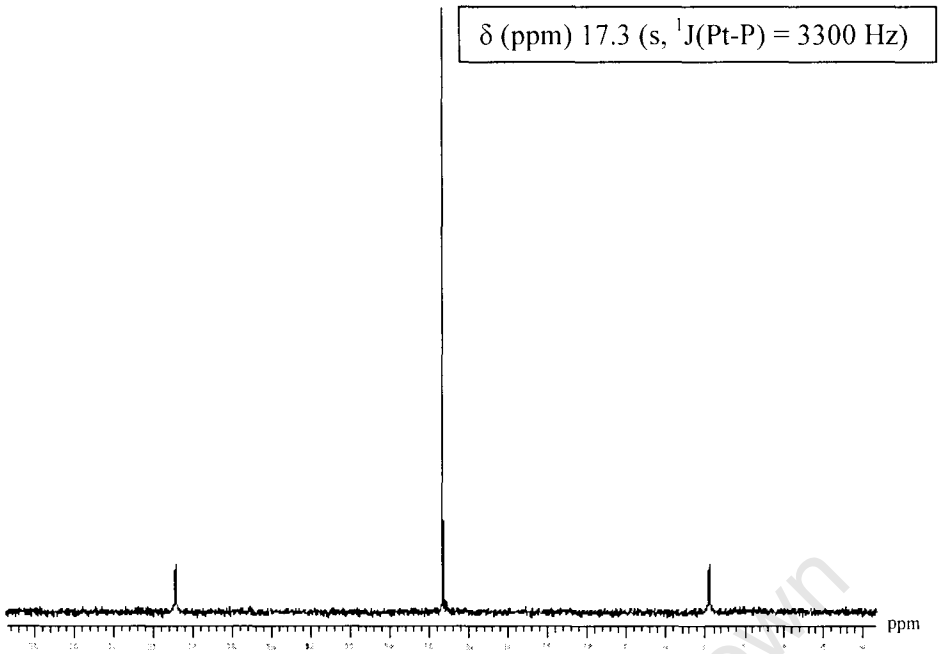

Figure 2.14: ^{31}P NMR spectrum of **2-15** ($CDCl_3$, RT, internal standard: H_3PO_4).

2.7.1.3. *^{13}C NMR*

Table 2.12: ^{13}C NMR of **2-3** to **2-5** and **2-13** to **2-16**.

Compound	Carbon				
	Ar-C	$\underline{C}H_2$	C_g	C_f	C_e
2-3	127.9 - 139.8	56.1	-	-	-
2-13	129.1 - 133.9	53.5	-	-	-
2-4	121.4 - 139.6	57.8	-	-	-
2-14	123.1 - 133.7	54.7	-	-	-
2-5	128.4 - 132.9	-	54.9	24.7	10.9
2-15	133.4 - 133.1	-	51.5	23.0	11.1
2-16	133.2 - 132.2	-	48.3	22.8	11.4

($CDCl_3$, room temp, internal standard: TMS).

The aromatic carbons displayed signals in the range of δ 123.1 - 133.9 ppm for **2-13** to **2-15** (Table 2.12). The characteristic methylene carbons of **2-13** and **2-14** appeared as singlets at δ 53.5 and 54.7 ppm respectively. Both were upfield shifts to that observed in the ligand.

Complexes **2-15** and **2-16** showed no significant variations in chemical shifts for the carbons on the alkyl chain of the propylamino group when compared to the ligand. However, **2-16** did display a sizeable upfield shift for the methylene carbon, C_g, from δ 54.9 to 48.3 ppm.

2.7.2. Mass spectrometry

Figure 2.15 shows the mass spectrum (EI) obtained for complex **2-15.** The spectrum shows a weak peak corresponding to the parent ion with loss of a chloride ion (Table 2.13). The complex fragments by loss of the remaining chloride ion and subsequent loss of a phenyl group as well as the propyl chain (m/z = 502.6 $[M\text{-}(Cl)_2\text{-}Ph\text{-}(CH_2)_2\text{-}CH_3]^+$). This is followed by sequential loss of the remaining phenyl groups.

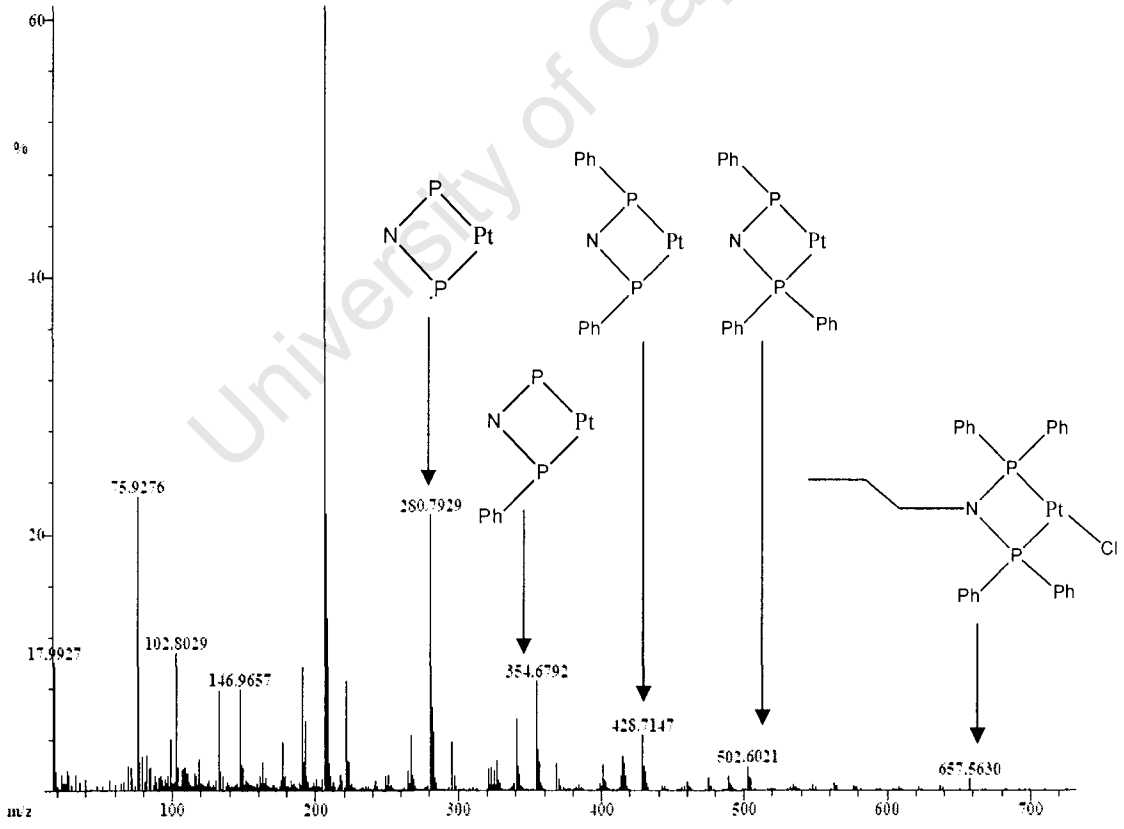

Figure 2.15: Mass Spectrum (EI) of **2-15.**

Table 2.13: Assignment of fragment ions in the mass spectrum of **2-15**.

Fragment ion	m/z
$[M\text{-}Cl]^+$	657.5
$[M\text{-}(Cl)_2\text{-}Ph\text{-}(CH_2)_2\text{-}CH_3]^+$	502.6
$[M\text{-}(Cl)_2\text{-}(Ph)_2\text{-}(CH_2)_2\text{-}CH_3]^+$	428.7
$[M\text{-}(Cl)_2\text{-}(Ph)_3\text{-}(CH_2)_2\text{-}CH_3]^+$	354.7
$[M\text{-}(Cl)_2\text{-}(Ph)_4\text{-}(CH_2)_2\text{-}CH_3]^+$	280.8

2.8. Physical properties and IR spectroscopy of complexes 2-9 to 2-16

2.8.1. Physical properties

The platinum dichloride complexes **2-13** to **2–15** were isolated as white solids, while the diiodo complex **2-16** was found to be a pale yellow solid (Table 2.14). The complexes were all air stable and the yields obtained varied between 65 to 71 %. The complexes did not melt below 288 °C. Microanalysis was carried out on all complexes synthesized and are in agreement with proposed formulations.

The palladium dichloride complexes **2-9** to **2–12** were all air stable, yellow solids which did not melt or decompose below 300 °C. The data obtained agrees with those previously reported.[20] Experimental yields obtained varied between 68 to 72 %.

Table 2.14: Yields and physical properties of complexes **2-9** to **2-16**.

Complex	Yield (%)	Colour of Solid	Melting point (°C)
2-9	71	Yellow	292-293
2-10	74	Yellow	>300
2-11	68	Yellow	288-290
2-12	72	Yellow	>300
2-13	71	White	>300
2-14	61	White	>300
2-15	67	White	>300
2-16	65	Pale yellow	>300

2.8.2. IR spectroscopy

While the assignment of P=N groups is well known, the assigned frequency of the P-N bond varies considerably for many different compounds.[34] However, from reported values, the expected frequency for P-N bonds is near 1000 cm^{-1}.[35,36] The possible reason for discrepancies in values is due to coupling of the P-N and adjacent groups resulting in varying position and intensity of peaks. The spectra of alkylaminodiphosphine ligands however, appear to be more easily assigned with bands near 880 cm^{-1} that do not change with complexation.[31]

Table 2.15 summarizes selected peaks observed in the IR spectra of **2-9** to **2-16**. These P-N stretching frequencies are characteristic of these compounds and the values agree with those previously reported.[20] Figure 2.16 shows the P-N peak observed in the IR spectra of ligand **2-5** and metal complexes **2-11** and **2-15**.

Table 2.15: Selected IR peaks of **2-9** to **2-16**.

Complex	ν(P-N) (cm^{-1})[a]
2-9	803
2-10	813
2-11	829
2-12	828
2-13	803
2-14	816
2-15	826
2-16	834

[a]IR obtained using KBr pellets.

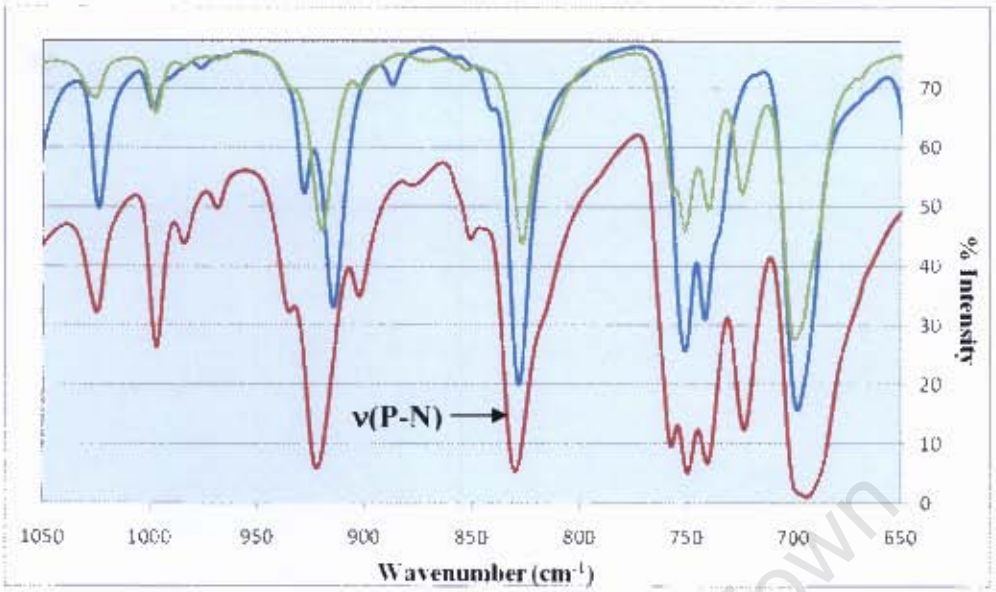

Figure 2.16: IR spectra of **2-5** (——), **2-11** (——) and **2-15**(——).

2.9. Synthesis and characterization of Pt complexes (2-17 to 2-21)

Platinum complexes **2-17** to **2-21** (Table 2.16) were prepared by reacting the appropriate diphosphine ligand with [$PtCl_2$(cod)] in dichloromethane (Scheme 2.7). The complexes were isolated as white solids which did not melt or decompose below 300 °C. The spectroscopic data obtained agree with literature reported values for complexes **2-17** to **2-20**.[37-40] To our knowledge, complex **2-21** has not previously been reported.

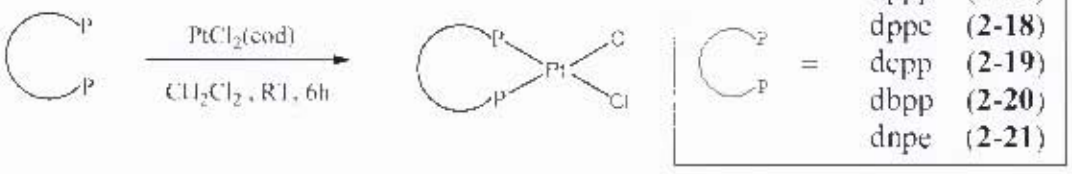

Scheme 2.7: Complexation reactions using diphosphine ligands and [$PtCl_2$(cod)].

Table 2.16: Complexes containing diphosphine ligands.

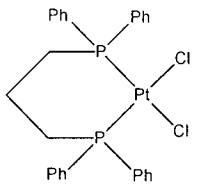	**2-17**	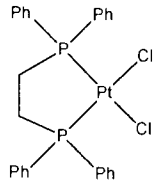	**2-18**
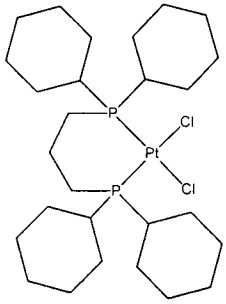	**2-19**	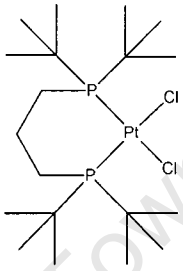	**2-20**
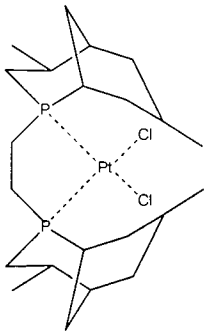	**2-21**	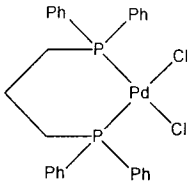	**2-22**

2.9.1. NMR spectroscopy

2.9.1.1. *^{1}H NMR*

The NMR data for complexes **2-17** to **2-21** were obtained in d_6-dmso due to poor solubility in most common organic solvents. Compound **2-17** was prepared by reacting the ligand dppp with $[PtCl_2(cod)]$ in dichloromethane. This complex was previously used as a hydroformylation catalyst and will be used to compare relative activity to complexes **2-18** to **2-21**.[41]

The aromatic protons of **2-17** appeared in the region of δ 7.46 – 8.01 ppm. The methylene groups on the bridging three-carbon chain between the phosphorus atoms displayed multiplets at δ 2.84 and 1.86 ppm respectively, with the latter being the

peak for the internal methylene group. The methylene groups were differentiated based on integration of peaks as well as peak intensity with the internal methylene peak intensity half that of its counterpart. The corresponding palladium complex [$PdCl_2$(dppp)] (**2-22**) was also prepared to compare relative activity of the palladium complexes synthesized. The methylene groups on the ligand of this complex displayed multiplets at δ 2.67 and 1.78 ppm, with the latter being the peak for the internal methylene group.

Complex **2-18** contains a two-carbon chain on the ligand backbone, thus both sets of protons are present on carbon atoms in the same chemical environment and one triplet peak at δ 2.51 ppm (^2J(H-H) = 6 Hz) is displayed in the ^{1}H NMR spectrum. Complex **2-19** displayed overlapping of the methylene groups from both the carbon chain and cyclohexyl groups in the region of δ 2.28 – 2.71 ppm. Similarly, for complex **2-21**, containing a nine-membered ring, overlapping of the proton signals in the aliphatic region ranged between δ 1.08 to 2.42 ppm. Complex **2-20** displayed a singlet peak at 0.89 ppm for the methyl groups of the tertiary-butyl substituents and multiplets for the methylene groups on the carbon chain at δ 1.14 and 1.53 ppm.

The carbon chain bridging the phosphorus atoms on the ligand backbone were varied in these complexes with complexes **2-17**, **2-19** and **2-20** each containing a three-carbon group, while complexes **2-18** and **2-21** contain two-carbon chains. The size of the metallacycle formed depends on the length of the bridging carbon chain and thus determines the bite angle of the complex. Bite angle has been found to play an important role in the hydroformylation of metal complexes containing diphosphine ligands.[42]

The second variation considered was the substituents on the phosphorus atoms. For complexes **2-17** and **2-18** the substituents are phenyl groups, while for **2-19**, **2-20** and **2-21** the substituents are cyclohexyl, tertiary-butyl and 8-bicyclo–2-6-dimethylphospha(3.3.1)nonyl groups respectively.

2.9.1.2. *^{31}P NMR*

Complexes **2-17** to **2-20** displayed singlet resonances flanked by platinum satellites. For complex **2-17** this was observed at δ -3.6 ppm in the ^{31}P NMR spectrum (^{1}J(Pt-P) = 3414 Hz). This was a significant shift from the position of the free ligand (dppp) occurring at δ -16.8 ppm. Table 2.17 summarizes the ^{31}P NMR peaks observed in the spectra of complexes **2-17** to **2-21**.

Table 2.17: ^{31}P NMR spectra of complexes **2-17** to **2-21**.

Complex	δ (ppm)[a]	^{1}J(Pt-P) (Hz)
2-17	-3.6 (s)	3414
2-18	-3.41 (s)	3610
2-19	26.6 (s)	3396
2-20	17.6 (s)	3558
2-21	29.1 (d), 28.8 (s), 27.9 (s)	3538, 3527, 3518

[a](d_6-dmso, room temp, internal standard: H_3PO_4).

The platinum complexes revealed coupling constants in the range of 3414 - 3558 Hz (^{1}J(Pt-P)) for **2-17** to **2-20**. Complexes **2-17** and **2-18** consisting of phenyl substituents on the phosphorus atoms displayed singlets at negative shifts of δ -3.6 and -3.41 ppm respectively. Complexes **2-19** and **2-20** consisting of cyclohexyl and tertiary-butyl substituents displayed peaks at positive shifts of δ 26.6 and 17.6 ppm respectively. Complex **2-21** contains three chiral centres on each bicyclo-nonyl substituent. While the substituent on one phosphorus atom is of R configuration, the other would be in either the R or S configuration. Thus, the complex exists in the R,R, R,S and S,S configurations. This translated in the ^{31}P NMR spectrum as a doublet at δ 29.1 ppm for the R,S configuration due to the phosphorus atoms being in different chemical environments. Also, singlets were observed for the R,R and R,S configurations at δ 28.8 and 27.9 ppm respectively. Complex **2-21** was further characterised by elemental analysis and mass spectrometry.

2.9.1.3. *^{13}C NMR*

The ^{13}C NMR spectra of **2-17** displayed singlets for the carbons attached to the phosphorus atoms and the internal carbons at δ 18.2 and 54.7 ppm respectively. In contrast, the spectra of **2-18** displayed a singlet peak at δ 28.1 ppm for the identical carbons of the ethyl chain. Complexes **2-19**, **2-20** and **2-21** displayed overlapping signals for the aliphatic carbons of the phosphorus substituents and bridging alkyl chains between δ 13.7 – 34.8 ppm.

2.10. Mechanistic studies of intermediates in Pt catalyzed hydroformylation

The role of $SnCl_2$ in promoting steps in the hydroformylation cycle, such as alkene and CO insertion as well as hydrogenolysis, have been thoroughly investigated in Pt complexes containing monodentate phosphine ligands.[43-52] However, the role of the $SnCl_3^-$ anion and the mechanism of hydroformylation in Pt complexes containing chelating diphosphine ligands have been scarcely studied.[53] Four- or five-coordinate Pt-alkyl-carbonyl compounds containing bidentate ligands have not previously been synthesized or characterized. This is partly due to the drastic reaction conditions required for these systems, particularly in carbonylation reactions.[54,55]

2.10.1. Hydroformylation cycle of a platinum complex containing a bidentate ligand

Based on the well established mechanisms of both Rh and Co hydroformylation and studies carried out to elucidate the role of $SnCl_2$, a reaction pathway of platinum catalyzed hydroformylation can be envisaged (Scheme 2.8).

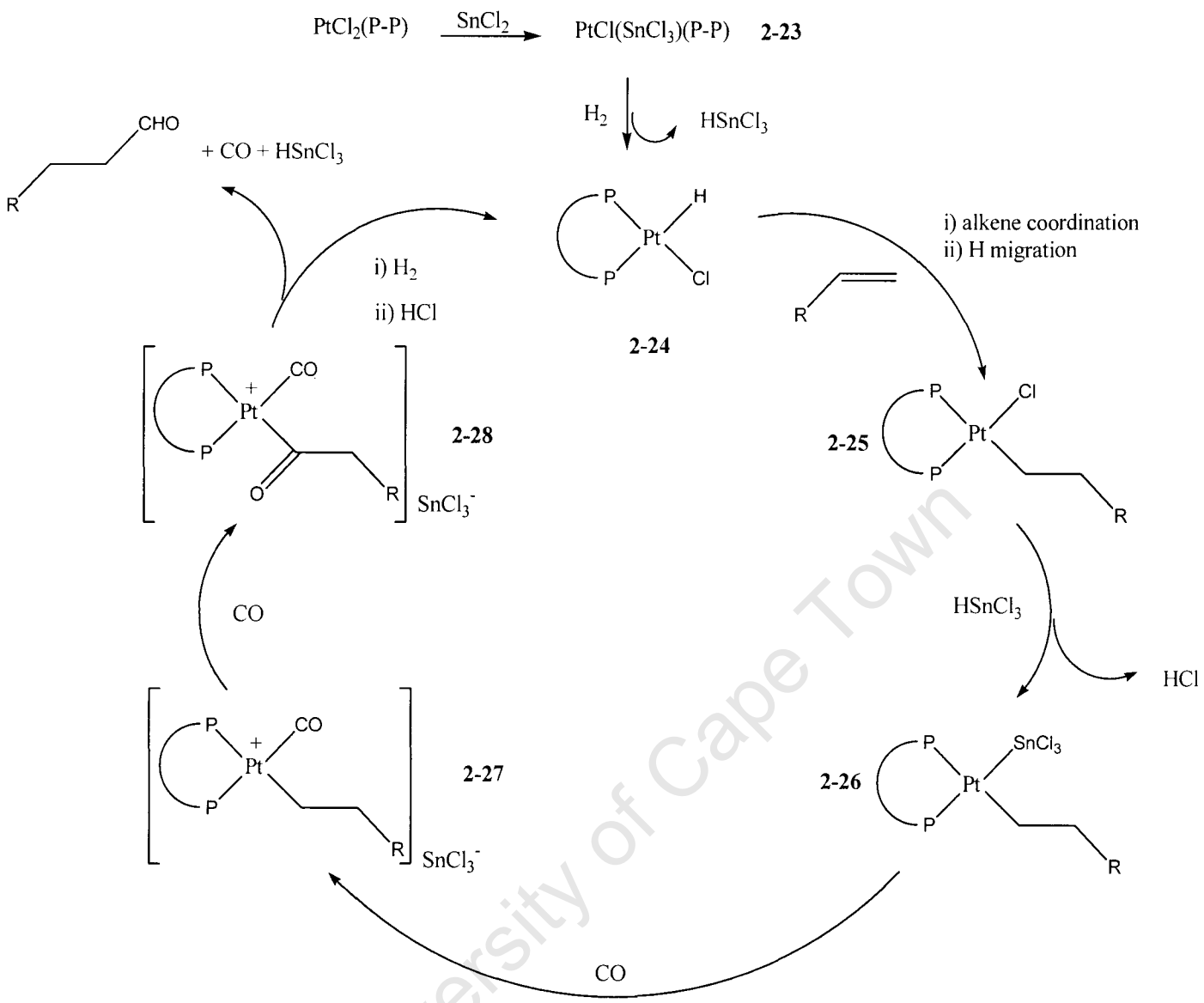

Scheme 2.8: Proposed steps in the Pt/Sn catalyzed hydroformylation cycle ((P-P) = bidentate diphosphine ligand).[53,56-64]

A number of studies have investigated the role of $SnCl_2$ in various reaction steps.[56-59] Kollar *et al.* reported the first ^{119}Sn NMR evidence for the presence of a platinum-tin bond in solution.[60] Complexes of the type $[PtCl_2L_2]$ (L_2 = P-P, P-O, P-N, P-S chelating ligands) were prepared and it was found that $SnCl_2$ inserts into the Pt-Cl bond *trans* to the harder donor atom of the chelating ligand.[60] These findings suggest that a platinum complex such as **2-23** (Scheme 2.8) is a likely catalytic intermediate.

Scrivanti *et al.* studied the reactivity of Pt-alkyl complexes containing chelating diphosphine ligands and reported a Pt(II)-hydride species [*cis*-PtHCl(dppb)].[53] The ^1H

NMR signals observed were similar to those reported by Moulton and Shaw for a Pt(II)-hydride complex containing a bidentate ligand.[61] This provides evidence for a catalytic intermediate such as complex **2-24**. As in Co and Rh catalyzed hydroformylation, alkene coordination is followed by H migration to form a Pt-alkyl intermediate such as **2-25**. Similar complexes of the type [PtRCl(P-P)] (R = Me, Et, (P-P) = dppe, (S,S)-bdpp) have been reported.[58, 62]

The $SnCl_3^-$ species becomes important again in the formation of complex **2-26** and analogous compounds such as [Pt($SnCl_3$)(C_2H_5)(dppb)] and [Pt($SnCl_3$)(CH_3)((S,S)-bdpp)] have been reported.[53,62] The by-product in the formation of **2-26** is HCl. Pregosin and co-workers have also detected the presence of HCl in reactions of [*cis*-$PtCl_2(PPh_3)_2$] with $SnCl_2$ under hydrogen.[63] The importance of the role of an acidic species was also pointed out by Marchionna and co-workers.[64]

Tóth *et al.* showed that the CO insertion and hydrogenolysis steps takes place *via* ionic four-coordinate intermediates such as **2-27** and **2-28**.[58] The study showed that the reaction of [Pt($SnCl_3$)(Me)((S,S)-bdpp)] with CO (25 bar) at 193 K produced the ionic four-coordinate species [Pt(Me)(CO)((S,S)-bdpp)]$^+SnCl_3^-$.[58] This compound suggests substitution of $SnCl_3$ by CO and was characterized using ^{31}P and ^{13}C NMR spectroscopy. Conductivity studies in a CO atmosphere confirmed the ionic nature of the complex.[58] The cationic acetyl-carbonyl compound [Pt(COMe)(CO)((S,S)-bdpp)]$^+SnCl_3$ was subsequently formed by increasing the temperature to 293 K under 25 bar of CO pressure.[58]

The proposed catalytic cycle (Scheme 2.8), shows that the hydrogenolysis step, which includes aldehyde formation and regeneration of **2-24**, produces $HSnCl_3$ as well as HCl. Toth *et al.* found that the reaction of [Pt(COMe)(CO)((S,S)-bdpp)]$^+SnCl_3$ with hydrogen (25 bar) at 293 K produced the aldehyde product and an unidentified Pt species.[58] This unidentified species was presumed to be a Pt-H species but the detection of a Pt-H resonance by ^1H NMR was difficult even at 193 K due to ongoing exchange processes.[53,58]

2.10.2. Attempted synthesis of a Pt-trichlorostannate-acyl complex containing a bidentate ligand (2-32)

To gain further insight into the hydroformylation mechanism of Pt complexes containing bidentate ligands, a reaction pathway was proposed to arrive at an intermediate species such as complex **2-32** (Scheme 2.9). This complex is vital to the hydroformylation mechanism since subsequent hydrogenolysis forms the nonanal product and regenerates the active catalyst. Complex **2-17** was used as a model compound since it demonstrated good activity and selectivity in the hydroformylation study (**Chapter 3**).

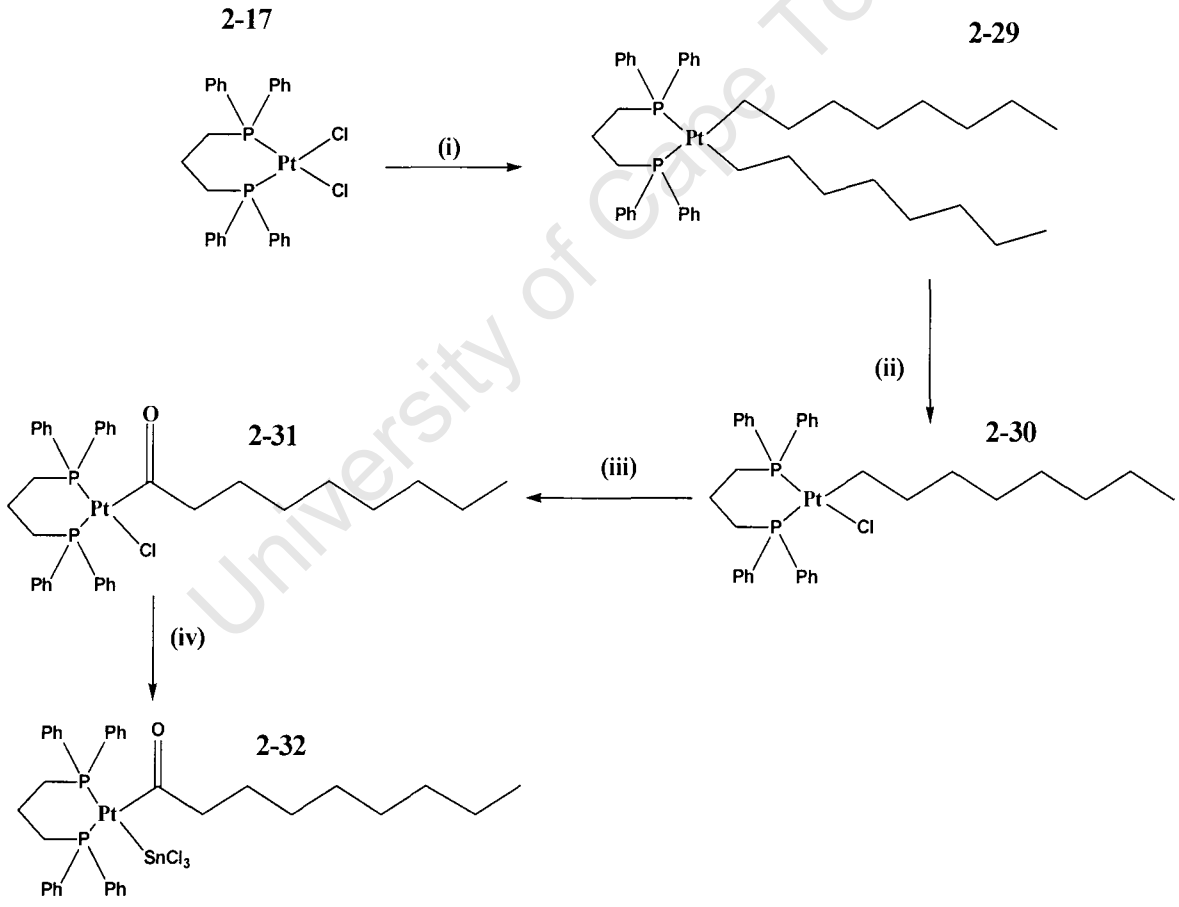

Scheme 2.9: Reaction Pathway: (i) $MgBr((CH_2)_7CH_3)$, Et_2O (ii) HCl, Et_2O (iii) CO, CH_2Cl_2 (iv) anhydrous $SnCl_2$, CH_2Cl_2.

2.10.3. Synthesis of [cis-Pt{$(CH_2)_7CH_3$}$_2$(dppp)] (2-29)

Complex **2-29** was prepared by reacting **2-17** with an excess of an octyl Grignard reagent in diethyl ether. This compound was previously prepared by Sivaramakrishna *et al.* in 2007.[65] The complex was isolated as an air stable yellow solid with a melting range between 85-87 °C. The ^{1}H NMR spectrum ($CDCl_3$) displayed peaks for the aliphatic protons of the alkyl chains between δ 2.49 - 2.69 ppm. The ^{31}P NMR spectrum displayed a singlet peak flanked by platinum satellites at δ 3.4 ppm (^{1}J(Pt-P) = 1601 Hz).[65]

2.10.4. Attempted synthesis of [PtCl{$(CH_2)_7CH_3$}(dppp)] (2-30)

The formation of **2-30** was a key step in the synthetic pathway since the target compounds **2-31** and **2-32** could then be accessed. A compound similar to complex **2-30,** containing an octenyl chain as opposed to an octyl chain, was prepared by Sivaramakrishna *et al.* in 2008.[66] Two methods have previously been used to cleave one alkyl chain from a Pt-bis(alkyl) compound i.e. by slowly adding a solution of HCl in Et_2O or by adding acetyl chloride to a methanol solution and producing the HCl *in situ.*[62]

Numerous attempts at reacting **2-29** with molar equivalents of HCl (0.01 M) resulted in the cleaving of both alkyl chains producing complex **2-17**, clearly evident from the ^{31}P NMR spectrum. This suggested that the concentration of the solution was greater than expected, resulting in rapid formation of the Pt-dichloride species **2-17** instead of the Pt-chloro-octyl species **2-30**. Since, the HCl solution was standardised prior to use, a possible explanation is that Et_2O evaporated readily during addition to the reaction mixture, increasing the HCl concentration and promoting formation of **2-17** rather than **2-30**. Shorter (0.5-3 h) and longer (5-10 h) reaction times as well as the exclusion of chlorinated solvents also produced **2-17**. Presumably, complex **2-30** forms prior to **2-17**. Thus, the reaction rate of **2-30** to **2-17** was faster than that of **2- 29** to **2-30**.

The reaction of **2-29** with acetyl chloride in methanol was also carried out in an attempt to isolate complex **2-30.** After numerous attempts at various reaction conditions, a mixture of **2-17** as well as **2-30** was observed when acetyl chloride was added to a solution of **2-29** in methanol at 0 °C. The ^{31}P NMR spectrum displayed a singlet peak for **2-17** as well as two doublet resonances flanked by platinum satellites resulting from the non-equivalent phosphorus atoms of **2-30**. Also evident from the ^{31}P NMR was that the major product was complex **2-17**. This provided evidence that the formation of **2-17** from **2-30** was indeed the favoured and far more rapid reaction. The solid containing both **2-17** and **2-30** was highly insoluble in most common organic solvents and after numerous attempts at separation, a pure sample of exclusively compound **2-30** was not obtained. Thus, the reaction pathway was not investigated further. More dilute acid solutions and longer reaction times at low temperatures may be required to reduce the reaction rate and isolate **2-30** exclusively.

2.10.5. Synthesis of [PtCl($SnCl_3$)(dppp)] (2-33)

Scheme 2.9 shows that formation of complex **2-30** was to be followed by a reaction with CO to produce the desired Pt-acyl species **2-31**. Therafter, a reaction with $SnCl_2$ produces the Pt-$SnCl_3$ species **2-32**. The reaction of **2-17** with $SnCl_2$ was carried out to observe the formation of the Pt-$SnCl_3$ bond. A pale yellow solid was isolated when **2-17** was reacted with anhydrous $SnCl_2$ in toluene at room temperature. Elemental analysis of the product identified the complex as [PtCl($SnCl_3$)(dppp)] (**2-33**). The product readily formed a white suspension upon addition of most common organic solvents such as dichloromethane, chloroform and acetone. NMR spectroscopy revealed that the white product formed was complex **2-17**, thus the Pt-$SnCl_3$ bond proved to be a weak bond that dissociates when exposed to chlorinated or oxygenated solvents.

2.11. Conclusion

A series of aminodiphosphine ligands of the type X-N($Ph_2P)_2$ (where X = benzyl, 2-picolyl, ^{n}Pr, *p*-anisidyl, 4-nitro-anilyl, ^{i}Pr) and subsequently a series of metal complexes of the type [MCl_2{X-N($Ph_2P)_2$}] (where M = Pt, Pd; X = benzyl, 2-picolyl, ^{n}Pr) were prepared. A range of spectroscopic and analytical techniques including NMR and IR spectroscopy, elemental analysis and mass spectrometry were applied to characterize the ligands and complexes. Physical methods such as melting point determinations as well as experimental yields and observations also assisted in synthesis and characterization. Detailed analysis, particularly of NMR data, allowed for differentiation between complexes that varied only slightly in molecular structure. Palladium complex **2-11** as well platinum complexes **2-15** and **2-16** are new complexes.

In addition, a series of platinum complexes consisting of diphosphine ligands of the type [$PtCl_2$(P-P)] (where (P-P) = dppp, dppe, dcpp, dbpp, dnpe) have been prepared of which [$PtCl_2$(dnpe)] (**2-21**) has not previously been reported. The complexes containing aminodiphosphine ligands have not previously been tested in hydroformylation. Thus, the diphosphine systems may provide an insightful means of comparison for relative catalytic activity. The platinum complexes were further employed as potential catalysts in the hydroformylation of 1-octene. The results of these studies will be discussed in **Chapter 3**.

Hydroformylation using platinum complexes containing bidentate ligands requires further investigation as the complete mechanism is still to be fully uncovered.[11] Previous studies have shown that the hydroformylation reaction may take place *via* cationic square-planar intermediates such as **2-27** and **2-28** (Scheme 2.8).

Attempts in this project to isolate possible intermediates has proven challenging since complexes such as **2-31** and **2-32** are vital to understanding the mechanism but not easy to access synthetically. The Pt-$SnCl_3$ bond was found to be weakly coordinated lending evidence that the role of $SnCl_3$ is to provide a vacant coordination site as it is a better leaving group than Cl^-.[16]

2.12. References

1. B. Cornils, W. A. Herrman, *Applied Homogeneous Catalysis with Organometallic Compounds*, Vol 1, Wiley-VCH, Weinheim, 2002, pp 29-33.
2. J. A. Godfrey, R. A. Searles, *Chemie-Technik*, 1981, **10**, 1271.
3. B. Cornils, L. Marko, *Methoden Org. Chem. (Houben-Weyl), 4th Ed*, 1986, Vol E18, 759.
4. J. Gauthier-Lafaye, R. Perron, *LActualite Chimique*, *Mars/Avril*, 1989, 49.
5. E. Drent, W. W. Jager, Shell Int. Res., GB 2.282.137, 1995.
6. C. Abu-Gnim, I. Amer, *J. Chem. Soc., Chem. Commun.*, 1994, 115.
7. A. Bader, E. Lindner, *Coord. Chem. Rev.*, 1991, **108**, 27.
8. C. Vaecher, A. Mortreux, F. Petit, J. P. Picaret, H. Sliwa, N. W. Murall, A. J. Welch, *Inorg. Chem.*, 1985, **24**, 2338.
9. S. Gladiali, L. Pinna, C. G. Arena, E. Rotondo, F. Faraone, *J. Mol. Catal.*, 1991, **66**, 183.
10. C. A.Ghilardi, S. Midollini, S. Moneti, A. Orlandini, G. Scapacci, *J. Chem. Soc., Dalton Trans.*, 1992, **23**, 3371.
11. R. E. Rülke, V. E. Kaasjager, P. Wehman, C. J. Elsevier, P. W. N. M van Leeuwen, K.Vrieze, *Organometallics*, 1996, **15**, 3022.
12. J. C. Jeffery, T. B. Rauchfuss, P. A. Tucker, *Inorg. Chem.*, **19**, 3306.
13. G. Petőcz, G. Rangits, M. Shaw, H. de Bod, D. B. G. Williams, *J. Org. Chem*, 2009, **694**, 219.
14. K. G. Gaw, M. B. Smith, J. W. Steed, *J. Organomet. Chem.*, 2002, **664**, 294.
15. A. M. Z. Slawin, H. L. Milton, J. Wheatley, J. D. Woollins, *Polyhedron,* 2004, **23**, 3125.
16. Z. Fei, R. Scopeletti, P. J. Dyson, *Eur. J. Inorg. Chem.*, 2003, 3527.
17. T. Appleby, J. D. Woollins, *Coord. Chem. Rev.*, 2002, **235**, 121.
18. H. H. Sisler, L. Smith, *J. Org. Chem.*, 1961, **26**, 611, 4733.
19. K. D. Berlin, G. B. Butler, *Chem. Rev.*, 1960, **60**, 243.
20. N. Biricik, F. Durap, C. Kayan, B. Gümgüm, N. Gurbuz, I. Ozdemir, W. Han Ang, Z. Fei, R. Scopelliti, *J. Org. Chem.*, 2008, **693**, 2693.
21. I. Bachert, P. Braunstein, R. Hasselbring, *New J. Chem*, 1996, **20**, 993.
22. J. Reedijk, *J. Chem. Soc., Chem. Commun.*, 1996, 801.
23. P. Bhattacharya, T. Q. Ly, A. M. Z. Slawin, J. D. Woollins, *Polyhedron*, 2001, **20**,

1803.

24. B. Gümgüm, O. Akba, F. Durap, L.T. Yildirim, D. ÜLkü, S.Özkar, *Polyhedron*, 2006, **25**, 3133.
25. S. Goldschmidt, H. L. Krauss, *Annalen*, 1955, **595**, 193.
26. R. Jefferson, R. Keat, J. F. Nixon, T. M. Painter, L. Stobbs, *J. Chem. Soc., Dalton Trans.*, 1973, 1414.
27. H. Noth, L. Meinel, *Inorg. Chem.*, 1967, **349**, 225.
28. R. J. Cross, T. H. Green, R. Keat, *J. Chem. Soc., Dalton Trans.*, 1976, **14**, 1424.
29. A. H. Cowley, M. J. S. Dewar, W. R. Jackson, W. B. Jennings, *J. Am. Chem. Soc.*, 1970, **92**, 5206.
30. E. Hedburg, L. Hedburg, K. Hedburg, *J. Am. Chem. Soc.*, 1974, **96**, 4417.
31. G. Ewart, A. P. Lane, J. Mckechnie, D. S. Payne, *J. Chem. Soc.*, 1964, 1543.
32. Killian, K. Blann, A. Bollmann, J. T. Dixon, S. Kuhlmann, M. C. X. Maumela, H. Maumela, D. H. Morgan, P. Nongodlwana, M. J. Overett, M. Pretorius, K. Hofener, P. Wasserscheid, *J. Mol. Catal.*, 2007, **270**, 214.
33. M. Filby, A. J. Deeming, G. Hogarth, M. Lee, *Can. J. Chem.*, 2006, **84**, 319.
34. B. Holmstedt, L. Larsson, *Acta. Chem. Scand.*, 1951, **5**, 1179.
35. J. E. Mayhood, B. Harvey, *Canad. J. Chem.*, 1955, **33**, 1552.
36. R. A. McIvor, C. E. Hubley, *Canad. J. Chem.*, 1959, **57**, 869.
37. D. A. Slack, and M. C. Baird, *Inorg. Chim. Acta*, 1977, **24**, 277.
38. I. Pantcheva, K. Osakada, *Organometallics,* 2006**, 25**, 1735.
39. M. Harada, Y. Kai, N. Yasuoka, N. Kasal, *Bull. Chem. Soc. Jpn.,* 1979, **52**, 390 394.
40. R. McCrindle, G. J. Arsenault, A. Gupta, M. J. Hampden-Smith, R. E. Rice, A. J. McAlees, *J. Chem. Soc. Dalton Trans.*, 1991, 949.
41. L. Kollar, P. Sandor, G. Szalontai, B. Heil, *J. Org. Chem.*, 1990, **393**, 153.
42. P. Dierkes, P. W. N. M van Leeuwen, *J. Chem. Soc., Dalton Trans.*, 1999, 1519.
43. R. W. Glyde, R. J. Mawby, *Inorg. Chem.*, 1971**, 10**, 854.
44. C. J. Wilson, M. Green, R. J. Mawby, *J. Chem. Soc., Dalton Trans.*, 1974, 421.
45. P. E. Garrou, R. F. Heck, *J. Am. Chem. Soc.,* 1976, **98**, 4115.
46. N. Sugita, J. V. Minkiewich, R. F. Heck, *Inorg. Chem.,* 1978, **17,** 2809.
47. G. K. Anderson, R. J. Cross, *J. Chem. Soc., Dalton Trans.,* 1979**,** 1246.
48. M. Kubota, D. A. Phillips, J. E. Jacobsen, *J. Coord. Chem.,* 1980, **10**, 125.
49. G. K. Anderson, H. C. Clark, J. A**.** Davies, *Organometallics,* 1982**, 1,** 64**.**

50. K. G. Anderson, R. J. Cross, *Ace. Chem. Res.,* 1984, **17,** 67.

51. M. Gomez, G. Muller, D. Sainz, J. Sales, *Organometallics,* 1991, **10,** 4036.

52. P. J. Stang, Z. Zhong, A. M. Arif, *Organometallics,* 1992**, 11**, 1017.

53. A. Scrivanti, C. Botteghi, L. Toniolo, A**.** Berton, *J. Organomet. Chem.,* 1988**,** **344**, 261.

54. G. P. C. M. Dekker, A. Buijs, C. J. Elsevier, K. Vrieze, P. W. N. M. van Leeuwen, W. J. J. Smeets, A. L. Spek, Y. F. Wang, C. H. Stam, *Organometallics,* 1992**, 11**, 1937.

55. G. K. Anderson, G. J. Lumetta, *Organometallics,* 1985**, 4,** 1542.

56. A. Scrivanti, A. Berton, L. Toniolo, A. Berton, C. Botteghi, *J. Organomet. Chem.*, 1986, **314**, 369.

57. H. C. Clark, J. A. Davies, *J. Organomet. Chem.*, 1981, **213,** 503.

58. Tóth, T. Kégl, C. J. Elsevier, L. Kollár, *Inorg. Chem.*, 1994, **33**, 5708.

59. T. Kégl, L. Kollár, L. Radics, *Inorg. Chim. Acta.*, 1997, **265**, 249.

60. L. Kollár, S. Gladiali, M. J. Tenorio, W. Weissensteiner, *J. Cluster Sci.*, 1998, **9**, 321.

61. C. J. Moulton, B. L. Shaw, *J. Chem. Soc., Chem. Commun.*, 1976, 365.

62. D. A. Slack, M. C. Baird, *Inorg. Chim. Acta*, 1977, **24**, 277.

63. K. A. O. Starzewski, H. Ruegger, P. S. Pregosin, *Inorg. Chim. Acta*, 1979, **36**, L445.

64. F. Lancillotti, M. Lami, M. Marchionna, *XVI Congress of Italian Chemical Society*, Abstract no. O16.

65. A. Sivaramakrishna, H. Su, J. R. Moss, *Organometallics*, 2007, **26**, 5786.

66. A. Sivaramakrishna, H. Su, J. R. Moss, *Dalton Trans*, 2008, 2228.

Chapter 3

Hydroformylation of 1-octene using platinum complexes containing bidentate ligands

3.1. Hydroformylation of 1-octene using [$PtCl_2$(dppp)] (2-17)

The complex [$PtCl_2$(dppp)] was tested in the hydroformylation of 1-octene at various reaction times to identify a period that would yield a suitable conversion. Short reaction times of 3 to 4 h resulted in 0 % conversion of the substrate while extended reaction times of 18 to 20 h resulted in complete (100 %) conversion. Although complete conversion suggests good activity of the catalyst, it is of greater importance to analyze the performance of the catalyst when conversion is slightly below 100 %. This gives a more accurate indication of the selectivity from the aldehydes formed by ensuring that they do not undergo further reactions (e.g. aldol condensation) to form what is referred to as 'heavies' due to extended periods in the reaction mixture at high temperature and pressure. In addition, in the absence of gas uptake data, the % conversion over the same time period for different systems can be used as a relative indication of activity. For an 8 h reaction, the conversion obtained was 92 % (Table 3.1).

Table 3.1: Hydroformylation of 1-octene using [$PtCl_2$(dppp)]/$SnCl_2$.

Complex	**[$PtCl_2$(dppp)]/$SnCl_2$**
Conversion (%)	92
Heavies (%)	22
Hydrogenation (%)	21
Yield Nonanal (%)	57
Linearity (%)	58
n:i	1.9
TOF (mol 1-octene/(mol Pt.h))	1351

Reaction conditions: 80 bar syngas ($CO:H_2$ = 1:1), 100 °C, 600 rpm stirring, 8 h, n[$PtCl_2$(dppp)]:n($SnCl_2$) = 1:1.

The reaction produced a good nonanal yield of 57 % and showed good selectivity for the linear aldehyde as indicated by the 58 % linearity of the products. The reaction times studied were 3, 4, 8, 14, 18 and 20 h using this catalyst system. The 3 to 4 hr catalytic runs were initially attempted as these were the reaction times previously reported using this catalyst in the hydroformylation of styrene.[1] Kollar *et al.* used an autoclave reactor, a thermostated oven for heating and an arm shaker for mixing when they carried out the hydroformylation. Thus, the substrate and reaction equipment used in that study were different to those used in the present study (1-octene, pipe reactors and stirrer/hot plates) which may explain why there is a discrepancy in the reaction time required to obtain good conversions.

Figure 3.1 depicts the trend observed for the conversion of 1-octene with time. The plot shows that little or no conversion takes place between 3 to 4 hr and that there is a steep increase in conversion from 4 to 8 hours (0 – 92 %). This increase in conversion suggests a direct relationship between conversion and time during this period. The behaviour suggests that the catalyst requires an induction period before promoting rapid conversion of the substrate. Thereafter, a much smaller increase in the conversion (92 – 100 %) from 14 to 20 hours is observed. This considerably slower reaction at a later stage can be attributed to the hydroformylation of internal olefins produced as a result of isomerisation of the substrate.

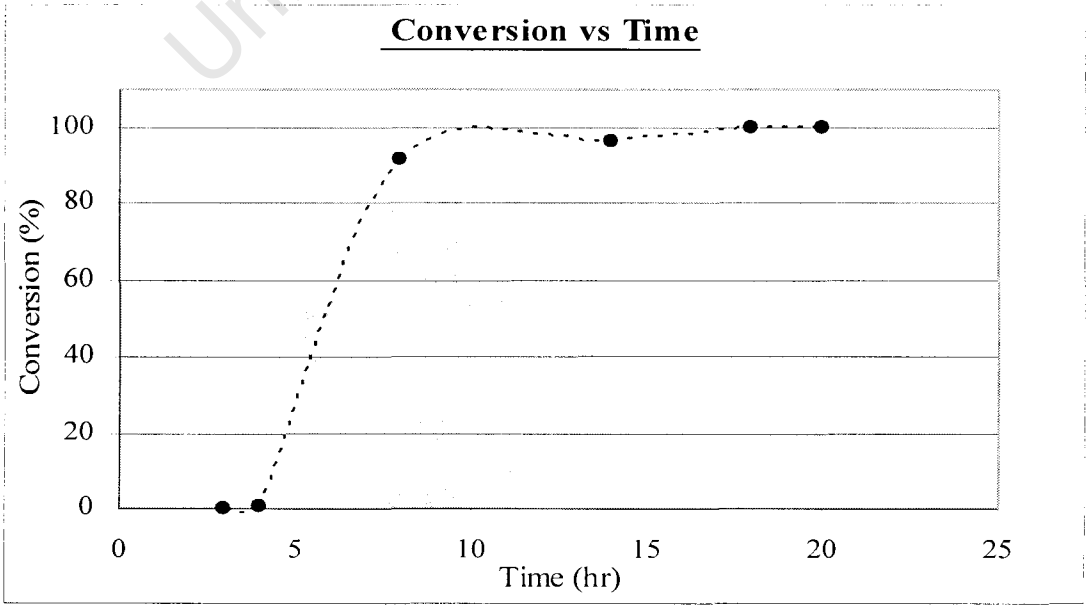

Figure 3.1: Conversion of 1-octene vs Time using a $[PtCl_2(dppp)]/SnCl_2$ catalyst.

When considering the yield of nonanal over time it would be useful to study the period between which we observe good conversion, thus excluding the points at 3 and 4 hours (Figure 3.2). The nonanal yield increased between 8 to 18 hours from 57 – 61 %. Thereafter a slight decrease in the yield was observed between 18 to 20 hours. This behaviour indicates that the nonanal yield increases with time until complete conversion is reached, after which time the yield of nonanal starts to diminish. Since the nonanal yield is expressed as a percentage of moles of nonanal produced per mole of 1-octene converted, we can conclude that the quantity of nonanals in the product mixture have been reduced as the mole of 1-octene converted remains unchanged. This suggests that nonanals that have accumulated in the reaction mixture have now been utilized in subsequent reactions to form aldol condensation products.

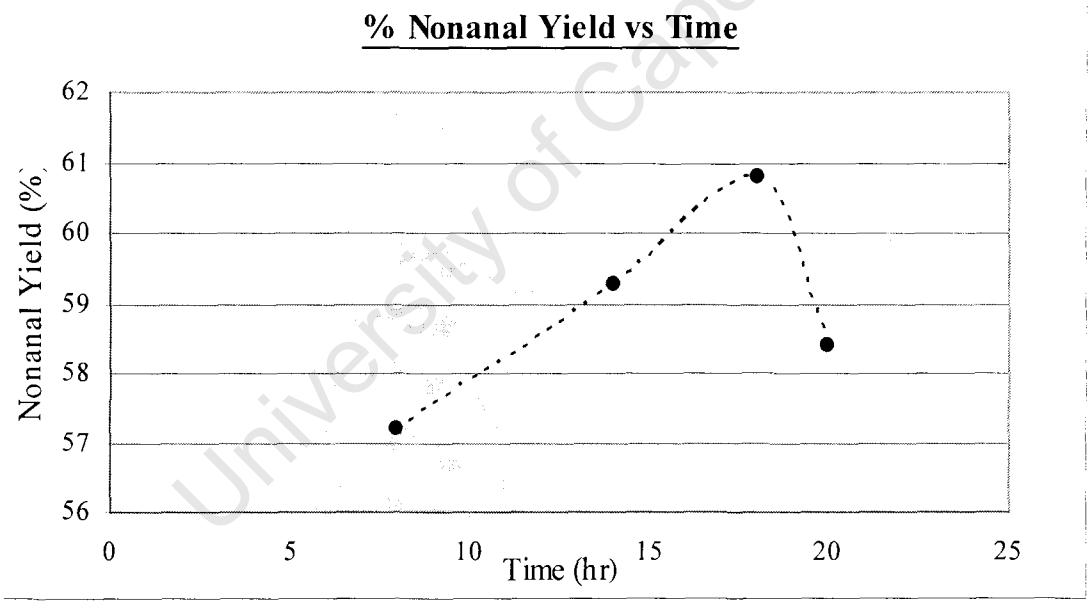

Figure 3.2: Nonanal yield vs Time using a $[PtCl_2(dppp)]/SnCl_2$ catalyst.

Figure 3.3 indicates that the hydrogenation of 1-octene fell within a range of 19.6 ± 1.5 % for all reaction times.

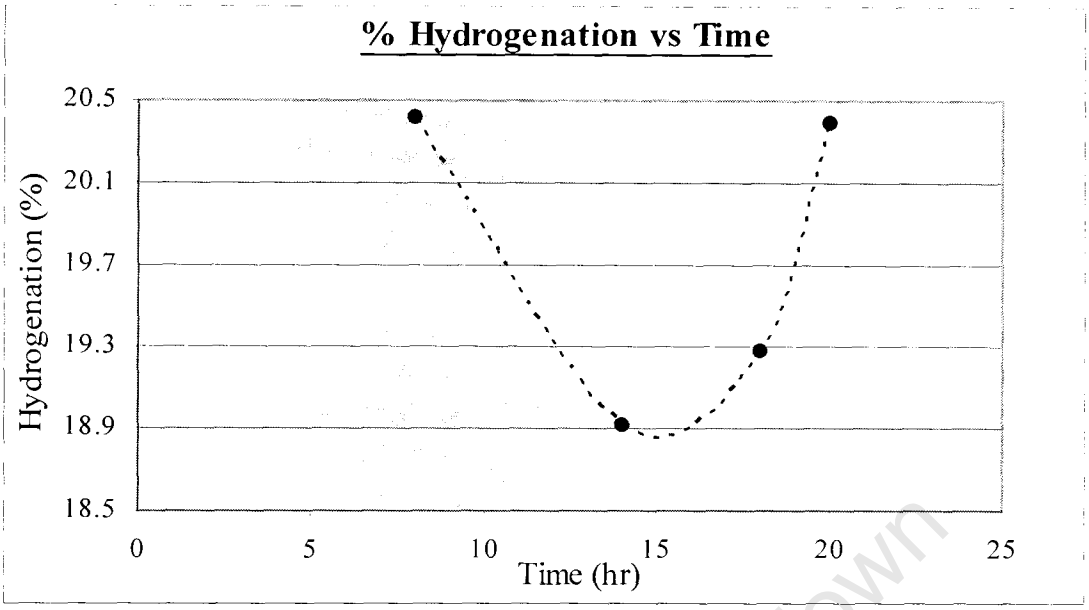

Figure 3.3: Hydrogenation vs Time using a $[PtCl_2(dppp)]/SnCl_2$ catalyst.

The plot of linearity versus time (Figure 3.4) shows 58.5 – 59.9 % linearity from 8 to 18 hours and then a significant decline in linearity from 18 to 20 hours. This is evidence that the formation of branched products increases after 18 h and linear aldehyde products are being depleted. This can be attributed to the hydroformylation of isomerised 1-octene prevalent at this stage contributing to a greater quantity of branched aldehydes. Also, this supports the hypothesis that linear aldehydes produced undergo subsequent condensation reactions if left for extended periods in the product mixture.

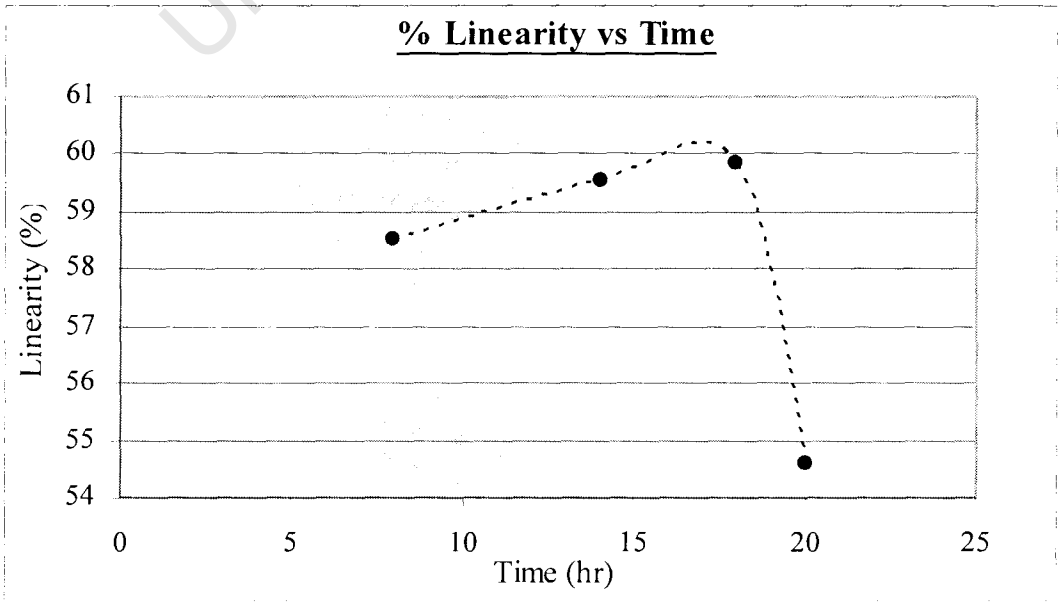

Figure 3.4: % Linearity vs Time using a $[PtCl_2(dppp)]/SnCl_2$ catalyst.

Since the turnover frequency (TOF) is a measure of the moles of 1-octene converted per mole of catalyst used per hour, an inverse relationship between TOF and time is expected once the catalyst has been activated. This trend is observed after 8 hours in this system as shown in Figure 3.5. We observe a steady decline in the TOF because substrate conversion is approaching 100 % i.e the moles of 1-octene converted does not change considerably but reaction times are extended.

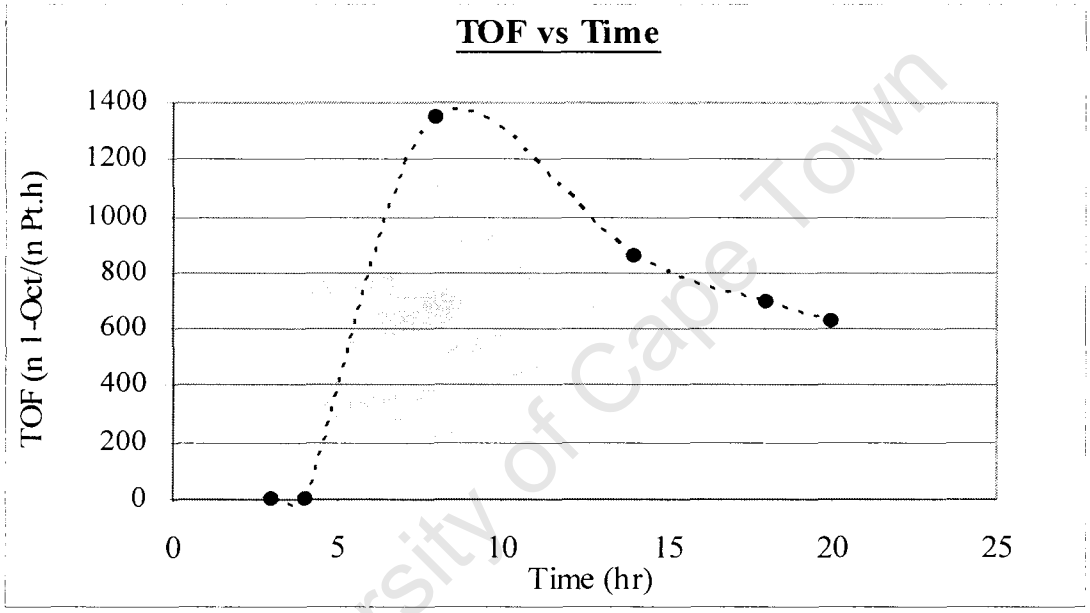

Figure 3.5: TOF vs Time using a $[PtCl_2(dppp)]/SnCl_2$ catalyst.

3.2. Hydroformylation of 1-octene using Pt complexes containing aminodiphosphine ligands (2-13 to 2-15)

Complexes **2-13** to **2-15** were tested in the hydroformylation of 1-octene. Complex **2-17** was tested simultaneously under identical reaction conditions to compare relative activity (Table 3.2).

Table 3.2: Complexes tested for their hydroformylation activity.

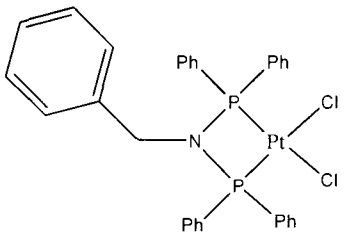 **(2-13)**	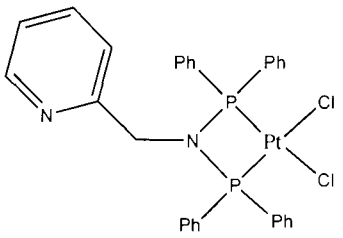 **(2-14)**
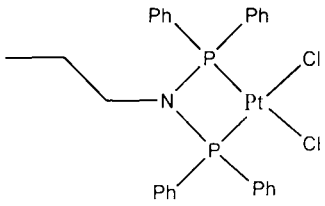 **(2-15)**	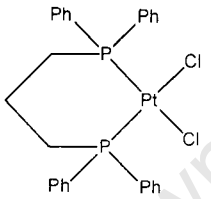 **(2-17)**

Complexes **2-13** to **2-15** fit the criteria of platinum complexes containing a bidentate diphosphine ligand with the added effect of an amino group coordinated to both phosphorus atoms. The complexes are air stable solids (m.p > 300 °C) due to strong coordination to the metal centre provided by the phosphorus atoms. However, the stability of the complexes under hydroformylation conditions and their ability to promote alkene coordination due to structural constraints are factors which the catalysis would assist in determining.

These complexes exhibited low activity when subjected to 80 bar syngas at 100 °C for short periods of 3 to 4 hours and the conversion obtained was less than 1 % for all three complexes. When the reaction time was increased to 20 hours the conversion increased to 4 %, 2 % and 5 % for **2-13**, **2-14** and **2-15** respectively (Table 3.3).

Table 3.3: Hydroformylation of 1-octene using complexes **2-13** to **2-15** with $SnCl_2$.

Complex	**2-17**	**2-13**	**2-14**	**2-15**
Conversion (%)	100	4	2	5
Hydrogenation (%)	20	19	23	19
Yield Nonanal (%)	58	26	23	22
Linearity (%)	55	85	77	85
n:i	1.7	6	3	6
TOF (mol 1-octene/ (mol Pt.h))	626	23	10	28

Reaction conditions: 80 bar syngas ($CO:H_2$ = 1:1), 100 °C, 600 rpm stirring, 20 h, Pt:Sn = 1:1.

Increasing the length of reaction time did not greatly increase the conversion. This suggests that the complexes were retarding the catalytic reaction and either a structural or electronic effect was causing the low activity rather than an induction period required for the catalysis to commence as was the case with catalyst **2-17**. Alternatively, catalyst decomposition may have resulted in the catalyst system deactivating.

The hydrogenation observed for complexes **2-13** and **2-15** (19 %) was similar to **2-17** (20 %), while it was slightly higher for complex **2-14** (22 %). This is an interesting observation since **2-14** has the added electronic effect of the nitrogen on the pyridyl group of the ligand when compared to **2-13,** suggesting that this functional group is increasing the hydrogenating ability of the catalyst.

The yield of nonanal was considerably lower than that observed for **2-17** at 26 %, 23 % and 22 % for **2-13**, **2-14** and **2-15** respectively. This coincides with the low conversions achieved by these catalysts.

Surprisingly, a high percentage of the products formed were linear aldehydes as reflected by the 85 %, 77 % and 85 % linearity for **2-13**, **2-14** and **2-15** respectively. This was considerably higher than the linearity achieved by complex **2-17** (55 %), suggesting that these catalysts are contributing to a considerable steric effect resulting

in the formation of predominantly linear aldehydes. However, due to the low conversions of these catalysts the high linearity observed cannot be emphasized since the formation of branched aldehydes may be underestimated.

Hayashi *et al.* found that diphosphine ligands with rigid ring skeletons resulted in remarkable linearity in the platinum catalyzed hydroformylation of 1-pentene.[3] The significant linearity found in this study provides evidence that the low activity exhibited by complexes **2-13** to **2-15** under hydroformylation conditions is a result of structural features of the ligand backbone rather than electronic properties.

Complex **2-14** containing the picolylamino group showed the lowest conversion and its counterparts were almost twice as active in the catalysis. Since complexes **2-13** and **2-14** differ only in the group attached to the nitrogen we can attribute the lower activity of **2-14** to the presence of the pyridyl group. Complex **2-15** containing a propylamino group was more active than its counterparts as demonstrated by the superior TOF and conversion. Thus, the benzylamine and picolylamine groups present on complexes **2-13** and **2-14** respectively have proven to be unfavorable substituents when considering the hydroformylation ability of these catalysts.

Kollar *et al.* carried out the Pt/Sn-catalyzed hydroformylation of styrene in the presence of amine additives.[1] They reported that the very basic amines such as Et_3N obstructed the reaction completely. This effect was attributed to the abstraction of $HSnCl_3$ by an amine from the [PtH(diphosphine)($SnCl_3$)] intermediate which renders the catalyst inactive.[4] Thus, the interference of the nitrogen atoms of the ligands used in our study with intermediates in the hydroformylation cycle cannot be ruled out as a possible cause of low activity.

The bite angle of these complexes is also a factor which needs to be taken into account when considering activity. The natural bite angle has been reported to have a decisive effect on activity, stability and selectivity in hydroformylation studies.[5,6] This parameter can be obtained by molecular mechanics calculations and has been extensively applied for diphosphine ligands.[7] The bite angle can further be described as a combination of two different effects. The first, the steric bite angle effect is related to the steric interactions such as ligand-ligand or ligand-substrate interactions.

This effect occurs when the backbone of the ligand is modified while the substituents at the phosphorus atom remain the same. Activity and selectivity of a catalytic system can be varied when the steric interactions cause changes in energies of the transition and catalyst resting states.[7] The second effect, the electronic bite angle effect is the electronic changes incurred when the bite angle is changed.[8] This effect is essentially an orbital effect as the bite angle determines metal hybridization which in turn influences metal orbital energies and reactivity. This effect also contributes to the overall stability of transition states in a reaction. These two bite angle effects can be differentiated but work mutually when the bite angle is varied in diphosphine systems. Although it is not always clear which of the two effects is the reason for activity or selectivity obtained, rational design of ligands can lead to conclusions that changes are due to mainly one of these two effects.

Many examples, especially in Pt(diphosphine)/Sn systems, show that catalytic efficiency is directly related to bite angle.[3,9] Dierkes *et al.* reported a good agreement between ligand bite angles obtained from molecular modelling calculations and those observed from the crystal structures.[8] In the case of complexes **2-13** and **2-14** these bite angles are 72.54° and 72.71° respectively.[8,10] This correlates well with the bite angle and activity of the platinum complex containing the ligand dppm (71.53°) which proved almost ineffective in the platinum catalyzed hydroformylation of 1-pentene.[3]

Work performed on the Rh catalyzed hydroformylation of 1-octene using a family of xanthphos ligands provided evidence that the steric bite angle effect had a significant effect on regioselectivity as well.[11-13] Ligands with larger bite angles were proposed to increase steric congestion around the metal centre favouring the less sterically demanding transition state and assisting the reaction in producing predominantly the linear aldehyde.[7] The studies also showed that ligands with exceptionally large bite angles showed sharp increases in reaction rates. Since steric effects have little influence in the CO insertion reactions, the elevated rates were proposed to be a result of a more stabilised square planar Rh intermediate. This led to the hypothesis that faster migratory insertion was taking place and therefore a higher concentration of [RhH(diphosphine)(CO)] intermediates were present which accelerated the reaction.[7]

3.3. Hydroformylation of 1-octene using Pt complexes containing alkyldiphosphine ligands (2-18 to 2-21)

The bridging group located between the two phosphorus atoms on the bidentate diphosphine ligands has proven to be an important functionality in hydroformylation catalysts.[3] This bridging group would be the three-carbon chain present in **2-17**. Studies have shown that the length of the carbon chain dramatically affects the catalytic activity since [$PtCl_2$(dppm)] complexes show little activity while [$PtCl_2$(dppb)] complexes show very high activity. More than 4 carbons on this alkyl chain have been reported to reduce activity again.[3]

The substituents on each phosphorus atom such as the phenyl groups in **2-17** have also been found to affect overall activity. An interesting study and the one which was carried out next was to observe the influence that various substituents on the phosphorus atoms had on the overall activity.

The remarkable activity of complex **2-17** confirmed that the presence of a flexible bridging group in the backbone of the bidentate ligand, as well as the phenyl substituents on the phosphorus atoms are vital components of a highly active hydroformylation catalyst. Thus, a series of complexes which are variations of complex **2-17** were tested to provide further insight into the influence of particular functional groups on overall activity (Table 3.4). The activities and selectivities observed using these complexes in the hydroformylation of 1-octene is shown in Table 3.5.

Table 3.4: Complexes tested for their hydroformylation activity.

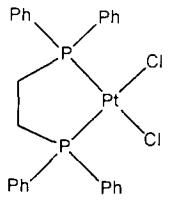 **2-18**	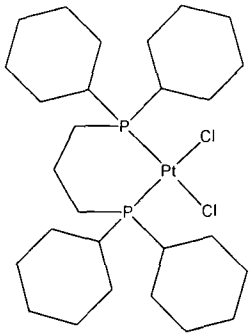 **2-19**
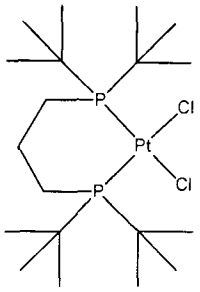 **2-20**	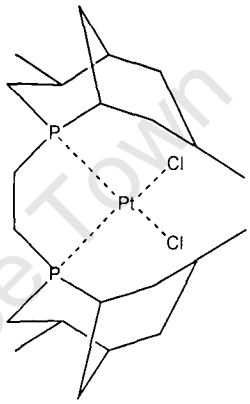 **2-21**

Table 3.5: Hydroformylation of 1-octene using complexes **2-18** to **2-21** with $SnCl_2$.

Complex	**2-18**	**2-19**	**2-20**	**2-21**
Conversion (%)	68	6	4	15
Hydrogenation (%)	46	12	31	5
Yield Nonanal (%)	41	72	51	64
Linearity (%)	87	98	90	97
n:i	7	60	37	28
TOF (mol 1-octene/(mol Pt.h))	610	50	36	101

Reaction conditions: 80 bar syngas ($CO:H_2$ = 1:1), 100 °C, 600 rpm stirring, 14 h, Pt:Sn = 1:1.

Complex **2-18** showed good activity after 14 h and this was not surprising as the structural properties of **2-18** are similar to that of **2-17** (Table 3.5). The only structural difference was the presence of a two-carbon instead of a three-carbon bridging group in the ligand backbone. This proved to have a significant effect on the catalysis since

96 % conversion was achieved after 14 hours using **2-17** while **2-18** achieved only 68 % conversion over the same reaction time.

Table 3.6 shows the activity and selectivity of these two catalysts under identical reaction conditions. Firstly, **2-17** achieves a higher conversion of the substrate. Complex **2-18** produces a lower nonanal yield (41 % vs 59 %) but superior linearity (87 % vs 60 %). Also, complex **2-18** produces 28 % more hydrogenated products than **2-17**. The quantity of heavies produced was less than 20 % for both catalysts. The results indicated that reduced flexibility in the bridging group on these ligands lowered the conversion achieved as well as nonanal yield but increased the linearity of the aldehyde products.

Table 3.6: Hydroformylation of 1-octene using complexes **2-17** and **2-18** with $SnCl_2$.

Complex	**2-17**	**2-18**
Conversion (%)	96	68
Hydrogenation (%)	18	46
Yield Nonanal (%)	59	41
Linearity (%)	60	87
n:i	2.1	7
TOF (mol 1-octene/(mol Pt.h))	862	610

Reaction conditions: 80 bar syngas ($CO:H_2$ = 1:1), 100 °C, 600 rpm stirring, 14 h, Pt:Sn = 1:1.

Kollar *et al.* investigated the hydroformylation of styrene using complex **2-17** and **2-18**.[1] They reported that reasonable conversions were only achieved with diphosphine ligands that had the ability to form six or seven-membered chelate rings and that increasing ring size showed a marked decrease in hydrogenation. Also, **2-17** showed superior conversion, lower chemoselectivity and greater selectivity for the branched aldehyde when compared to **2-18** (Table 3.7).[1] The results reported are in agreement with those obtained in this study.[1]

Table 3.7: Hydroformylation of styrene using [Pt/($PPh_2(CH_2)_nPPh_2$/$SnCl_2$] catalysts.[1]

Diphosphine (n)	Conversion (%)	R[a] (%)	R_L[b] (%)
1	2 (4)[b]	80	45
2	9 (36)	72	28
3	76	86	73

Reaction conditions: 80 bar syngas ($CO:H_2$ = 1:1), 100 °C, 4 h.

[a] (mol aldehyde / mol substrate converted)*100.

[b] (mol linear aldehyde / mol aldehyde)*100.

Hayashi *et al.* reported that catalytic activity strongly depended on the length of the bridging group when catalysts of the type [($Ph_2P(CH_2)_nPh_2P$)$PtCl_2$/$SnCl_2$] (n = 1 - 4) were tested in the hydroformylation of 1-pentene.[3] They found that dppb was the most active bidentate diphosphine. The linearity achieved was in the range of 91–94 % and activity was found to be independent on the value of n. However, linearity was reduced to 69 % for n = 3. They attributed this effect to the steric repulsion due to the 1,3–diaxial phenyl groups on the phosphorus atoms causing instability in the six-membered chelate ring.[3]

The testing of catalyst **2-19** provided evidence that the phenyl substituents on the phosphorus atoms in **2-17** were important structural and electronic features for the performance of this catalyst (Table 3.5). The conversion obtained for **2-19** was 6 %, suggesting that electron withdrawing groups with a spatial arrangement such as that provided by the phenyl substituents are necessary for good activity. The co-planar spatial arrangement adopted by two phenyl groups in close proximity would provide sufficient space around the metal for alkene coordination and CO insertion reactions. Predominantly linear aldehydes were formed (98 %) emphasizing a significant steric contribution by the cyclohexyl substituents. The bridging group of **2-19** contains three carbons compared to the two carbons of **2-18**. Previous results indicate that this serves to improve activity but in this case the steric effect of the phosphorus substituents outweighs the flexibility induced by the longer bridging carbon chain.

Hayashi *et al.* found that diphosphine ligands with rigid ring skeletons resulted in remarkable linearity and this was attributed to the bulkiness of the ring skeletons causing a large steric hinderance or 'steric fence'. The proposed process of linear aldehyde formation from a terminal alkene is depicted in Scheme 3.2.[3] The scheme shows the favoured formation of the linear aldehyde which is more sterically feasible in the presence of bulky diphosphine ligands.

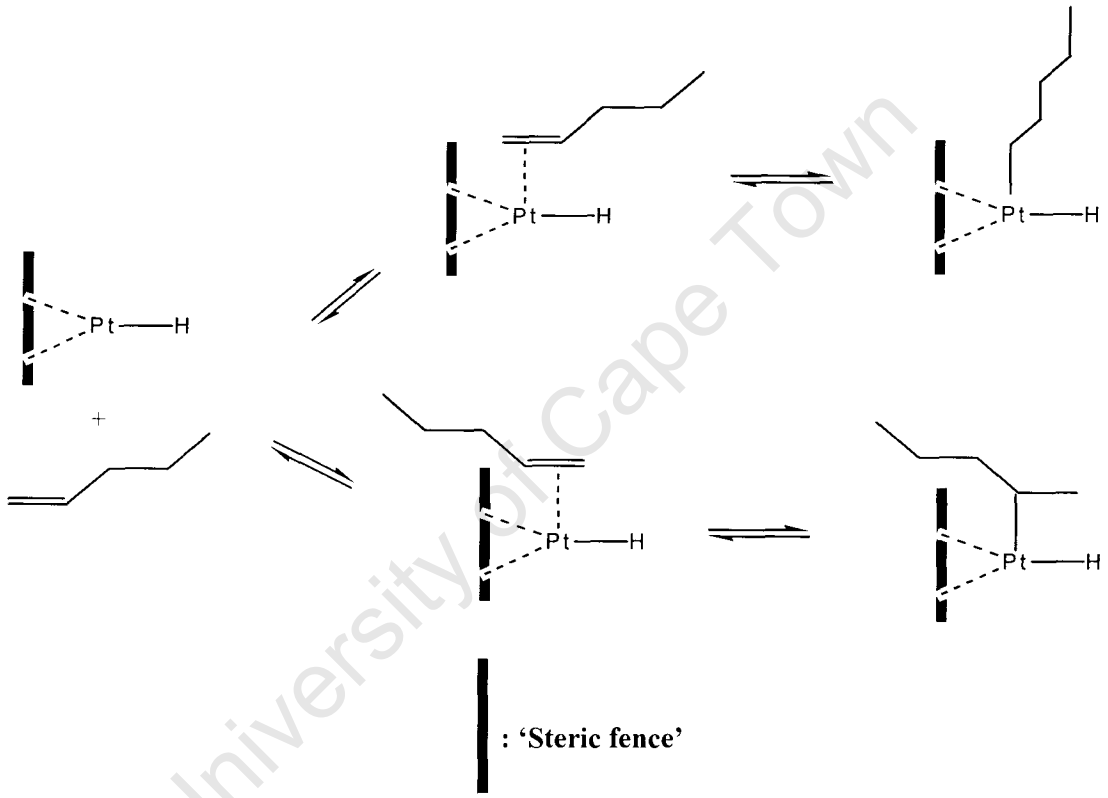

Scheme 3.2: Proposed process of linear and branched aldehyde formation from an alkene.

Complex **2-20** also contains bulky substituents on the phosphorus atoms and a three-carbon bridging chain giving reason to believe that the performance of the catalyst would be similar to that of **2-19**. As expected, the catalysts performed similarly to **2-19** with the only significant difference arising from the linearity of the products (98 % for **2-19** vs 90 % for **2-20**). Thus, the ^{t}Bu substituents on the phosphorus atoms have proven too sterically demanding and electronically unsuitable for efficient hydroformylation.

The catalytic testing of complex **2-21** provided an investigation using a platinum complex that also contains a bridging two-carbon chain between the phosphorus atoms and a bulky ligand system that has not previously been observed in platinum complexes. This tertiary bicyclic phosphine ligand and variations thereof have previously been used in the cobalt catalyzed hydroformylation of alkenes to good effect.[14] In this ligand system, the phenyl groups of **2-18** were replaced by 8-bicyclo–2-6-dimethylphospha(3.3.1)nonyl groups. The conversion obtained after 14 hours was 15 %, almost twice that of **2-19** and **2-20**. This was interesting since the ligand was expected to achieve similar conversions to its counterparts containing bulky ligands. The catalyst performed similarly to **2-19** with high linearity (97 %) and nonanal yield (64 %) but showed low hydrogenation of 1-octene (5 %) compared to catalysts **2-18**, **2-19** and **2-20**.

3.4. Conclusion

The hydroformylation reaction was used to investigate the catalytic activity of platinum complexes containing bidentate diphosphine ligands in the presence of $SnCl_2$. The complex $[PtCl_2(dppp)]$ (**2-17**) achieved 92 % conversion of 1-octene and a nonanal yield of 57 % after 8 hours at 100 °C using 80 bar syngas ($CO:H_2$ = 1:1).

Complexes of the type $[PtCl_2\{X\text{-}N(Ph_2P)_2\}]$ (X = benzyl (**2-13**), 2-picolyl (**2-14**), ^{n}Pr (**2-15**)), of which **2-15** was new, had not previously been tested in hydroformylation and showed low activity even after extended reaction times. This was attributed to the small bite angle of these complexes since $[PtCl_2(dppm)]$ consisting of a similar bite angle, previously showed comparable catalytic activity.

Complexes of the type $[PtCl_2(P\text{-}P)]$ (where (P-P) = dppe (**2-18**), dcpp (**2-19**), dbpp (**2-20**), dnpe (**2-21**)) showed significant activity and demonstrated that a combination of both steric and electronic effects contributes to the overall activity and selectivity of a hydroformylation catalyst. Surprisingly, new complex **2-21** containing a bulky ligand system showed higher activity than both its counterparts **2-19** and **2-20**.

Finally, we have re-established that the group linking the phosphorus atoms is an important feature of the ligand backbone in [$PtCl_2$(P-P)] complexes. The more flexible three-carbon chain such as that in [$PtCl_2$(dppp)] (**2-17**) has produced a more active catalyst as compared to the rigid two-carbon bridge present in [$PtCl_2$(dppe)] (**2-18**). The substituents on the phosphorus atoms have also proven to be vital in hydroformylation since catalyst **2-17** containing phenyl groups as substituents on the phosphorus atom exhibits 17 times higher activity than its cyclohexyl containing counterpart [$PtCl_2$(dcpp)] (**2-19**).

3.5. Future Work

From the results obtained in this study it is clear that the hydroformylation of 1-octene using platinum(II) complexes containing small bite angles (**2-13** to **2-15**) results in low catalytic activity. Future studies investigating the structural integrity of aminodiphosphine ligands under hydroformylation conditions will assist in explaining the diminished activity. The selectivity achieved by complexes **2-17** to **2-21** demonstrates the great potential of platinum(II) complexes containing bidentate diphosphine ligands as hydroformylation catalysts.

3.6. References

1. L. Kollar, P. Sandor, G. Szalontai, B. Heil, *J. Org. Chem.*, 1990, **393**, 153.
2. G. Petocz, G. Rangits, M. Shaw, H. de Bod, D. B. G. Williams, L. Kollár, *J. Org. Chem.*, 2009, **694**, 219.
3. T. Hayashi, Y. Kawabata, T. Isoyama, I. Ogata, *Bull. Chem. Soc. Jpn.*, 1981, **54**, 3438.
4. H. J. Ruegg, P. S. Pregosin, A. Scrivanti, L. Toniolo, C. Botteghi, *J. Organomet. Chem.*, 1986, **316**, 233.
5. C. P. Casey, G. T. Whiteker, *Isr. J. Chem.*, 1990, **30**, 299.
6. M. Kranenburg, Y. E. M van der Burgt, P. C. J. Kamer, P. W. N. M. van Leeuwen, D. Vogt, W. Keim, *Chem. Commun.*, 1995, 2177.
7. Z. Freixa, P. W. N. M. Van Leeuwen, *Dalton Trans.*, 2003, **10**, 1890.
8. P. Dierkes, P. W. N. M. van Leeuwen, *J. Chem. Soc., Dalton Trans.*, 1999, 1519.
9. Y. Kawabata , T. Hayashi, T. Isoyama, I. Ogata, *J. Chem. Soc., Chem. Commun.*, 1979, 462.
10. N. Biricik, F. Durap, C. Kayan, B. Gümgüm, N. Gurbuz, I. Ozdemir, W. Han Ang, Z. Fei, R. Scopelliti, *J. Org. Chem.*, 2008, **693**, 2693.
11. L. A. van der Veen, P. H. Keeven, G. C. Schoemaker, J. N. H. Reek, P. C. J. Kamer, P. W. N. M. van Leeuwen, M. Lutz, A. L. Spek, *Organometallics*, 2000, **19**, 872.
12. L. A. van der Veen, M. D. K. Boele, F. R. Bregman, P. C. J. Kamer, P. W. N. M. van Leeuwen, K. Goubitz, J. Fraanje, H. Schenk, C. Bo, *J. Am. Chem. Soc.*, 1998, **120**, 11616.
13. L. A. van der Veen, P. C. J. Kamer, P. W. N. M. van Leeuwen, *Organometallics*, 1999, **18**, 4765.
14. P. N Bungu, S. Otto, *Dalton Trans.*, 2007, **27**, 2876.

Chapter 4

Experimental

4.1. General procedures and Instrumentation

4.1.1. General procedures

All reactions were conducted under nitrogen using a dual high-vacuum/nitrogen line to carry out standard Schlenk techniques unless otherwise stated. Solvents used were all of analytical grade and were further purified by distillation under a nitrogen atmosphere. Solvents were dried over the appropriate drying agent. Diethyl ether and tetrahydrofuran were dried over sodium wire using benzophenone as an indicator, while dichloromethane and toluene were dried over calcium hydride. Once purification procedures were complete, the dry solvents were transferred under vacuum into a Teflon-valve storage vessel.

K_2PtCl_4 and $PdCl_2$ were obtained from Johnson Matthey. All other reagents including deuterated chloroform and dimethylsulfoxide were obtained from Sigma-Aldrich and used as received without further purification unless otherwise stated.

4.1.2. Instrumentation

NMR spectroscopy was carried out at the University of Cape Town and recorded on Varian Mercury-XR300 and Varian Unity-XR400 MHz spectrometers. Tetramethylsilane (TMS) was used as an internal standard for ^{1}H as well as ^{13}C NMR and phosphoric acid (H_3PO_4) as an external standard for ^{31}P NMR. Microanalyses were performed using a Fisons EA 1108 CHNS Elemental Analysis apparatus at UCT. Mass spectra (EI) were recorded using a JEOL-MATE(II) GC-MS instrument at UCT. Melting points were obtained using a Kofler hot stage microscope (Riechert Thermovar). FT-IR spectra were recorded on a Perkin Elmer Spectrum One FT-IR spectrophotometer. GC analyses were performed using a Varian 3900 gas chromatograph equipped with a packed DB-WAX column (25 m x 320 μm (internal diameter) x 1.20 μm film thickness). The carrier gas was nitrogen with a constant flow at 25 ml/min. The GC instrument required a 1 μl sample volume at an injection

temperature of 220 °C and an injection pressure of 30.8 kPa. The oven was programmed to maintain an initial temperature of 50 °C for 2 min and ramp to a final temperature of 220 °C at 10 deg/min held for 5 min.

4.2. Experimental details pertaining to Chapter 2

4.2.1. Synthesis of *o*-$Ph_2PC_6H_4CH=N^nPr$ (2-1)

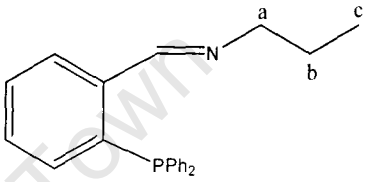

o-(Diphenylphosphino)benzaldehyde (0.5 g, 1.72 mmol) was added to propylamine (0.16 ml, 1.89 mmol) in dry toluene (15 ml) containing anhydrous $MgSO_4$ (40 mg). The resulting mixture was refluxed for 4 h. Thereafter, the solution was cooled to room temperature, the solvent removed and a yellow oil was recovered. Degassed hot ethanol was then added to the crude product and the solution was filtered. The solvent was then removed under high vacuum and a pale yellow oil was obtained. The data obtained agrees with literature values.[6] Yield: 61 % (0.35 g), ^{1}H NMR (300 MHz, $CDCl_3$) δ (ppm) 8.85 (d, 1H, HC=N), 8.01 - 6.98 (m, 14H, ArH), 3.42 (m, 2H, H_a), 1.46 (m, 2H, H_b), 0.68 (t, 3H, H_c, ^{2}J(H-H) = 7 Hz). ^{31}P NMR (121 MHz, $CDCl_3$) δ (ppm) -13.4 (s). IR (DCM, NaCl plates), ν (cm^{-1}) 1637 (C=N).

4.2.2. Synthesis of $[PtCl_2(cod)]$

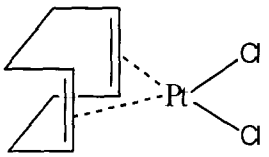

$[PtCl_2(cod)]$ was prepared using the procedure reported by Clark and Manzer.[1] K_2PtCl_4 (1g, 2.41 mmol) was added to distilled water (80 ml) resulting in a clear orange solution. Thereafter, isopropanol (40 ml) followed by 1,5-cyclooctadiene (5 ml) and a catalytic amount of $SnCl_2.H_2O$ (0.015g, 0.064 mmol) was added to the reaction mixture. Vigorous stirring resulted in a milky white solution. The reaction was left stirring for 3 days after which time a white solid was filtered and washed with distilled water (20 ml) and ethanol (10 ml). The product was obtained as a white solid and dried under vacuum for 3 hours. Yield: 88 % (0.79 g), m.p: 280 °C. ^{1}H NMR (300 MHz, d_6-dmso) δ (ppm) 5.54 (m, 4H, =CH), 2.51 (m, 4H, CH_2), 2.31 (m, 4H, CH_2). ^{13}C (d_6-dmso, 75 MHz) δ (ppm) 101.9 (s, 4C, CH), 31.1 (s, 4C, CH_2).[1]

4.2.3. Synthesis of [$PtCl_2$(*o*-$Ph_2PC_6H_4CH=N^nPr$)] (2-2)

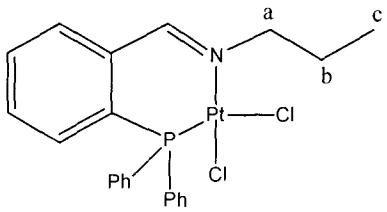

This complex was prepared by adding **2-1** (0.18 g, 0.54 mmol) to a solution of [$PtCl_2$(cod)] (0.2 g, 0.53 mmol) in dry DCM (10 ml). The mixture was stirred for 3 h after which time the solvent was removed under high vacuum and a yellow solid recovered. The product was recrystallized using a DCM/hexane solution (10ml/10ml) and the yellow solid was dried under vacuum for 3 hours. Yield: 69 % (0.23 g). ^{1}H NMR (300 MHz, $CDCl_3$) δ (ppm) 8.79 (d, 1H, HC=N), 7.91 - 6.95 (m, 14H, ArH), 4.45 (m, 2H, H_a), 1.72 (m, 2H, H_b), 0.49 (t, 3H, H_c, ^{2}J(H-H) = 7 Hz). ^{31}P NMR (121 MHz, $CDCl_3$) δ 5.81 ppm (s, ^{1}J(Pt-P) = 3741 Hz). IR (DCM, NaCl plates), ν (cm^{-1}) 1606 (C=N). Anal. Calc. for $C_{22}H_{22}NPPtCl_2$: C, 44.23; H, 3.71; N, 2.34. Found: C, 44.37; H, 3.66; N, 2.18 %.

4.2.4 Synthesis of aminodiphosphine ligands 2-3 to 2-8

4.2.4.1. Synthesis of benzyl-N(Ph_2P)$_2$ (2-3)

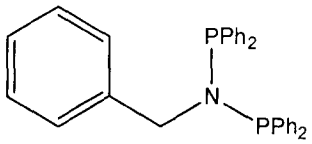

The benzylaminodiphosphine ligand was prepared by slowly adding Ph_2PCl (4.1 g, 18.5 mmol) to a solution of benzylamine (1 g, 9.33 mmol) and Et_3N (1.87 g, 18.5 mmol) in dry DCM (30 ml) at 0 °C. The white suspension was stirred for 3 h after which time the solvent was removed revealing a white solid. The solid was washed with degassed water (3 x 10 ml), air-dried and then recrystallized from a DCM/EtOH (10 ml/5 ml) solution to give the product as a white powder. Yield: 87 % (3.86 g), m.p: 146-148 °C. ^{1}H NMR (300 MHz, $CDCl_3$) δ (ppm): 6.82 – 7.33 (m, 25H, ArH), 4.55 (s, 2H, CH_2). ^{13}C (75 MHz, $CDCl_3$) δ (ppm): 127.9 – 139.8 (m, 30 C, ArC), 56.1 (CH_2).^{31}P NMR (121 MHz, $CDCl_3$) δ (ppm): 60.2 (s). IR (KBr pellet), ν (cm^{-1}) 833 (P-N).[7]

4.2.4.2. Synthesis of 2-picolyl-N($Ph_2P)_2$ (2-4)

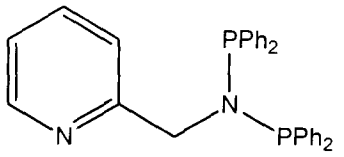

The picolylaminodiphosphine ligand was prepared in the same way as outlined for **2-3** but using picolyamine (1.01 g, 9.33 mmol) as the appropriate amine. The product was isolated as a white powder. Yield: 89 % (3.94 g), m.p: 162-164 °C. ^{1}H NMR (300 MHz, $CDCl_3$) δ (ppm): 6.98 – 8.44 (m, 24H, ArH), 4.67 (s, 2H, CH_2).^{13}C (75 MHz, $CDCl_3$) δ (ppm): 121.4 – 139.6 (m, 29 C, ArC), 57.8 (CH_2). ^{31}P NMR (121 MHz, $CDCl_3$) δ (ppm): 62.6 (s). IR (KBr pellet), ν (cm^{-1}) 858 (P-N).[7]

4.2.4.3 Synthesis of ^{n}Pr-N($Ph_2P)_2$ (2-5)

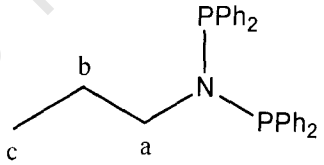

The propylaminodiphosphine ligand was prepared in the same way as outlined for **2-3** but using propylamine (0.55 g, 9.33 mmol) as the appropriate amine. The product was isolated as a white powder. Yield: 71 % (2.85 g), m.p: 85-87 °C, ^{1}H NMR (300 MHz, $CDCl_3$) δ (ppm): 7.31 – 7.41 (m, 20H, ArH), 3.20 (m, 2H, H_a), 1.11 (m, 2H, H_b), 0.59 (t, 3H, H_c, ^{2}J(H-H) = 7 Hz). ^{13}C ($CDCl_3$, 75 MHz) δ (ppm): 128.4 – 132.9 (m, 24C, ArC), 54.8 (C_a), 24.7 (C_b), 10.9 (C_c).^{31}P NMR (121 MHz, $CDCl_3$) δ (ppm): 62.9 (s). IR (KBr pellet), ν (cm^{-1}) 828 (P-N).[8]

4.2.4.4 Synthesis of *p*-MeO(C_6H_4)-N($Ph_2P)_2$ (2-6)

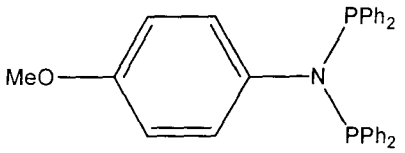

This ligand was prepared was prepared in the same way as outlined for **2-3** but using 4-methoxy-aniline (1.2 g, 9.33 mmol) as the appropriate amine. The product was isolated as a yellow powder. Yield: 75 % (3.42 g), m.p: 118-120 °C. ^{1}H NMR (300 MHz, $CDCl_3$) δ (ppm): 6.49. – 7.41 (m, 24H, ArH), 3.69 (s, 3H, O-CH_3). ^{13}C (75 MHz, $CDCl_3$) δ (ppm): 113.2 – 139.5 (m, 30C, ArC), 55.24 (O-CH_3). ^{31}P NMR (121 MHz, $CDCl_3$) δ (ppm): 70.5 (s). IR (KBr pellet), ν (cm^{-1}) 882 (P-N).[9]

4.2.4.5. Synthesis of *p* -$N_2OC_6H_4$-$N(Ph_2P)_2$ (2-7)

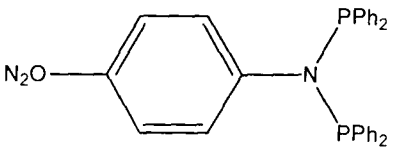

This ligand was prepared was prepared in the same way as outlined for **2-3** but using 4-nitro-aniline (1.27 g, 9.33 mmol) as the appropriate amine. The product was isolated as a yellow powder. Yield: 66 % (3.1 g), m.p: 141-143 °C. ^{1}H NMR (300 MHz, $CDCl_3$) δ (ppm): 6.91 – 8.21 (m, 24H, ArH). ^{13}C (75 MHz, $CDCl_3$) δ (ppm): 126.1 – 134.51 (m, 30 C, ArC). ^{31}P NMR (121 MHz, $CDCl_3$) δ (ppm): 68.7 (s). IR (KBr pellet), ν (cm^{-1}) 891 (P-N).[9]

4.2.4.6. Synthesis of ^{i}Pr-$N(Ph_2P)_2$ (2-8)

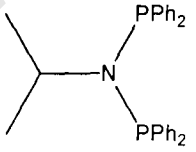

The isopropylaminodiphosphine ligand was prepared in the same way as outlined for **2-3** but using isopropylamine (0.55 g, 9.33 mmol) as the appropriate amine. The product was isolated as a white powder. Yield: 63 % (2.5 g), m.p: 133-134 °C. ^{1}H NMR (300 MHz, $CDCl_3$) δ (ppm): 7.31 – 7.35 (m, 20H, ArH), 3.68 (m, 1H, CH), 1.17 (d, 6H, CH_3, ^{2}J(H-H) = 6 Hz). ^{31}P NMR (121 MHz, $CDCl_3$) δ (ppm): 48.8 (br s). IR (KBr pellet), ν (cm^{-1}) 873 (P-N).[10]

4.2.5. Synthesis of Pd complexes 2-9 to 2-12

4.2.5.1. Synthesis of $[PdCl_2(cod)]$

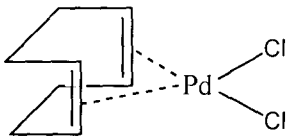

$[PdCl_2(cod)]$ was prepared using the procedure reported by Bailey and Linsesky.[11] Palladium(II) chloride (2.11 g, 11.90 mmol) was dissolved in concentrated hydrochloric acid (10 ml). Ethanol (100 ml) was added to the resulting dark orange solution and immediately a brown residue appeared. The solution was filtered and the residue washed with ethanol (25 ml). Thereafter, 1,5-cyclooctadiene (3.4 ml, 27.37 mmol) was added to the orange solution and a yellow precipitate formed. The solution was stirred for 3 hours. The yellow solid was filtered, washed with ethanol (50 ml) as well as diethyl ether (25 ml) and dried under vacuum for 3 hours. Yield: 88 % (3.31 g), m.p: 204 – 206° C. ^{1}H NMR (300 MHz, d_6-dmso) δ (ppm) 5.49 (m, 4H, =CH), 3.54 (m, 4H, CH_2), 2.28 (m, 4H, CH_2).^{13}C (75 MHz, d_6-dmso,) δ (ppm) 128.19 (s, 4C, CH), 27.31 (s, 4C, CH_2).[11]

4.2.5.2. Synthesis of [$PdCl_2${benzyl-N($Ph_2P)_2$}] (2-9)

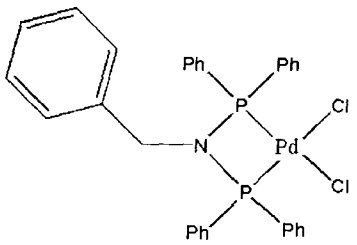

Ligand **2-3** (0.083 g, 0.175 mmol) was added to a solution of [$PdCl_2$(cod)] (0.050 g, 0.175 mmol) in freshly distilled DCM (10 ml). The reaction mixture was stirred for 3 hours after which time the reaction volume was reduced to approximately 2 ml *in vacuo*. Thereafter, diethyl ether (20 ml) was added and the resulting yellow precipitate was filtered and dried for 3 hours *in vacuo*. The data obtained agrees with literature values.[7] Yield: 71 % (0.081 g), m.p: 292-293 °C. ^{1}H NMR (300 MHz, $CDCl_3$) δ (ppm): 6.44 – 7.81 (m, 25H, ArH), 4.21 (s, 2H, CH_2). ^{13}C (75 MHz, $CDCl_3$) δ (ppm): 128.6 – 133.8 (m, 30C, ArC), 52.9 (CH_2). ^{31}P NMR (121 MHz, $CDCl_3$) δ (ppm): 34.6 (s). IR (KBr pellet), ν (cm^{-1}) 803 (P-N). Anal. Calc. for $C_{31}H_{27}NP_2PdCl_2$: C, 57.03; H, 4.17; N, 2.15. Found: C, 57.29; H, 4.31; N, 2.02 %.

4.2.5.3. Synthesis of [$PdCl_2${2-picolyl-N($Ph_2P)_2$}] (2-10)

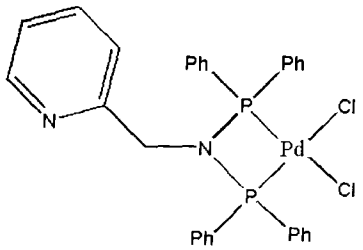

Complex **2-10** was prepared in the same way as outlined for **2-9** using the appropriate ligand **2-4** (0.083 g, 0.175 mmol). The product was isolated as a white solid. The data obtained agrees with literature values.[7] Yield: 74 % (0.084 g), m.p: > 300 °C, ^{1}H NMR (300 MHz, $CDCl_3$) δ (ppm): 6.35 – 7.92 (m, 24H, ArH), 4.26 (s, 2H, CH_2). ^{13}C (75 MHz, $CDCl_3$) δ (ppm): 123.2 – 139.3 (m, 29C, ArC), 54.1 (CH_2). ^{31}P NMR (121 MHz, $CDCl_3$) δ (ppm): 34.5 (s) IR (KBr pellet), ν (cm^{-1}) 813 (P-N). Anal. Calc. for $C_{30}H_{26}NP_2PdCl_2$: C, 55.11; H, 4.01; N, 4.28. Found: C, 54.88; H, 4.16; N, 4.17 %.

4.2.5.4. Synthesis of [$PdCl_2${^{n}Pr-N($Ph_2P)_2$}] (2-11)

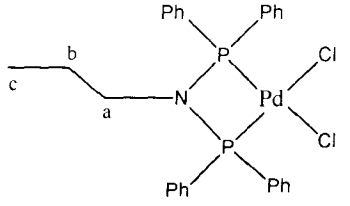

Complex **2-11** was prepared in the same way as outlined for **2-9** using the appropriate ligand **2-5** (0.075 g, 0.175 mmol). The product was isolated as a white solid. Yield: 68 % (0.072 g), m.p: 288-290 °C. ^{1}H NMR (300 MHz, $CDCl_3$) δ (ppm): 7.54 – 7.89 (m, 20H, ArH), 2.95 (m, 2H, H_a), 1.2 (m, 2H, H_b), 0.52 (t, 3H, H_c, ^{2}J(H-H) = 7 Hz). ^{13}C ($CDCl_3$, 75 MHz) δ (ppm): 129.4 - 133.6

(m, 24C, ArC), 51.1 (C_a), 23.1 (C_b), 11.2 (C_c). ^{31}P NMR (121 MHz, $CDCl_3$) δ (ppm): 31.3 (s). Selected IR (KBr), ν (cm^{-1}): 829 (P–N). Anal. Calc. for $C_{27}H_{27}NP_2PdCl_2$: C, 53.62; H, 4.50; N, 2.32. Found: C, 53.77; H, 4.45; N, 2.12 %.

4.2.5.5 Synthesis of [$PdCl_2${*p*-OMe(C_6H_4)-N(Ph_2P)$_2$}] (2-12)

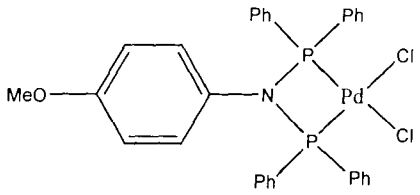

Complex **2-12** was prepared in the same way as outlined for **2-9** using the appropriate ligand **2-6** (0.086 g, 0.175 mmol). The product was isolated as a yellow solid. Yield: 72 % (0.084 g), m.p: > 300 °C. ^{1}H NMR (300 MHz, $CDCl_3$) δ (ppm): 6.51 - 7.96 (m, 24 H, ArH), 4.26 (s, 3H, O-CH_3). ^{13}C ($CDCl_3$, 75 MHz) δ (ppm): 129.5 - 135.1 (m, 30C, ArC), 56.1 (O-CH_3). ^{31}P NMR (121 MHz, $CDCl_3$) δ (ppm): 70.1 (s). Selected IR (KBr), ν (cm^{-1}): 828 (P–N). Anal. Calc. for $C_{31}H_{27}NOP_2PdCl_2$: C, 55.67; H, 4.07; N, 2.09. Found: C, 55.39; H, 4.05; N, 2.08 %.

4.2.6. Synthesis of Pt complexes 2-13 to 2-16

4.2.6.1. Synthesis of [$PtCl_2${benzyl-N(Ph_2P)$_2$}] (2-13)

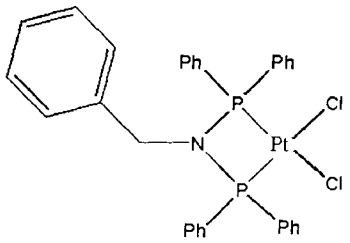

Ligand **2-3** (0.041 g, 0.086 mmol) was added to a solution of [$PtCl_2$(cod)] (0.032 g, 0.086 mmol) in freshly distilled DCM (10 ml). The reaction mixture was stirred for 3 hours after which time the reaction volume was reduced to approximately 2 ml *in vacuo*. Thereafter, diethyl ether (20 ml) was added and the resulting white precipitate was filtered and dried for 3 hours *in vacuo* to give a white solid product. The data obtained agrees with literature values.[7] Yield: 71 % (0.045 g), m.p: > 300 °C. ^{1}H NMR (300 MHz, $CDCl_3$) δ (ppm): 6.25 – 7.33 (m, 25H, ArH), 4.14 (s, 2H, CH_2). ^{13}C (75 MHz, $CDCl_3$) δ (ppm): 129.1 – 133.9 (m, 30 C, ArC), 53.5 (CH_2). ^{31}P NMR (121 MHz, $CDCl_3$) δ (ppm): 20.5 (s,^{1}J(Pt-P) = 3305) Hz, IR (KBr pellet), ν (cm^{-1}) 803 (P-N). Anal. Calc. for $C_{31}H_{27}NP_2PtCl_2$: C, 50.21; H, 3.67; N, 1.89. Found: C, 49.97; H, 3.48; N, 1.76 %.

4.2.6.2. Synthesis of $[PtCl_2\{2\text{-picolyl-N}(Ph_2P)_2\}]$ (2-14)

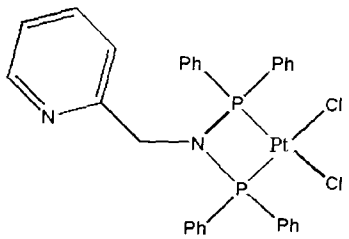

Complex **2-14** was prepared in the same way as outlined for **2-13** using the appropriate ligand **2-4** (0.041 g, 0.086 mmol). The product was isolated as a white solid. The data obtained agrees with literature values.[7] Yield: 61 % (0.039 g), m.p: > 300 °C. ^{1}H NMR (300 MHz, $CDCl_3$) δ (ppm): 6.49 – 8.11 (m, 24H, ArH), 4.18 (s, 2H, CH_2). ^{13}C (75 MHz, $CDCl_3$) δ (ppm): 123.1 – 133.7 (m, 29C, ArC), 54.7 (CH_2). ^{31}P NMR (121 MHz, $CDCl_3$) δ (ppm): 20.3 (s, ^{1}J(Pt-P) = 3309 Hz), IR (KBr pellet), ν (cm^{-1}) 816 (P-N).[4] Anal. Calc. for $C_{30}H_{26}NP_2PtCl_2$: C, 48.53; H, 3.53; N, 3.77. Found: C, 48.28; H, 3.59; N, 3.65 %.

4.2.6.3. Synthesis of $[PtCl_2\{^n\text{Pr-N}(Ph_2P)_2\}]$ (2-15)

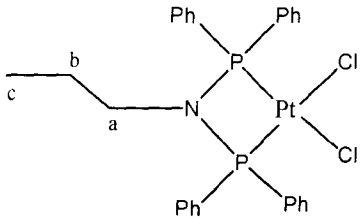

Complex **2-15** was prepared in the same way as outlined for **2-13** using the appropriate ligand **2-5** (0.037 g, 0.087 mmol). The product was isolated as a white solid. Yield: 67 % (0.040 g), m.p: > 300 °C. ^{1}H NMR (300 MHz, $CDCl_3$) δ (ppm): 7.26 - 7.87 (m, 20H, ArH), 2.94 (m, 2H, H_a), 1.15 (m, 2H, H_b), 0.51 (t, 3H, H_c, ^{2}J(H-H) = 7 Hz). ^{13}C (75 MHz, $CDCl_3$) δ (ppm): 133.4 - 133.1 (m, 24C, ArC), 51.5 (C_a) 23.0 (C_b), 11.1 (C_c). ^{31}P NMR (121 MHz, $CDCl_3$) δ (ppm): 17.3 (s, ^{1}J(Pt-P) = 3300 Hz). Selected IR (KBr pellet), ν(cm^{-1}): 826 (P–N). Anal. Calc. for $C_{27}H_{27}NP_2PtCl_2$: C, 46.77; H, 3.92; N, 2.02. Found: C, 46.54; H, 4.04; N, 1.86 %.

4.2.6.4. Synthesis of $[PtI_2\{^n\text{Pr-N}(Ph_2P)_2\}]$ (2-16)

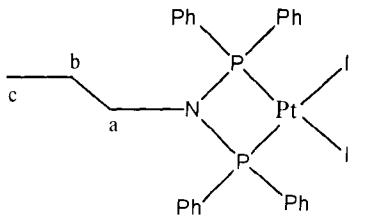

Complex **2-16** was prepared by adding complex **2-15** (0.12 g, 0.173 mmol) to a solution of NaI (0.052g, 0.346 mmol) in acetone (50 ml). The reaction mixture was stirred for 45 min after which time the solvent was removed under high vacuum. Distilled water (2 x 10 ml) was used to wash the excess salt and the product was extracted using DCM. The yellow product was recrystallized using a DCM/hexane solution (10ml/10ml) to give a pale yellow solid. Yield: 65 %

(0.098 g), m.p: > 300 °C. ^{1}H NMR (300 MHz, $CDCl_3$) δ (ppm): 7.18–7.49 (m, 20H, ArH), 2.75 (m, 2H, H_a), 1.05 (m, 2H, H_b), 0.44 (t, 3H, H_c, ^{2}J(H-H) = 7 Hz). ^{13}C (75 MHz, $CDCl_3$) δ (ppm): 133.2-132.2 (m, 24C, ArC), 48.3 (C_a) 22.8 (C_b), 11.4 (C_c). ^{31}P NMR (121 MHz, $CDCl_3$) δ (ppm): 13.3 (s, ^{1}J(Pt-P) = 3019 Hz). Selected IR (KBr pellet), ν (cm^{-1}): 834 (P–N). Anal. Calc. for $C_{27}H_{27}NP_2PtI_2$: C, 37.00; H, 3.11; N, 1.60. Found: C, 37.22; H, 3.38; N, 1.44 %.

4.2.7. Synthesis of Pt complexes 2-17 to 2-21

4.2.7.1. Synthesis of [$PtCl_2$(dppp)] (2-17)

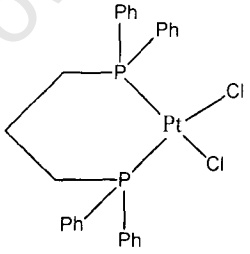

[$PtCl_2$(cod)] (0.68 g, 1.81 mmol) was added slowly to a solution of dppp (0.75 g, 1.81 mmol) in DCM (50 ml). Immediately, a clear solution was observed and within 10 minutes a white turbid solution formed. The reaction mixture was then stirred overnight after which time the white precipitate was filtered and washed with Et_2O (25 ml). The data obtained agrees with literature values.[2] Yield: 79 % (0.98 g), m.p: > 300 °C. ^{1}H NMR (300 MHz, d_6-dmso) δ (ppm) 7.46 – 8.01 (m, 20H, ArH), 2.84 (m, 4H, CH_2), 1.86 (m, 2H, CH_2). ^{13}C (75 MHz, d_6-dmso) δ (ppm) 128.1 – 134.3 (m, 24C, ArC), 18.2 (s, 2C, CH_2), 54.7 (CH_2). ^{31}P NMR (121 MHz, d_6-dmso) δ (ppm) -3.6 (s, ^{1}J(Pt -P) = 3414 Hz).

4.2.7.2 Synthesis of [$PtCl_2$(dppe)] (2-18)

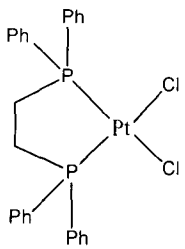

Complex **2-18** was prepared in the same way as outlined for **2-17** using the appropriate ligand dppe (0.72 g, 1.81 mmol). The product was obtained as a white solid. The data obtained agrees with literature values.[13] Yield: 63 % (0.76 g), m.p > 300 °C, ^{1}H NMR (300 MHz, d_6-dmso) δ (ppm) 7.52 -7.55 (m, 20H, ArH), 2.51 (t, 4H, CH_2, ^{2}J(H-H) = 12 Hz).[13]C (75 MHz, d_6-dmso) δ (ppm) 127.02 – 133.19 (m, 24C, ArC), 28.1 (s, 2C, CH_2). ^{31}P NMR (121 MHz, d_6-dmso) δ -3.41 ppm (s, ^{1}J(Pt-P) = 3610 Hz).

4.2.7.3. Synthesis of [$PtCl_2$(dcpp)] (2-19)

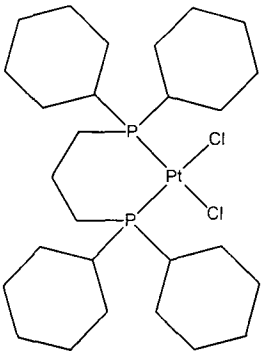

Complex **2-19** was was prepared in the same way as outlined for **2-17** using [$PtCl_2$(cod)] (0.2 g, 0.53 mmol) and the ligand (dcpp) (0.23 g, 0.53 mmol). The product was obtained as a white solid. The data obtained agrees with literature values.[14] Yield: 69 % (0.26 g), m.p > 300 °C, ^{1}H NMR (300 MHz, d_6-dmso) δ (ppm) 2.28 – 2.71 (m, 50H, CH and CH_2). ^{31}P NMR (121 MHz, d_6-dmso) δ 26.6 ppm (s, ^{1}J(Pt-P) = 3396 Hz). Anal. Calc. for $C_{27}H_{50}P_2PtCl_2$: C, 46.15; H, 7.17. Found: C, 46.38; H, 7.31 %.

4.2.7.4. Synthesis of [$PtCl_2$(dbpp)] (2-20)

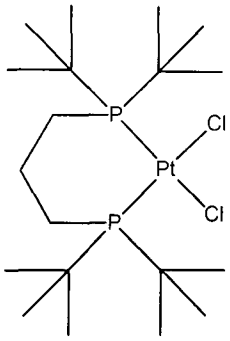

Complex **2-20** was prepared in the same way as outlined for **2-17** using [$PtCl_2$(cod)] (0.2 g, 0.53 mmol) and the ligand dbpp (0.18 g, 0.53 mmol). The product was obtained as a white solid. The data obtained agrees with literature values.[14] Yield: 75 % (0.24 g), m.p > 300 °C, ^{1}H NMR (300 MHz, d_6-dmso) δ (ppm) 0.89 (d, 36 H, CH_3, ^{2}J(H-H) = 11 Hz), 1.14 (m, 4H, CH_2), 1.53 (m, 2H, CH_2). ^{13}C (75 MHz, d_6-dmso) δ (ppm) 31.4 (C-C), 29.4 (s, 2C, CH_2), 22.4 (CH_2), 13.73 (CH_3). ^{31}P NMR (121 MHz, d_6-dmso) δ 17.6 ppm (s, ^{1}J(Pt-P) = 3558 Hz).

4.2.7.5. Synthesis of [$PtCl_2$(dnpe)] (2-21)

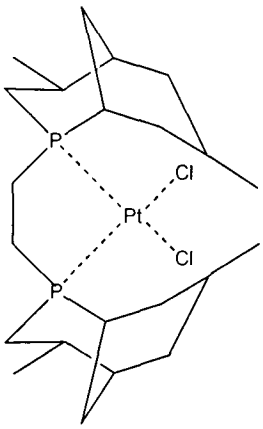

Complex **2-21** was prepared in the same way as outlined for **2-17** using [$PtCl_2$(cod)] (0.2 g, 0.53 mmol) and the ligand dnpe (0.21 g, 0.53 mmol). The product was obtained as a white solid. Yield: 82 % (0.29 g), m.p: > 300 °C, ^{1}H NMR (300 MHz, $CDCl_3$) δ (ppm) 3.21 (br m, 4H, CH_2), 1.56 - 2.52 (br m, 24H, CH and CH_2) 1.12 (d, 12H, CH_3, ^{2}J(H-H) = 6 Hz). ^{31}P NMR (121 MHz, $CDCl_3$) δ 29.1 ppm (d, ^{1}J(Pt-P) = 3538 Hz), 28.8 ppm (s, ^{1}J(Pt-P) = 3527 Hz), 27.9 ppm (s, ^{1}J(Pt-P) = 3518 Hz). Anal. Calc. for $C_{24}H_{46}P_2PtCl_2$: C, 43.61; H, 7.00, Found: C, 43.82; H, 6.76 %. MS (EI): $[M\text{-}Cl]^+$ = 611.2.

4.2.7.6. Synthesis of [$PdCl_2$(dppp)] (2-22)

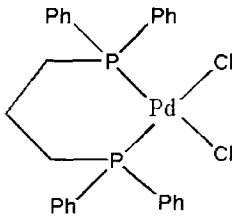

To a solution of dppp (1.44 g, 3.5 mmol) in freshly distilled DCM (10 ml) was added [$PdCl_2$(cod)] (1 g, 3.5 mmol). The reaction mixture was stirred for 3 hours after which time the reaction volume was reduced to approximately 2 ml *in vacuo*. Thereafter, diethyl ether (20 ml) was added and the resulting precipitate was filtered and dried for 3 hours *in vacuo* to give a solid yellow product. The data obtained agrees with literature values.[12] Yield: 77 % (1.6 g), m.p: > 300 °C, ^{1}H NMR (300 MHz, d_6-dmso) δ (ppm) 7.4 – 7.91 (m, 20H, ArH), 2.67 (m, 4H, CH_2), 1.78 (m, 2H, CH_2). ^{31}P NMR (121 MHz, d_6-dmso) δ 13.5 ppm (s). ^{13}C (75 MHz, d_6-dmso) δ (ppm) 128.1 – 133.5 (m, 24C, ArC), 24.4 (s, 2C, CH_2), 17.8 (CH_2).

4.2.8. Preparation of Grignard reagent $MgBr(CH_2)_7CH_3$

A three-necked round bottomed flask containing dry diethyl ether (60 ml) and an excess of Mg turnings (2 g, 0.08 mol) was fitted with a reflux condenser.[4] Thereafter, 1-bromooctane (5 ml, 0.03 mol) was added at -78 °C and the reaction mixture was stirred for 24 hours at 0 °C. The resulting grey reaction mixture was refluxed at 50 °C for 4 hours turning the solution a dark grey colour. The concentration of the resulting solution was determined by hydrolysing the Grignard reagent (1 ml) with distilled water (2 ml) and titrating against HCl (1M) using phenolpthalein as an indicator (2-3 drops).

4.2.9. Synthesis of [cis-Pt{$(CH_2)_7CH_3$}$_2$(dppp)] (2-29)

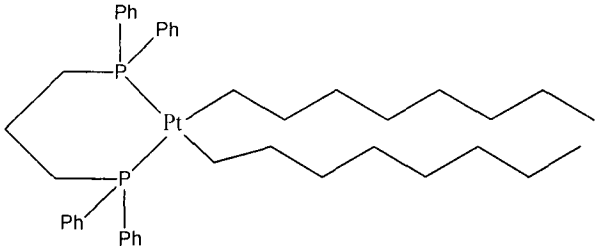

Dry diethyl ether (25 ml) was added to [$PtCl_2$(dppp)] (0.8 g, 1.18 mmol) in a Schlenk flask. The flask was cooled to -78 °C and $MgBr(CH_2)_7CH_3$ (8.1 ml, 6.48 mmol) was added to the flask using a syringe. The reaction mixture was stirred for 24 hours. Thereafter, saturated aqueous NH_4Cl (15 ml) was added at -78 °C to the colourless reaction mixture to hydrolyze the excess Grignard reagent and immediately form a white precipitate. The aqueous layer was washed with dichloromethane (3 x 5 ml) and the organic layer

added to anhydrous $MgSO_4$. The solution was then filtered and the solvent removed under reduced pressure. The yellow residue recovered was recrystallized from a dichloromethane/hexane solution (5 ml/10 ml). The yellow solid was recovered by decanting the mother liquor and drying under vacuum for 3 hours. The data obtained agrees with literature values.[5] Yield: 73 % (0.72 g), m.p: 92 – 93 °C. ^{1}H NMR (300 MHz, $CDCl_3$) δ (ppm): 7.25–7.58 (m, 20H, ArH), 2.49-2.69 (m, 6H, P-CH_2), 0.8-1.86 (br m, 34H, CH_2). ^{31}P NMR (121 MHz, $CDCl_3$) δ (ppm): 3.4 (s, ^{1}J(Pt -P) = 1601 Hz).

4.2.10. Synthesis of [PtCl($SnCl_3$)](dppp) (2-33)

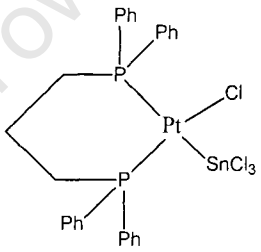

Anhydrous $SnCl_2$ (0.021 g, 0.178 mmol) was added to a solution of [$PtCl_2$(dppp)] (0.12 g, 0.178 mmol) in toluene (10 ml). The reaction mixture was stirred for 6 hours after which time a yellow solution was observed. The solvent was reduced and diethyl ether (20 ml) was added. The yellow solid was filtered and dried under vacuum for 2 hours. Yield: 72 % (0.11 g). Anal. Calc. for $C_{27}H_{26}P_2PtSnCl_4$: C, 37.32; H, 3.13; N; Found: C, 37.33; H, 3.20 %.[3]

4.3. Experimental details pertaining to Chapter 3

4.3.1. Hydroformylation reaction

In a typical experiment, [$PtCl_2$(diphosphine)] (19 mg, 0.029 mmol) and anhydrous $SnCl_2$ (5 mg, 0.029 mmol) were added to a solution of dry toluene (11.1 ml) and 1-octene (8.9 ml, 0.06 mmol) in a stainless steel pipe reactor. The reactor was initially pressurized to 50 bar total pressure ($CO:H_2$ = 1:1) and placed in an oil bath at 100 °C for 15 minutes with stirring at 600 rpm. The total pressure was then increased to 80 bar and syngas was supplied on demand to maintain the reaction pressure at 80 bar throughout the reaction period. After the reaction time was reached, the syngas supply was shut down and the reactor was cooled in an ice bath. The excess pressure was then vented from the cooled reactor and the resulting pale yellow solution was transferred into vials for GC analysis.

4.3.2. Description of multi-cell reactor setup

Dr S. Otto and fellow contributors at the Research and Development department at SASOL designed, constructed and evaluated this multi-reactor system for rapid screening in homogeneous catalysis in 2007. The design of this multi-reactor system consists of five high pressure pipe reactors connected in parallel to a constant syngas pressure supply (Figure 4.1).

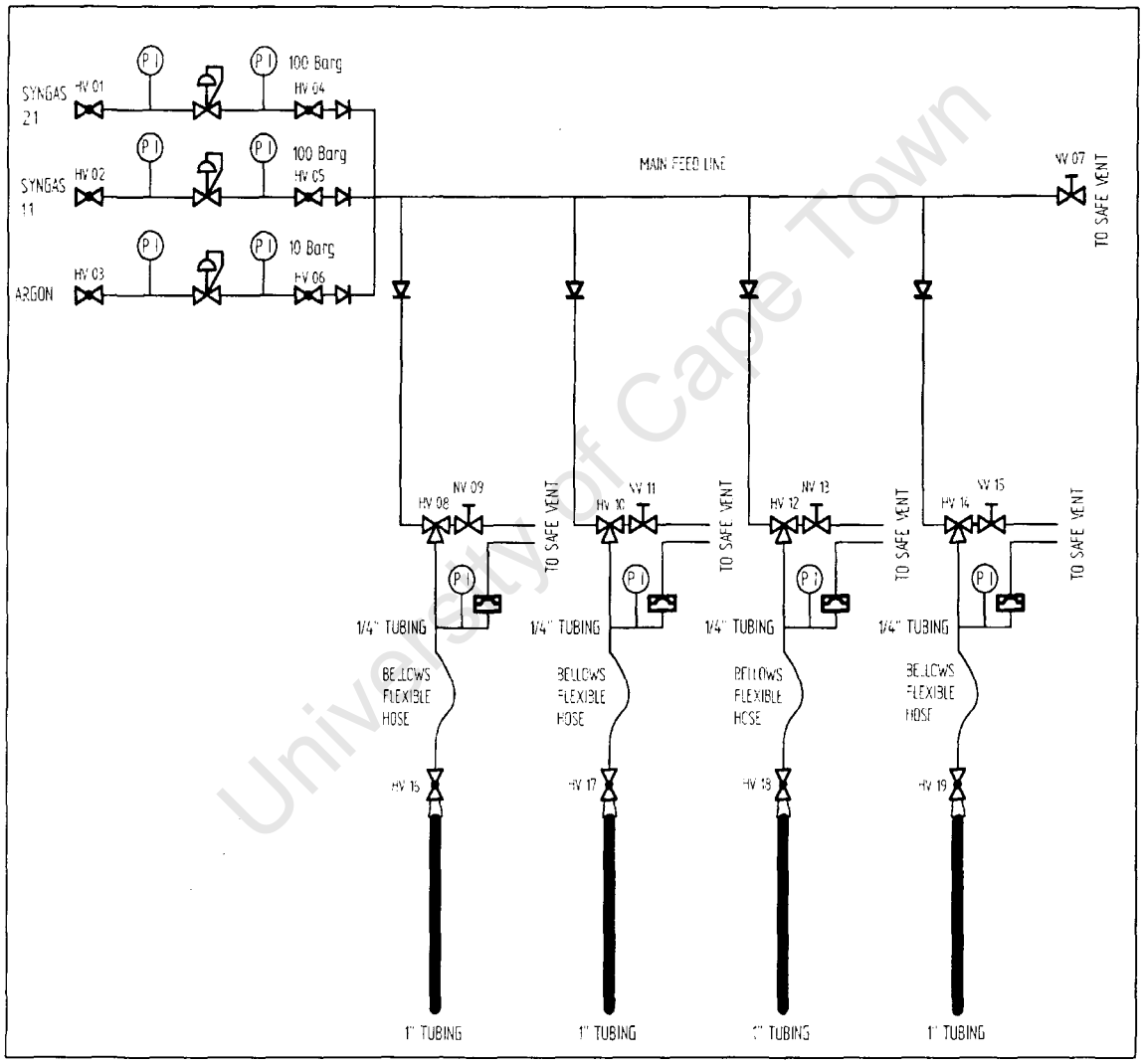

Figure 4.1: Schematic of pipe reactor system.

The temperature is regulated using oil baths which are placed on hotplate stirrers. The system was evaluated for reproducibility of results in all cells by performing modified Co (modCo) hydroformylation reactions using 1-octene for 3 hrs. Performance testing was carried out using the modCo system as a standard of comparison and parameters

including % conversion, % yield of alcohol and % hydrogenation were evaluated. The system was found to achieve acceptable reproducibility (i.e good correlation of data and low statistical spread). The appropriate risk assessment was performed on the reactor system and a Written Safe Work Procedure and Operating Procedure were established to ensure the system is safe for conducting experiments. This well-developed system is advantageous as it can accommodate small reaction volumes and is further beneficial as it allows reactions to be conducted at different temperatures while subjected to identical syngas pressure at five individual reactors (Figure 4.2).

Figure 4.2: Two of the five individual reactors.
Syngas and argon regulators are visible in the top right of the picture.

Thus, this multi-reactor system is ideal for catalysis to be carried out using the metal complexes prepared in this study and facilitates the output of results rapidly when numerous comparative experiments are required. The subsequent analysis of product distribution in the reaction mixture using GC-FID analysis provided an efficient method of measuring the relative activity and selectivity of the catalyst systems used.

The pipe reactors are 1" 316 stainless steel pipes which are 25 cm in length. The end of each pipe is enclosed with a cap using a high pressure Swagelock nut and ferrule (Figure 4.3).

Figure 4.3: High pressure Swagelock nut and ferrule of the reactor cap. The inlet for syngas supply is clearly visible through the centre of the cap.

The flexible hose enables easy handling for the reactor to be placed in the oil bath and a connection from the reactor to the three way valve. This three way valve provides a connection to the supply/vent line for each individual reactor (Figure 4.4).

Figure 4.4: Picture of flexible hose, three way valve and supply/vent line.

4.3.3. Operating procedure of multi-cell pipe reactors

4.3.3.1 Temperature

The temperature required for each pipe reactor was regulated using a standard oil bath on a stirrer/hot plate and was set prior to catalyst loading as the oil bath took several minutes to equilibrate.

4.3.3.2. Stirring

The stirring was set to 600 revolutions per minutes (rpm) by selecting the stirring option on the stirrer/hot plate.

4.3.3.3. Loading of pipe reactors

The pipe reactor was placed in a fume-hood for catalyst loading and a small magnetic stirrer bar was included. The closing cap of the pipe reactor was securely tightened with a spanner and bench vice in the reactor room. The shut-off valve on the reactor was closed to transport the contents under an inert atmosphere before attaching it to the flexible hose (Figure 4.1, HV 16 – 19).

4.3.3.4. Assembly of system

The reactors were clamped above the heated oil baths to perform pressure checks. Initially, all needle valves were closed (NV 07, 09, 11, 13, 15). Three way valves (HV 08, 10, 12, 14) of each reactor were closed to the syngas line when the supply line was opened. The first pressure test was carried out by opening the argon supply line and opening the three way valves to each reactor. The reactors were checked for gas leaks by applying snoop (soap agent). The reactors were then shut off to argon using the three way valves and then vented using the needle valve. The argon supply was stopped by closing the shut off valve (HV 03) and the main feed line was vented. The second argon shut off valve was then closed (HV 06). A second pressure test using syngas was performed in the same manner to confirm that the system was leak free. The reactors were then closed to the syngas supply using the three way valves and each reactor opened to syngas and then vented to ensure that all argon was replaced. Finally, the shut off valve on each reactor was closed and the three way valves opened to the gas supply to pressurise the line just before the reactors.

4.3.3.5. Operation

Checks were then performed to ensure correct temperature, pressure and stirring rate. The reactors were then lowered into the oil bath. The shut off valve to the reactors were opened individually and syngas delivered to each reactor. This time was recorded as the initiation time for each reaction.

4.3.3.6. Reaction termination

When the reaction time had expired, the shut off valve to the reactor was closed and the reactor was placed in an ice bath to cool. The excess pressure in the reactor line was vented by opening the three way valve to the vent line and opening the needle valve to the vent system. After the reactor cooled down sufficiently, the shut off valve of the reactor was opened slowly and the pressure vented by opening the needle valve to the vent system. The shut off valve (HV 02) was then closed and the supply line vented by opening the needle valve to the vent line. Shut off valve (HV 05) was then closed. The reactor was opened using a bench vice and spanner and the cap was removed. GC analysis was conducted by pouring the contents into a beaker and transferring a sample into a GC vial.

4.4 References

1. H. C. Clark and L. E. Manzer, *J. Org. Chem.*, **59**, 1973, 411.
2. D. A. Slack, M. C. Baird, *Inorg. Chim. Acta*, 1977, **24**, 277.
3. A. Scrivanti, C. Botteghi, L. Toniolo, A. Berton, *J. Org. Chem.*, 1988, **344**, 261.
4. G. S. Silverman and P. E. Rakita, *Handbook of Grignard Reagents*, Marcel Dekker, Inc., New York, 1996.
5. A. Sivaramakrishna, H. Su, J. R. Moss, *Organometallics*, 2007, **26**, 5786.
6. C. A. Ghilardi, S. Midollini, S. Moneti, A. Orlandini, G. Scapacci, *J. Chem. Soc., Dalton Trans.*, 1992, **23**, 3371.
7. N. Biricik, F. Durap, C. Kayan, B. Gümgüm, N. Gurbuz, I. Ozdemir, W. H. Ang, Z. Fei, R. Scopelliti, *J. Org. Chem.*, 2008, **693**, 2693.
8. G. Ewart, A. P. Lane, J. Mckechnie, D. S. Payne, *J. Chem. Soc.*, 1964, 1543.
9. Killian, K. Blann, A. Bollmann, J. T. Dixon, S. Kuhlmann, M. C. X. Maumela, H. Maumela, D. H. Morgan, P. Nongodlwana, M. J. Overett, M. Pretorius, K. Hofener, P. Wasserscheid, *J. Mol. Catal.*, 2007, **270**, 214.
10. R. J. Cross, T. H. Green, R. Keat, *J. Chem. Soc., Dalton Trans.*, 1976, **14**, , 1424.
11. C. T. Bailey, G. C. Linsesky, *J. Chem Edu.*, 1985, **62**, 896.
12. D. L. Oliver and G. K. Anderson, *Polyhedron*, 1992, **11**, 2415.
13. I. Pantcheva, K. Osakada, *Organometallics,* 2006, **25**, 1735.
14. M. Harada, Y. Kai, N. Yasuoka, N. Kasal, *Bull. Chem. Soc. Jpn.*, 1979, **52**, 390.

5. Appendix

5.1. GC analysis

Figure 5.1 shows the GC-FID spectrum obtained from the feed mixture. Two major peaks are clearly visible. The peaks at retention times of 2.81 min and 7.28 min are indicative of 1-octene and toluene respectively. The GC-FID output data is summarised in Table 5.1. Table 5.2 shows how the output data can be used to obtain the mass (g) of each component in 100 g of feed.

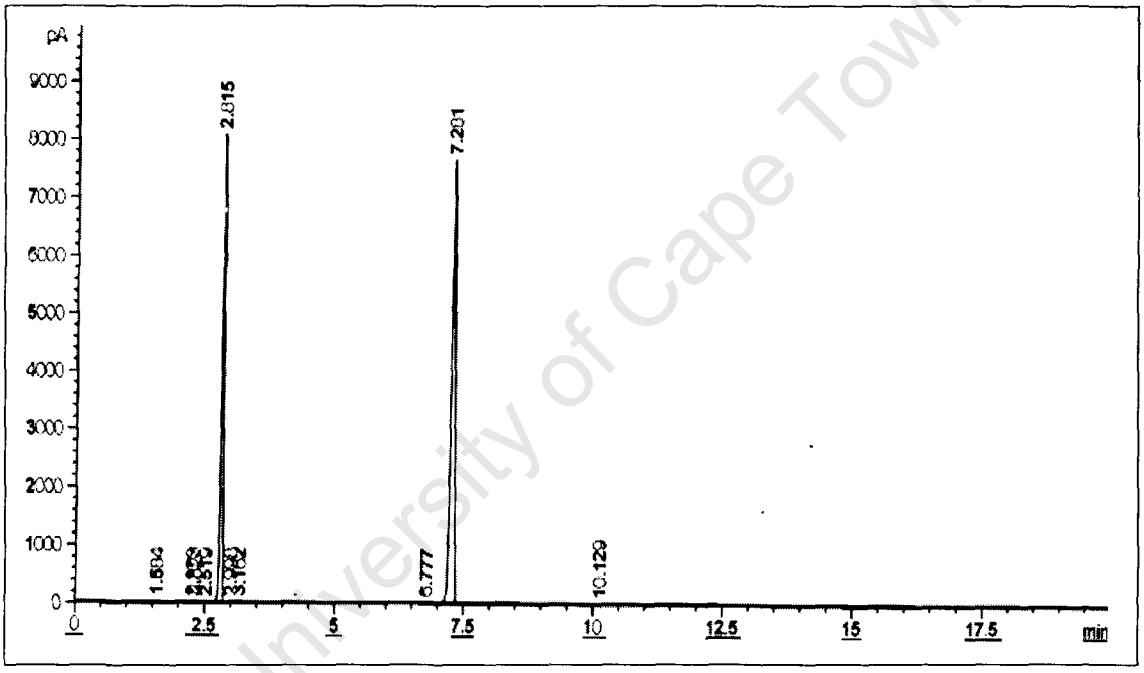

Figure 5.1: GC-FID spectrum of feed mixture.

Table 5.1: GC-FID output data for peaks in the feed mixture.

Component	Retention time (min)	Height (pA)	Area (%)
1-Octene	2.82	5051.06	38.21
Toluene	7.28	7656.59	61.53

Table 5.2: GC-FID data of feed used to calculate component mass in 100g feed.

Component	Area (%)	Mass (g)[a]	Mass (%)[b]
1-Octene	38.21	38.21	39.92
Toluene	61.53	57.51	60.08

[a] Mass (g) = Area (%) / Response Factor (RF: 1-Octene = 1, Toluene = 1.07)

[b] Mass (%) = [Mass (g) / (Mass (g) 1-octene + mass (g) toluene)]* 100

= mass in 100 g feed.

The response factor (RF) is calculated for each substance with a particular detector (Table 5.2). The response factor is obtained experimentally by analyzing a known quantity of the substance into the GC instrument and measuring the area of the relevant peak (RF for toluene = 1.07, 1-octene = 1, octane = 1, aldehydes = 0.8).

When comparing the GC-FID spectrum of the feed with that of the products it is evident that the solvent peak does not seem to change, thus it is a component of the reaction mixture that is not taking part in the reaction. This peak is then selected in the feed GC-FID spectrum and labelled T-feed. The mass (g) of toluene in 100 g of feed is calculated using the % mass (Table 5.2). Thus, 100 g of feed contains 60.08 g toluene and 39.92 g 1-octene. The toluene peak is also selected in the product spectrum and labelled T-prod. The mass ratio of T-feed/T-prod is calculated. The peaks in the product spectrum are then multiplied by this ratio to obtain the corrected mass which is the mass of the component produced when 100 g of feed is used. This calculation is demonstrated in Table 5.3.

Figure 5.2 shows the chromatograph obtained when a sample from the $[PtCl_2(dppe)]$ (**2-18**) reaction mixture was analyzed. Peaks occur at specific retention times and each peak can be identified as either a reactant or product when compared to internal standards of the instrument. Toluene and 1-octene peaks occur at the expected retention times. The aldehyde products, 1-nonanal, 2-methyl-octanal and 3-ethyl-heptanal appear at 21 (not shown here), 17 and 16 mins respectively. Peaks appearing in the region of 2-4 min are that of isomerised 1-octene, while that of octane appears at 2.3 min.

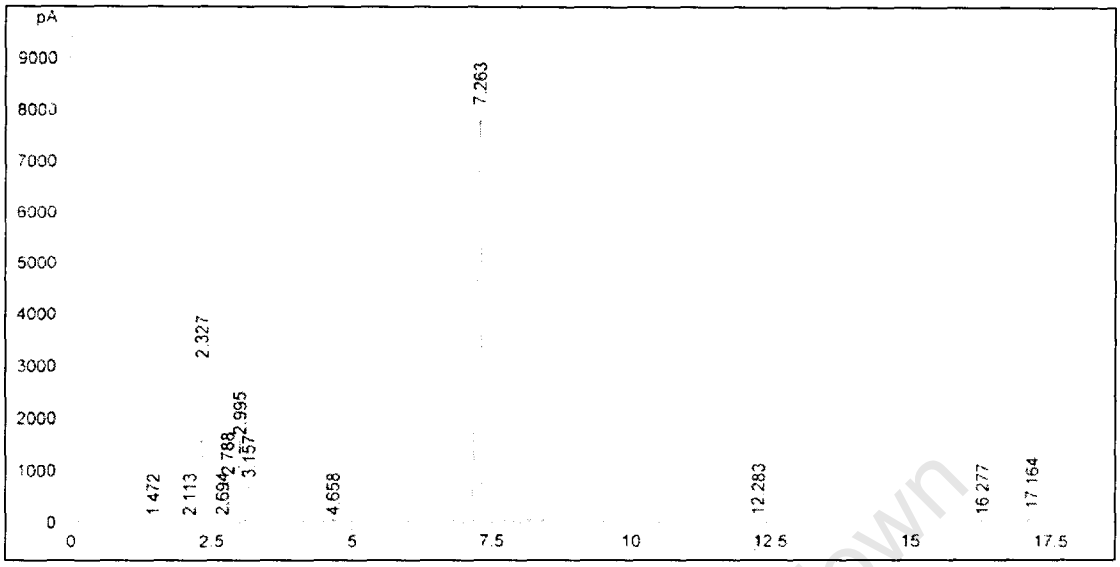

Figure 5.2: GC spectrum showing retention times of reaction products.

5.1. Sample calculations using GC data

Table 5.3 shows the calculation of molar quantities of the [$PtCl_2$(dppe)] catalyzed reaction starting from the area percent of components obtained from the GC-FID output data.

Table 5.3: Molar quantities of products from [$PtCl_2$(dppe)/$SnCl_2$] catalyzed hydroformylation.

Compound	[a]Area (%)	[b]Mass %	[c]Corrected mass (g)	[d]Moles
Toluene	62.76	58.65	60.06	0.652
1-Octene	14.15	14.15	14.85	0.132
Octane	11.79	11.79	12.08	0.106
1- Nonanal	8.66	10.83	11.09	0.0779
2-Me-octanal	1.09	1.36	1.39	0.00981
3-Et-heptanal	0.02	0.025	0.026	0.000183

[a]Area % as reported by GC-FID output data.

[c]Corrected Mass = mass (g) compound x [(T-feed / T-prod)]

= mass (g) compound x [60.08 g / 58.65 g]

= mass (g) x [1.024]

[d]Moles = Corrected mass (g) / Molar mass (g/mol).

Table 5.4 lists the criteria analyzed when considering the performance of the catalyst and shows the calculation of these parameters. Duplicate runs were performed and average molar quantities calculated for each catalyst under identical reaction conditions.

Table 5.4: Performance of catalyst in [$PtCl_2$(dppe)/$SnCl_2$] catalyzed hydroformylation.[a]

Moles of 1-octene in feed	0.358
Moles of 1-octene converted	0.226
% Conversion	63
% Hydrogenation	47
% Yield Nonanal	39
% Linearity	89
% Heavies	14
n:i	7.9
TOF (mol 1-oct.(mol Pt.h)$^{-1}$)	565

[a]Sample calculations:

(i) Moles of 1-octene converted = n(1-octene) in – n(1-octene) out
= 0.358 – 0.132
= <u>0.226 mol</u>

(ii) % Conversion = 100 – (n(1-octene) out / n(1-octene) in) * 100)
= 100 – ((0.132 / 0.358) * 100)
= <u>63 %</u>

(iii) % Hydrogenation = n(octane) / n(1-octene converted) * 100
= (0.106 / 0.226) * 100
= <u>47 %</u>

(iv) % Yield Nonanal = n(nonanal) / n(1-octene converted) * 100
= (0.0879 / 0.226) * 100
= <u>39 %</u>

(v) % Linearity = n(1-nonanal) / n(all aldehydes) * 100

= (0.0779 / (0.0879)) * 100

= 89 %

(vi) % Heavies = [(n(1-octene converted) – n(octane) – n(nonanal)] /

n(1-octene converted)]* 100

= [(0.226 – 0.106 – 0.0879) / 0.226] *100

= 14 %

(vii) n:i = n(1-nonanal) : n(2-nonanal)

= 0.0779 : 0.00981

= 7.9

(viii) TOF = n(1-octene converted) / (n(Pt) x h)

= (0.226 / (2.86 x 10^{-5} x 14))

= 565 mol 1-octene.$(mol.Pt.h)^{-1}$